Minimal Model of Lung Mechanics for Optimising Ventilator Therapy in Critical Care

Toshinori Yuta

A thesis presented for the degree of
Doctor of Philosophy
in
Mechanical Engineering
at the
University of Canterbury,
Christchurch, New Zealand.

July 2007

Acknowledgements

To my family, especially my parents, for their true unconditional and continuous support,

To my supervisor Prof. Geoff Chase for his technical insight and not-so-subtle nudge on my back,

To my supervisor Dr. Geoff Shaw for his skill and creativity in the art of medicine,

To Prof. Andrew Bersten for that crucial clinical data,

To my fellow engineers, comedians, and/or philosophers at the Centre for Bio-engineering,

To my friends,

To Cassie,

Thanks.

Contents

List of Figures

List of Tables

Nomenclature

ALI	Acute Lung Injury
ARDS	Acute Respiratory Distress Syndrome
cmH_2O	centimetre of water (pressure unit)
CO_2	Carbon Dioxide
CPAP	Continuous Positive Airway Pressure
EEP	End Expiratory Pressure
EEV	End Expiratory Volume
EIV	End Inspiratory Volume
ET	Endotracheal (tube)
FRC	Functional Residual Capacity
ICU	Intensive Care Unit
IQR	Inter Quartile Range
LIP	Lower Inflection Point
LPM	Litre per minute (flow rate unit)
MV	Mechanical Ventilator
PEEP	Positive End Expiratory Pressure
PIP	Peak Inspiratory Pressure
PV	Pressure vs. Volume (curve)
SD	Standard Deviation
TCP	Threshold Closing Pressure
TOP	Threshold Opening Pressure
TP	Threshold Pressure
UC	Unit Compliance (curve)
UIP	Upper Inflection Point
VILI	Ventilator Induced Lung Injury
Vt	Tidal Volume
WoB	Work of Breathing
ZEEP	Zero End Expiratory Pressure

Abstract

Positive pressure mechanical ventilation (MV) has been utilised in the care of critically ill patients for over 50 years. MV essentially provides for oxygen delivery and carbon dioxide removal by the lungs in patient with respiratory failure or insufficiency from any cause. However, MV can be injurious to the lungs, particularly when high tidal pressures or volumes are used in the management of Acute Respiratory Distress Syndrome (ARDS) or similar acute lung injuries.

The hallmark of ARDS is extensive alveolar collapse resulting in hypoxemia and carbon dioxide retention. Application of Positive End Expiratory Pressure (PEEP) is used to prevent derecruitment of alveolar units. Hence, there is a delicate trade-off between applied pressure and volume and benefit of lung recruitment. Current clinical practice lacks a practical method to easily determine the patient specific condition at the bedside without excessive extra tests and intervention. Hence, individual patient treatment is primarily a mixture of "one-size-fits-all" protocols and/or the clinician's intuition and experience.

A quasi-static, minimal model of lung mechanics is developed based on fundamental lung physiology and mechanics. The model consists of different components that represent a particular mechanism of the lung physiology, and the total lung mechanics are derived by combining them in a physiologically relevant and logical manner. Three system models are developed with varying levels of physiological detail and clinical practicality. The final system model is designed to be directly relevant in current ICU practice using readily available non-invasive data.

The model is validated against a physiologically accurate mechanical simulator and clinical data, with both approaches producing clinically significant results. Initial validation using mechanical simulator data showed the model's

versatility and ability to capture all physiologically relevant mechanics. Validation using clinical data showed its practicality as a clinical tool, its robustness to noise and/or unmodelled mechanics, and its ability to capture patient specific responses to change in therapy.

The model's capability as a predictive clinical tool was assessed with an average prediction error of less than 9% and well within clinical significance. Furthermore, the system model identified parameters that directly indicate and track patient condition, as well as their responsiveness to the treatment, which is a unique and potentially valuable clinical result. Full clinical validation is required, however the model shows significant potential to be fully adopted as a part of standard ventilator treatment in critical care.

Part I

Introduction and Physiology

Chapter 1

Introduction

Modern health care is becoming increasingly driven by new technologies, which has resulted in an increased complexity in therapies. Nowhere is this trend more true than in the Intensive Care Unit (ICU). The typical ICU patient is monitored and managed via a series of invasive catheters, breathing (endotracheal) tubes, electrodes and infusion pumps. All of these technologies are used to deliver advanced drug therapies, support circulation and breathing, and provide maintenance treatment for sedation, analgesia, nutrition, hyperglycemia, and hydration, among others.

1.1 The Mechanically Ventilated ICU Patient

Mechanical ventilation (MV) is one of the most common treatments a patient receives in the ICU. It is used to aid patients with respiratory failure, due to illness, disease, or heavy sedation. MV provides for bulk movement of gases in and out of the lungs. This is achieved through the application of additional pressure to the patient's airway. The air may be delivered invasively via an endotracheal (ET) tube, or non-invasively via a tightly fitted face mask. The ET tube is sealed within the airway using a low pressure cuff to provide accurate delivery of pressure and flow, and to prevent aspiration of acid secretions or harmful particulate material. As many as 97% of patients are treated with mechanical ventilation on admission to ICU [Walsh et al., 2004], at a typical daily additional cost of over $1,500 per patient [Dasta et al., 2005].

Mechanical ventilation helps patients with respiratory failure and, in most cases, it is necessary to maintain appropriate oxygen and carbon dioxide levels in the blood. However, incorrect ventilator settings may cause further injury to the lungs through use of high pressure (barotrauma) and high tidal volume (volutrauma). Extended MV treatment may lead to dependence, prolonging the stay and thus cost of ICU treatment [Dasta et al., 2005; McLean et al., 2006]. Long term MV can also lead to other complications, such as ventilator associated pneumonia [Rello et al., 2002].

Ideally, MV should be applied for the minimal period of time to prevent ventilator dependence and other complications. Hence, optmising the ventilator treatment and preventing lung injury is paramount. The ideal setting of the ventilator is therefore to apply just enough support to maximise lung recruitment to enable the patient to recover while minimising the risk of Ventilator Induced Lung Injury (VILI). However, in the absence of readily measured gold standard metrics of lung recruitment, it is impossible to strike this optimal balance in real time therapy.

There are a few main parameters in ventilator treatment that the intensive care clinician applies to each patient. Positive End Expiratory Pressure (PEEP) is a pressure at the end of expiration. Rather than deflating the lung to the relaxed volume at atmospheric pressure, or Functional Residual Capacity (FRC), at each breathing cycle, PEEP is applied to maintain some additional volume above FRC at the end of each expiration. Tidal Volume (Vt) is the volume of air that enters the lung at each breathing cycle. Peak Inspiratory Pressure (PIP) is a maximum pressure applied to the patient's proximal airway.

There are also 2 basic modes of ventilation: 1) pressure controlled and 2) volume controlled. When the ventilator is operating in the pressure controlled mode, PEEP and PIP are directly set by the clinician, where as Vt is a result of these settings. When the ventilator is operating in the volume control mode, PEEP and Vt are set by the clinician, and PIP is determined as a result. The compliance (volume change per pressure change) is highly variable depending on lung injury and disease. Therefore, Vt in pressure controlled mode or PIP in volume controlled mode, may be highly variable.

There have been numerous attempts to standardise ventilator treatment [Ware and Matthay, 2000]. These studies focused primarily on controlling the PEEP [Amato et al., 1998; Brower et al., 2004; Rouby et al., 2002; Takeuchi et al., 2002], and tidal volume [ARDS Network, 2000; Brochard et al., 1998; Eichacker et al., 2002; Kallet et al., 2005]. While these studies demonstrated improved survival with their set ventilation protocols, there is still no gold standard in which to base the ventilation treatments.

The difficulty is in determining the condition and needs of the individual ICU patient. The lung condition can vary greatly between patients, and can evolve significantly over time. As a result, in the absence of a patient specific ventilator treatment protocol, the ventilator settings and protocols still strongly depend on the individual clinicain's experience and intuition [Ferguson et al., 2005].

1.2 Lung Physiology

Warm blooded animals have the advantage of being able to adapt and survive in the most extreme environments. By keeping the internal body temperature constant, usually higher than the environment, these animals are able to react to any situation quickly. In contrast, cold blooded animals depend on external sources of heat, such as the sun, to warm up the muscles, and thus may not be able to react as quickly in the same situation. This constant internal temperature in warm blooded animals also means that all the chemical reactions in the body can take place relatively quickly and reliably, including those in the brain and nervous system, creating a fast, responsive animal.

The cost of this great advantage is the need for a constant supply of energy, and in large quantity. This vast amount of energy that a body requires comes from the food consumed. The energy is released after it undergoes a chemical reaction with oxygen, or oxidative cellular metabolism, as part of the normal homeothermic (warm-blooded) physiology. However, unlike the energy in food, which can be stored in a body as fat, oxygen cannot be stored readily in the body. Thus, the body requires a constant supply of oxygen to maintain the agility and well being of the body, which is where the lungs come into play.

The primary function of the lungs is therefore to supply the body with this vital gas by extracting it from the air we breathe. The oxygen is extracted from the air and transferred to the blood via lung alveoli. At the same time, the bi-products of this chemical reaction, including primarily carbon dioxide (CO_2), are removed from the blood and expelled from the body. Therefore, the lungs provide oxygen and remove waste products from the blood via gas exchange in recruited/available alveoli in the lungs.

1.2.1 Lung Structure

The lungs are situated in the thoracic cavity, above the diaphragm and around both sides of the heart, as illustrated in Figure 1.1. Two layers of membranes separate the lungs and the rib cage, the inner and outer pleural membranes. The inner pleural membrane is attached to the lungs and the outer membrane is attached to the inside of the ribcage. A thin layer of fluid fills the gap between the two pleural membranes, which reduces friction and allows these membranes to slide freely relative to each other. There are no direct mechanical connections between the lungs and the chest wall or diaphragm. The overall general shape of the lung is maintained by the relatively rigid ribcage.

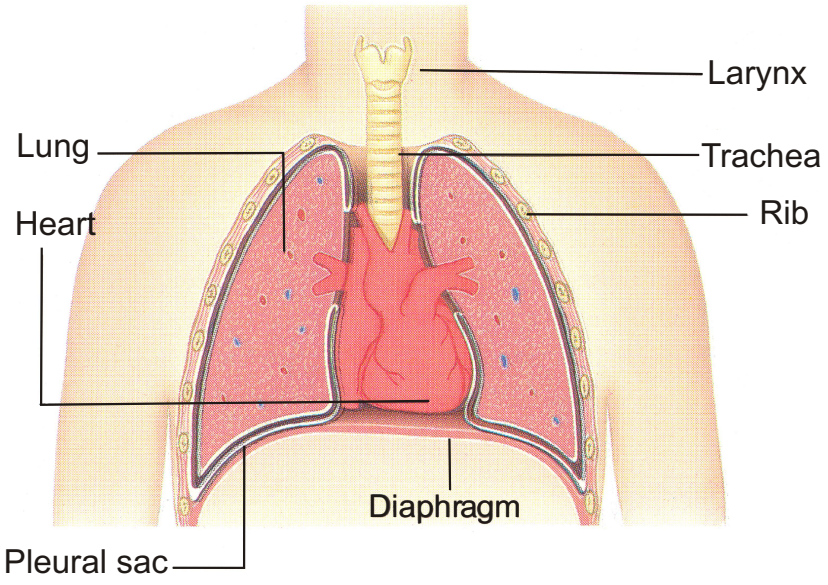

Figure 1.1 Location of lung and the surrounding structures. [Sebel et al., 1985]

Air enters the lung through the nose and/or mouth, moves past the larynx and into the trachea. The trachea is a c-shaped cartilage ring lined airway, about 2 cm in diameter on average. Stiff cartilages support the shape of the trachea and maintain this airway opening. It can withstand a pressure well above the normal intrathoracic cavity pressure [Sebel et al., 1985].

Just above the heart, the trachea bifurcates to airways slightly smaller in diameter, called bronchi. These airways branch off laterally, each feeding air to the lung on its respective side. The right bronchus is slightly larger than the left, which coincides with the relative size difference between the left and right lungs. The bronchi branch off further as they spread out deeper into the lungs, gradually reducing in diameter at each bifurcation. The cartilage on these airways also gradually becomes smaller, thinner and more irregular in shape. The overall structure is that of a branching tree with each successive branch becoming a smaller set of airways. Figure 1.2 illustrates the schematic drawing of major proximal airways.

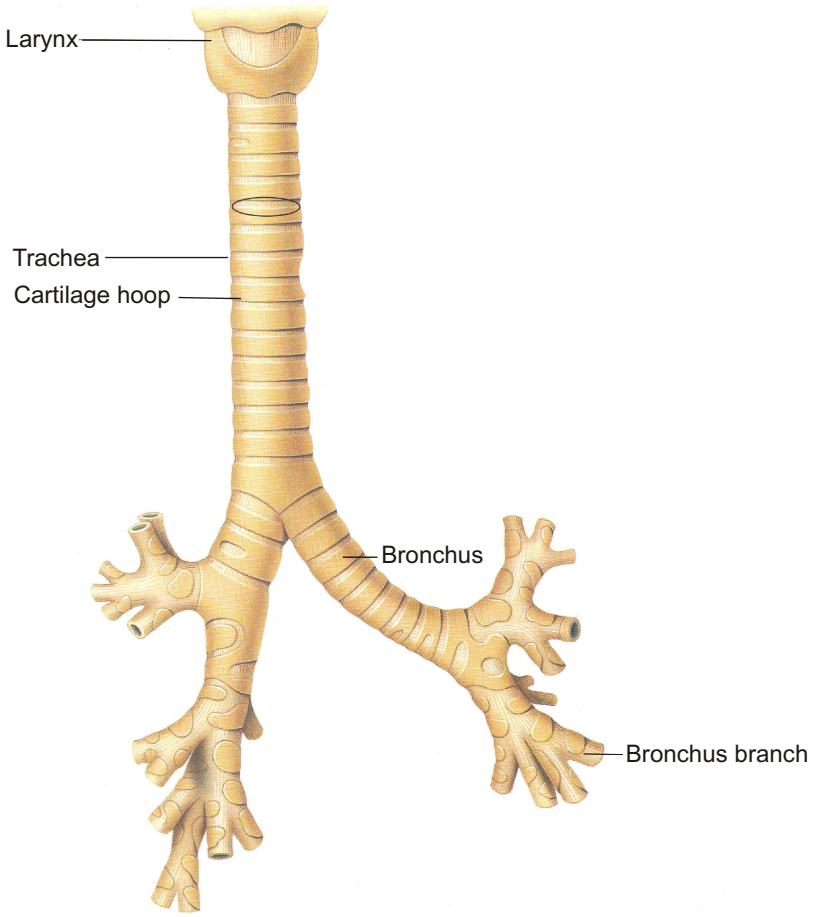

Figure 1.2 Major proximal lung airways. [Sebel et al., 1985]

By about the 11th generation of bronchial branches, the diameter is reduced to about 1 mm and the cartilage lining disappears. These smaller airways are called bronchioles. Their walls consist of helical bands of muscles and the airway relies on lung parenchyma, principal structural tissues, to maintain its shape. The bronchioles further branch for about another 8 generations. However, the diameters of these airways do not decrease as rapidly. Thus, the total surface area increases at every bifurcation in these generations. Up to this point, the sole purpose of these airways is to transport air, while controlling the temperature and humidity [Sebel et al., 1985; Vander et al., 2001].

At about the 17th total generation of bronchial branches, the alveoli start to appear on the walls of the bronchioles, known specifically as respiratory bronchioles. The number of alveoli gradually increases as the respiratory bronchiole further branches for about 3 more generations. The function of the airway also gradually changes from gas transport to gas exchange.

At about the 20th generation of bronchial branches, the wall of the airway is completely lined with alveoli, and the bands of muscles disappear from the walls. The diameters of these alveolar ducts and respiratory bronchioles do not decrease significantly as they bifurcate. Thus, the number of alveoli and surface area for gas exchange now increases rapidly. The very end of the bronchial branches, at about the 23rd generation, is the alveolar sac. The only difference from alveolar ducts is the fact that the alveolar sac is not a through passageway but a dead end. Each alveolar sac contains about 20 alveoli, and about half of the total number of all alveoli are located in alveolar sacs [Sebel et al., 1985; Vander et al., 2001].

The alveolus is where the primary function of the lung, gas exchange, occurs. There are about 600 million alveoli in the lungs of the average adult human and each alveolus is about 200 μm in diameter [Seeley et al., 2003]. The number of alveoli, however, varies greatly depending on the gender and the size of the lung of the individual [Ochs et al., 2004]. An alveolus is surrounded by capillaries, as the drawing of the alveolar sac terminus in Figure 1.3 illustrates. These capillaries are barely as large as the red blood cells they transport. The epithelium separating the blood and the gas is only about 0.2 μm thick, enabling rapid gas exchange between them [Vander et al., 2001]. The gas exchange occurs by diffusion, where gas is transferred from a high partial pressure region to lower partial pressure regions, in both directions, trading oxygen and CO_2.

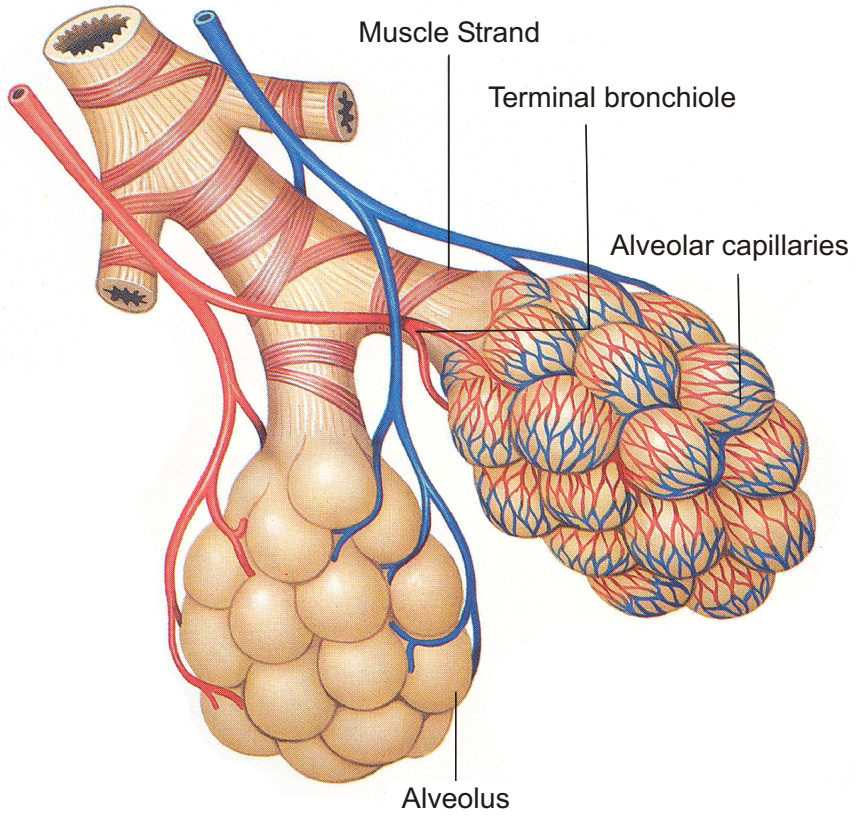

Figure 1.3 Alveoli sac and surrounding capillaries. [Sebel et al., 1985]

As any flexible elastic sphere, the inner pressure require to maintain its spherical shape is inversely related to its diameter. Thus, the smaller the sphere, the stronger its tendency to collapse. An alveolus is thought to react in a similar manner. To counteract this tendency at a reduced size, or low volume, the inside walls of the alveoli and distal bronchiole are lined with a fluid called surfactant. The surfactant is a mixture of protein and lipids, and works to control the surface tension and thus the shape of the alveoli. When the lung is deflated and the surface areas of alveoli and the airways are small, the concentration of surfactant molecules on the surface increases. This increase in concentration in turn decreases the surface tension, maintaining the volume in the air space. When the lung is inflated on inspiration, the surfactant molecules become more spread out, increasing the surface tension. This increase, in turn, prevents the alveoli and airways from overstretching during inspiration by providing a restoring force. The overall effect of the surfactant is therefore to maintain the structure of air spaces, based on equilibrium surface tension, over the wide range of volume experienced during breathing.

The lung itself does not participate in the actual muscular movement required for inflation. Instead, it is completely passive. The work is done by muscular movement of the diaphragm and the intercostal muscles of the ribs. During inspiration, the diaphragm moves downwards and the intercostal muscles move the ribs upward and outwards increasing the volume of chest cavity, as the illustration in Figure 1.4 shows. Since there are no direct mechanical connections between the surrounding tissues and the lung, this inflation is entirely based on the transmural pressure gradient between thoracic cavity and the lung. More specifically, when the inspiratory muscles contract, a negative pressure gradient is created between the thoracic cavity and the lung, which in turn creates negative pressure gradient between the lung and the environment. As a result, air is then drawn into this lung to equate the pressure gradient, creating the inspiratory pattern of normal breathing [Sebel et al., 1985; Seeley et al., 2003]

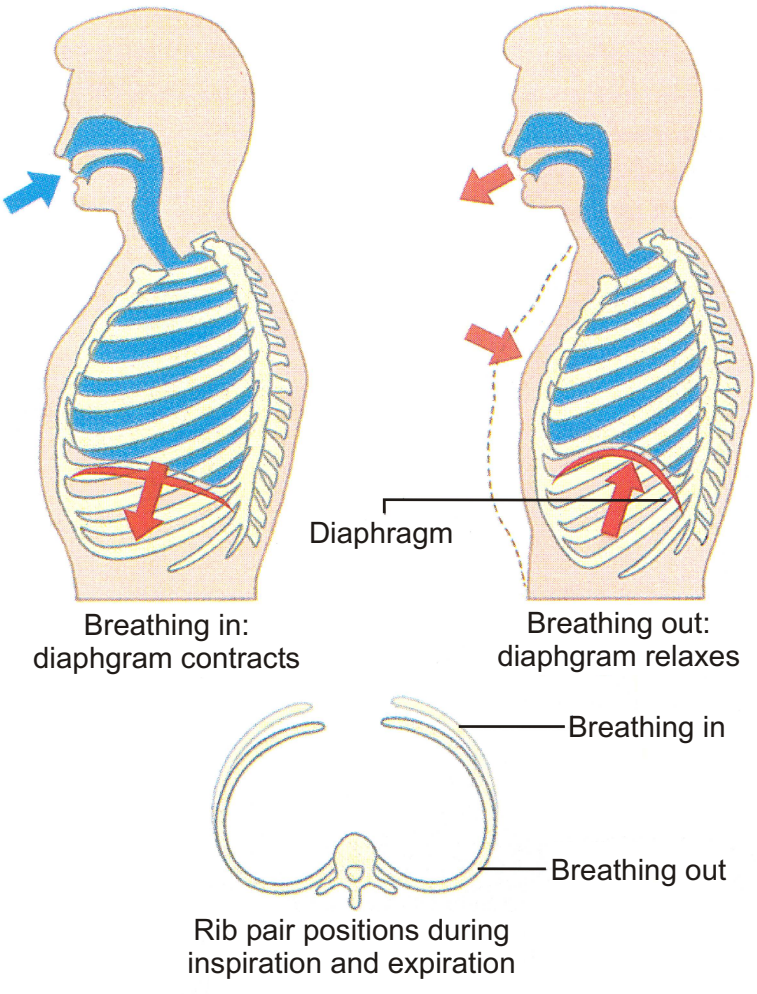

Figure 1.4 Muscle and rib cage movement during breathing. [Sebel et al., 1985]

Under normal, quiet breathing, deflation is a result of the simple elastic recoil of tissues. At the end of inspiration, all the respiratory muscles are relaxed and the lung volume resumes its original equilibrium value, forcing the air, now exchanged with CO_2 and waste products, out of the lungs. This movement is caused by elastic recoil of the surrounding tissues that were deformed during the inspiration phase. Most of this recoil force results from deformed lung tissues and the surface tension on alveoli and distal bronchioles.

1.2.2 ARDS

Acute Respiratory Distress Syndrome (ARDS), formerly known as Adult Respiratory Distress Syndrome, is a severe form of Acute Lung Injury (ALI). It is a condition where the lung is inflamed and fills with fluid, thus losing the ability to exchange gas effectively. Furthermore, the surfactant is denatured and its production is reduced due to inflammation causing alveoli to collapse. As a result, alveolar and bronchial passages collapse and/or fill with fluid, preventing them being filled with air during inspiration. Hence, severely affected lung units are "lost" to the disease, reducing the remaining effective lung volume as it were a "baby lung" [Gattinoni and Pesenti, 2005].

Patients affected by ARDS usually require mechanical ventilation to assist their breathing. A definition of ARDS has been discussed and evolving since it was first reported in 1967 [Ashbaugh et al., 1967]. The difficulty is that there are no specific criterias or tests that a clinician can follow to specifically diagnose ARDS because it does not have a distinguishable disease specific symptom [Artigas et al., 1998; Atabai and Matthay, 2002; Rouby et al., 2000]. Development of standardised definitions has helped, at least in terms of patient enrolment and results comparison in clinical trials [Esteban et al., 2002; Manzano et al., 2005; Reynolds et al., 1998].

Physiology / Symptoms/ Causes

ARDS is characterised by injury to the alveolar epithelial wall. Damage to this barrier between the blood and airspace causes an increase in permeability, and reduces the ability to remove the fluid from airspace. The result is alveolar flooding, or pulmonary edema. The damage to the cells also impairs surfactant

production causing the alveoli to collapse as they can no longer control or manage surface tension. The collapse is further encouraged by the additional pressure build up within the lung from the invading fluid. The fluid layer in flooded alveoli and lack of effective gas/blood interface in the collapsed alveoli makes efficient gas exchange impossible, thus starving the body of oxygen and increasing the CO_2 concentration.

The presence of injured tissues and additional fluid has the overall effect of making the lung stiffer. It therefore requires a larger pressure gradient to inflate. This additional required pressure greatly increases the work of breathing for the patient. Furthermore, flooded and injured alveoli do not participate in gas exchange, further reducing the functional volume of the lung. As a result, ARDS lungs are stiffer and smaller in volume, and the lung units are less effective at gas exchange.

The blood that flows through capillaries surrounding flooded and/or collapsed alveoli is circulated back to the body without undergoing gas transfer. A slight decrease in partial arterial oxygen pressure can cause a relatively large decrease in oxygen saturation. The result is a severe hypoxemia, or lack of oxygen in the body. Clinically, a patient is considered to be severely hypoxemic when partial arterial oxygen pressure falls below 50 mmHg, half the normal level. Such a severe hypoxemia requires immediate treatment or it can be fatal as vital organs, particularly the brain, cannot function without constant supply of oxygen. Cell damage and death can occur in a matter of minutes.

Furthermore, the ventilated tidal volume from the collapsed region is transferred to other regions of the lung, increasing the pressure of that region. This increase in pressure restricts the blood flow in the alveolar capillaries, or shunt, increasing the physiological dead space. This increase in dead space makes the elimination of CO_2 difficult. The result is hypercarbia, or an increased level of CO_2. Thus, ARDS is characterised by increased ventilator-perfusion abnormalities, causing hypoxemia and hypercarbia, a devastating combination, especially to those who are already weak from other injuries or illness.

There are various conditions that can cause ARDS. One of the obvious causes is a direct injury to the lung. These injuries include the inhalation of smoke and other toxic gases, pneumonia, near drowning, and direct physical injury to the

lung, such as lung surgery. Other causes are indirect, such as sepsis and severe trauma to other parts of the body including surgery, causing an inflammatory response at capillary level. Drug overdose and blood transfusion can also cause ARDS. In other words, anything that causes great stress to the body can lead to development of ARDS.

Incidence and Mortality

There are numbers of studies reporting the incidence and mortality of ARDS from various regions of the world. However, because the definition of ARDS is vague, the actual numbers are difficult to compare. Each study may have used different criteria to define ARDS. The reported number of incidences varies from about 10 to 80 cases per 100,000 persons per year [Bersten et al., 2002; Luhr et al., 1999; Manzano et al., 2005; Reynolds et al., 1998; Rubenfeld et al., 2005; Suchyta et al., 1997; Ware and Matthay, 2000; Zilberberg and Epstein, 1998].

The mortality rate for ARDS is reported as from 30% to as much as 80% [Bersten et al., 2002; Esteban et al., 2002; Luhr et al., 1999; Manzano et al., 2005; Reynolds et al., 1998; Rubenfeld et al., 2005; Suchyta et al., 1997; Ware and Matthay, 2000; Zilberberg and Epstein, 1998]. Older patients have a significantly higher risk of ARDS and higher mortality rate [Manzano et al., 2005; Rubenfeld et al., 2005; Suchyta et al., 1997]. A recent cohort study suggests that, in the United States, there are 190,600 cases of ALI, including ARDS, with 74,500 associated deaths and 3.6 million hospital hours every year [Rubenfeld et al., 2005].

1.3 Mechanical Ventilator Treatment

There are no specific treatments for ARDS. The only treatment clinicians can provide for the ARDS patient is to facilitate an environment that aids patients to recover on their own. There are a few suggested clinical therapies, such as anti-inflammatory and surfactant therapy. However, none has been proven to be clinically effective [Ware and Matthay, 2000].

One of the most important interventions for supporting the ARDS patient is the artificial or mechanical ventilation. The increase in work of breathing

with ARDS makes breathing difficult for the patients and most of them require additional support to reduce the work of breathing. Mechanical ventilation is the most common treatment to provide this artificial ventilation support in critical care.

Modern mechanical ventilators use positive pressure ventilation and the air is delivered to the lung through an endotracheal tube (ET tube), tracheotomy, or face mask. The ventilator itself is essentially a high precision air pump. It pumps a set amount of air into the lung at a set rate. The ventilator assists patient breathing by reducing the work of breathing. Alternatively, it can take over the work of breathing from the patient completely, if necessary.

Positive End Expiratory Pressure (PEEP) is one of the most important settings in mechanical ventilator usage. When PEEP is applied, rather than deflating to zero pressure, the ventilator stops the air flow at a certain positive pressure, preventing the lung from deflating to patient's abnormally low FRC. This additional pressure is especially important for the ARDS affected lung, because the lung units are vulnerable to collapse due to the presence of an additional superimposed pressure caused by the fluid and inflammation. Once collapsed, it takes significantly higher pressure to recruit those collapsed lung units. This collapse also increases the stiffness, or reduces compliance. PEEP prevents this impairment, thus maintaining the compliance and volume of functional lung units at a healthier, more effective level.

Tidal volume (Vt) is another fundamental setting in mechanical ventilator therapy. It determines the volume of air delivered to the lung in each breath. The Vt is determined by the patient's condition. A patient with a small functional volume requires a relatively small tidal volume. Too much Vt can over inflate the lung and cause further injury [Dreyfuss and Saumon, 1998].

There are two different ventilator modes typically used for delivering air to the lung: 1) Pressure Controlled and 2) Volume Controlled. The pressure controlled mode simply increases the pressure to a specified Peak Inspiratory Pressure (PIP) value from a preset PEEP and the air flows into the lungs passively as result. The volume control mode specifies a volume of air and delivers it at a set flow rate to the lung, and thus the pressure increases passively. The flow can be constant or varied over the inflation portion of the breathing cycle, and the actual flow rate

is determined by the combination of user-defined Vt and an Inspiration to Expiration Ratio (I:E). PEEP is also used with volume controlled ventilation. The ventilator actively control the inflation or inspiratory portion of breathing, and allows passive deflation to zero or prescribed PEEP under lung's own compliance.

1.3.1 Complications and Strategy

Optimal ventilator settings are difficult to determine. In normal condition, physiologically optimal Vt allows maximum gas exchange for minimum breathing effort [Otis et al., 1950]. However, for stiffer and reduced volume of ARDS lung, the normal tidal volume may be too high, and can lead to over inflation and further injury to the lung [Dreyfuss and Saumon, 1998; Lim et al., 2003]. Furthermore, PEEP should be kept relatively high, especially for the severely ARDS affected lungs, to prevent end expiratory collapse of the lung units and maintain the lung volume. This use of PEEP thus minimises the Vt that can be applied. Clinicians must therefore juggle these parameters to manage this trade-off between high PEEP and tidal volume, and low PIP.

The determination of the optimum ventilator settings is further complicated by the lack of any practical methods to determine the individual patient specific lung condition or status at bedside. Currently, the most reliable method of accurately determining the level of recruitment of the lung is by CT scanning. However, this method requires transport of patients out of ICU, expose them to significant radiation, and may require change of ventilation or setting during the scan. Therefore, this method poses additional danger to the patient as well as added cost for treating the patient. Furthermore, the condition of the patient can evolve significantly during ventilator treatment, and it would be very impractical to have such a scan every time their condition changes, or frequently enough to monitor these changes. As a result, the CT scan remains a research tool.

There have been numerous attempts to standardise ventilator protocols for optimising ARDS treatment based on readily obtainable Pressure vs. Volume (PV) curves. However, none of them have been a complete clinical success. Amato et al. [1998] conducted a clinical trial based on an "open lung" approach. The study showed that the mortality rate decreased when PEEP was set at 2 cmH_2O above the lower inflection point of inflation PV curve. This trial was based on

a theory that by having sufficient PEEP, the lung is kept inflated at the end of expiration and thus further collapse of the lung units is prevented, improving oxygenation. However, although the result shows the decrease in mortality, the reasoning behind this decrease has been challenged [Deans et al., 2005; Brower et al., 2004]. In particular, some argue that since derecruitment of the lung units occurs during deflation, the PEEP should be set according to the deflation curve, rather than inflation curve [Hickling, 2001, 2002; Girgis et al., 2006].

The ARDS Network [2000] also conducted a trial to compare high and low tidal volumes, which were chosen as 12 and 6 ml per predicted body weight (kg). They concluded that the low tidal volume resulted in lower mortality and suggested that ventilators should be set according to their findings. However, their results and conclusions have recently been criticised due to the impractically high tidal volume used (12 ml/kg, compared to normal practice of 8-10 ml/kg) during the trials for comparison [Eichacker et al., 2002] and for ignoring some negative aspects of low Vt [Kacmarek, 2005], suggesting that the result was skewed.

A significant problem with these suggested protocols is that they do not account for the unique conditions of individual patients. The condition of the ARDS patient varies greatly depending on many factors, such as age, gender, disease state, cause, and pre-existing conditions. It will also vary over time for each given patient, as their disease state evolves. Thus, simplified standard protocols may not be effective for every patient all the time [Deans et al., 2005], leading to mixed results in large trials using fixed protocols.

The optimal setting of the ventilator should facilitate maximum gas exchange and minimise further lung injury. However, choosing this setting requires a delicate trade-off between high PEEP and Vt for maximum gas exchange, and low PIP for minimising lung injuries. This trade-off is further complicated by the lack of an easy, practical way of determining the underlying, patient specific condition and lung recruitment status at bedside.

Still, there have been numerous attempts to standardise the ventilator treatment, and several protocols have been suggested [e.g. ARDS Network, 2000; Amato et al., 1998]. However, none of them has been well accepted by the entire ICU community. Because of the difficulties in determining the underlying patient specific condition and the lack of a well accepted adaptable protocol, clinicians

rely on their experience and intuition for optimising ventilation. As a result, ventilator settings are widely varied and inconsistent between patients [Ferguson et al., 2005] with equally variable patient mortality rates as a result [e.g. Bersten et al., 2002; Esteban et al., 2002; Reynolds et al., 1998; Rubenfeld et al., 2005].

1.4 Preface

The first goal of this thesis is to develop a model that accurately captures the essential mechanics of the mechanically ventilated lung. The model is based on simplified physiology and mechanics, and must have the capability to be individualised to capture the unique characteristics of the lung for each patient and condition without further invasive or impractical measurements. PV curves can easily be obtained from any modern ventilator in real-time and at the bedside. As a result, PV curves reflect the mechanical response and recruitment of the lung through a breathing cycle, embedded in which is the unique patient specific conditions. PV data is also widely used by clinicians to base their decision on the ventilator treatment and thus well accepted. However, to use PV curves to characterise the lung using this model, fundamental mechanisms of lung dynamics and the principal parameters governing their changes in ventilator therapy must be identified.

The second goal is to develop a system based on this model to determine the patient specific optimal ventilator treatment for artificially ventilated patients in a clinical situations. The system process consists of data acquisition, data processing, therapy simulation, and analysis. The entire process must be completed relatively quickly for the result to be applicable in clinical real-time. Furthermore, the data and the result must be presented in a clear and clinically relevant context to the clinicians. Once this system is developed, it can also be used to continuously monitor the patients' progress and lung status/condition at bedside. This system therefore allows clinicians to track the patient's condition and alter treatment accordingly. It can also be useful in research of ARDS and other acute lung injuries.

Part I of this thesis presents the background and basic physiology of the lung. The following chapter presents the fundamental physiology and a newly

hypothesised approach to modelling lung mechanics, on which this model is based.

Part II presents the lung model developed. Chapter 3 focuses on the components of the model and their physiological relevance. Chapter 4 combines those components to create the system model. A few different versions of the model are presented varying complexity and flexibility. Chapter 5 develops the fitting methods for clinical use and model validation.

Part III evaluates the model by validating its abilities to capture fundamental lung mechanics. Chapter 6 validates the model against a mechanical lung simulator and Chapter 7 validates it against clinical data. Finally, Chapter 8 evaluates the potential use of this model in clinical situations using clinical data.

Chapter 2

Lung Mechanics

The model is based on reported and well-accepted physiology and a newly hypothesised dynamic mechanism. It consists of several different components that work together to simulate the entire lung. Each component represents an element or mechanism of the actual lung. Thus, it can be applied and compared directly to the actual physiology. The model uses newly hypothesised lung mechanics that contradicts some traditional ideas of lung expansion and recruitment. However, this specific mechanism has already been recorded in clinical studies and also corresponds well to clinical observations. This chapter describes the fundamental lung mechanics on which the model is based.

2.1 The Lung Cycle and PV Curve

One of the fundamental pieces of data on which clinicians base their decisions for ventilator treatment is the Pressure vs. Volume (PV) curve. The curve indicates the characteristics of the lung over a breathing cycle, and this data can readily be extracted from any modern ventilator [e.g. Iotti and Braschi, 1999; Hamilton Medical, 2006; Maquet Medical Systems, 2006]. Typically, the pressure is measured at the mouthpiece or ventilator, however measurement or estimation of the true lung pressure at the trachea is possible with specialised equipment and techniques [e.g. Karason et al., 1999]. Clinicians often rely on this data to determine the condition and recruitment status of the lung and set the ventilator accordingly.

2.1.1 Definition and Interpretation

The shape of the PV curve indicates the fundamental phases of lung dynamics over a breathing cycle. A typical inflation portion of a PV curve follows a general sigmoid shape, where there is low compliance at lower and higher pressures, and relatively high compliance in the middle. This shape is especially apparent in a PV curve measured for total lung capacity over a full quasi-static PV range. The Lower Inflection Point (LIP) is the point at which the slope of the curve increases and the Upper Inflection Point (UIP) is the point at which the slope of the curve decreases, or plateaus at a higher pressure. Figure 2.1 shows the basic shape of a typical PV curve with a description of all the basic terminology.

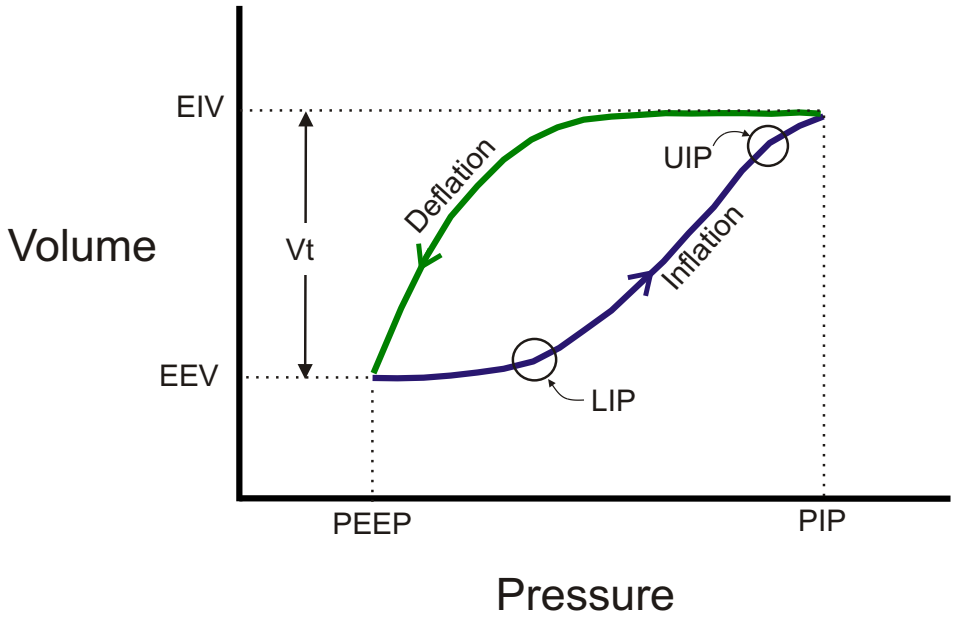

Figure 2.1 Lung Pressure vs. Volume (PV) curve. The illustration shows a basic shape of a typical PV curve with description and terminology. PEEP=Positive End Expiratory Pressure; PIP=Peak Inspiratory Pressure; LIP=Lower Inflection Point; UIP=Upper Inflection Point; EEV=End Expiratory Volume; EIV=End Inspiratory Volume; Vt=Tidal Volume

The first stage of inflation builds up pressure in the larger airways, such as the trachea and bronchi, as well as the topmost region of the lung. Since most of the larger airways are surrounded by cartilage and relatively rigid, the pressure builds up without resulting in any significant increase in volume. This phase thus corresponds to the initial low compliance portion of the PV curve. It also corresponds to the establishment of flow in the airways.

Once enough pressure is built up and the flow is established, the air flows to the distal airways and the lung starts to inflate. This phase corresponds to the higher compliance portion in the middle section of the PV curve. Finally, when the lung is inflated to near maximum capacity, the lung tissues are fully stretched and the lung becomes stiff. This last phase corresponds to the later lower compliance portion of the PV curve where the PV curve plateaus, or flattens at the end of inspiration.

The rate at which the lung is inflated partially depends on the superimposed pressure. Superimposed pressure is an additional pressure experienced by lung units due to the weight of the lung above them. Thus, in a supine position, the lung units towards the back or dorsal direction experience higher superimposed pressure, and require higher pressure to inflate. This effect is especially prominent in the ARDS lung because of the additional weight from the extra fluid build up in the lung [Ware and Matthay, 2000].

PV curves can potentially indicate unique characteristics and the condition of the lung, and clinicians have been relying on this data to determine ventilator settings [Jonson and Svantesson, 1999; Jonson, 2005]. ARDS lungs are stiffer and the functional volumes are smaller in comparison to healthy lungs. This difference can be clearly seen on PV curves where the stiffer lung has lower volume at a given pressure. A healthy lung has higher compliance and less hysteresis, while ARDS affected lungs have low compliance and significantly more hysteresis. Hence, PV curves show recruited or aerated lung volume as a function of pressure, clearly illustrating many fundamental measures of lung condition and status. The PV curves can also indicate other lung conditions, such as obstructive disease or asthma.

2.1.2 Limitations

There are a several limiting factors for using PV curves as an indicator for ventilator therapy. Ideally, the data would show the result of true lung mechanics for analysis. However, there are several aspects of the PV curve, especially those directly obtained from ventilators, that do not necessarily or fully reflect the true lung mechanics.

The measurement for a PV curve is essentially taken at a single point. Whether the pressure is measured at the mouthpiece or at trachea, one set of pressure data is associated with one volume data. Thus, the PV curve essentially represents the entire lung as one compartment. However, clinical studies found that ARDS/ALI affects the lung heterogeneously [Gattinoni et al., 2001; Puybasset et al., 2000]. Some regions of the lung are affected more than others. ARDS affected lung units exhibit different mechanics, and thus have different pressure and volume relations. Therefore, the PV curves, having a single point of measurement, cannot differentiate the healthy and injured lung units. For example, some clinically relevant information, such as the number and location of the affected lung units, cannot be directly extracted from PV curves.

The readily obtainable PV data is usually measured proximally at the ventilator or mouthpiece, because it does not require additional equipments or special techniques. However, the data obtained at these points also includes effects of airway resistance. Ventilated patients are usually intubated and thus are ventilated through an ET tube. ET tubes are usually less than 1 cm in diameter and provide significant flow resistance in certain flow patterns [Karason et al., 2000, 2001]. Therefore, the proximal PV measurement taken before the ET tube contains the effect of this resistance and can mask the true lung mechanics in the data, as clearly illustrated in Figure 2.2, which compares data measured at mouthpiece and trachea. This effect can be even more exaggerated for the data taken at the ventilator due to the additional connector tubes between ventilator and mouthpiece.

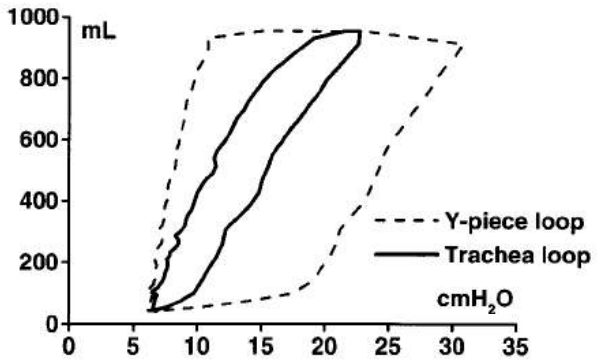

Figure 2.2 Effect of ET tube on PV curve. The outer loop shows the PV curve measured at Y-piece, before the ET tube, and the inner loops shows the trachea measurement. [Karason et al., 2001]

The ventilator inflates and deflates the lung by controlling the pressure and/or flow. At beginning of inspiration, the ventilator increases the pressure to a predefined PIP, or until the desired flow is established, depending on the operation mode. On expiration, the ventilator simply reduces the pressure to a predefined PEEP, and the lung deflates naturally. Therefore, the transition between inflation and deflation is rapid and highly dynamic, as illustrated in Figure 2.3. The plot in the figure shows clinical PV data [Bersten, 1998] sampled every 0.02 sec. The dynamic transition region of the PV curve is clearly illustrated by the sparse marker distributions indicating the rapid transition, resulting in reduced amount of sampled data in this region of the curve.

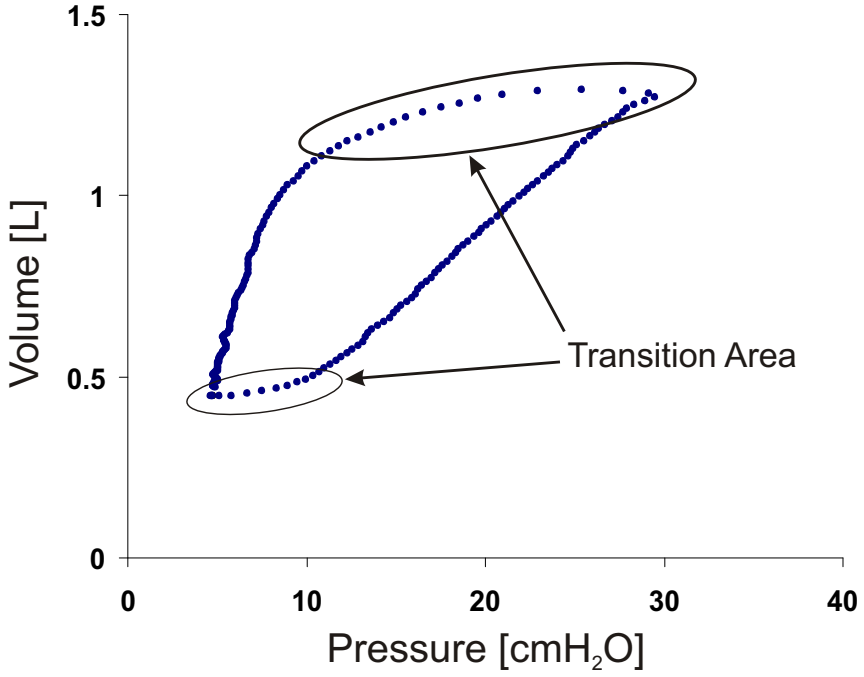

Figure 2.3 Effect of transition period on PV curve. The plot shows the clinical PV data [Bersten, 1998]. Each marker represents the data taken at every 0.02 sec. The highly dynamic portion of the curve is highlighted.

Due to combinations of some sensors' insensitivity to the lower flow and less sampled points, this transition phase of ventilation is prone to measurement errors. Furthermore, because the flow in the airways must be reversed during this transition period, the resulting mechanism is mostly due to the establishment of new flow. Therefore, the portion of PV data for the transition period is not necessarily an accurate reflection of the true lung mechanics, as well as being noisy and having lower data density.

2.2 Hypothesised Lung Mechanics

It is well known that PV curves can indicate the underlying condition of the lung [Jonson and Svantesson, 1999]. However, how to interpret the actual curve, particularly with regard to clinical decisions and protocols, is challenging and much debated [Deans et al., 2005; Kacmarek, 2005]. This difficulty is partially due to lack of a clear, well accepted, explanation of lung mechanics at the level of alveoli and distal airways, where recruitment, aeration, and gas exchange, the critical lung functions, take place. In addition, there is no clear readily available direct measure of these mechanics or behaviours in critical care [e.g. Gattinoni et al., 2001; Lee et al., 2002; Stenqvist et al., 2002; Stenqvist, 2003]. As a result, the interpretation is individualised between clinicians and inconsistent overall [Ferguson et al., 2005].

2.2.1 Traditional Theory of Lung Mechanics

Traditionally, the lung was thought to inflate mainly by isotropic, balloon-like, expansion of alveoli, and the PV curve is often interpreted accordingly [Hickling, 2002]. The LIP was thus thought to be a point where a single massive recruitment of alveoli occur, followed by high compliant isotropic balloon-like expansion of recruited alveoli. The analogy might be to a balloon making its initial stretching before the major volume change. The UIP is therefore thought to be a point where over-inflation of continuously expanding alveoli starts to occur. Thus, it exhibits lower compliance after the UIP as an interpreted metric of plastic, or elastic-plastic, expansion and potential damage.

The problem with this traditional interpretation is that it does not correspond well to clinical observation [Hickling, 2002]. For example, the recruitment and derecruitment of alveoli is thought to contribute greatly to hysteresis of the PV curve based on clinical observation [Cheng et al., 1995]. If the LIP was a single point of recruitment for most or all alveoli, then there should be minimum hysteresis for tidal ventilation with PEEP above LIP and the PV curves should thus be superimposed on the inflation limb of the total lung PV curve, which does not occur clinically [e.g. Bersten, 1998].

Furthermore, if LIP indicates a single massive recruitment, there should be no additional recruitment above LIP. However, clinical data shows an increase in volume at a given pressure as PEEP is increased. This additional increase indicates additional recruitment above LIP, contradicting the interpretation of LIP [Hickling, 2002].

Note that the question has been raised about the traditional interpretation of lung mechanics partially due to technological advancements in the medical field. New technology and equipment allow more precise control over the ventilator and real time data to be collected more easily. This in turn allowed the development of new strategies for ventilator treatment and generated results that could not be explained by the traditional theory. However, technological advancement has also allowed the development of new methods for further research and better understanding of lung mechanics.

2.2.2 New Theory of Lung Mechanics

Recent clinical studies have shown entirely different mechanisms of lung expansion from what was traditionally thought. They suggest that recruitment and derecruitment of alveoli greatly influence, if not dominate, the PV curve data and lung ventilation. In particular, it indicates that once recruited the alveoli show very small isotropic expansion as pressure increases. These studies also show that recruitment occurs continuously during inflation, well above LIP. These findings together suggest that lung inflation and deflation, particularly at the distal airways, is not caused by isotropic movement of alveoli, but predominantly by continuous recruitment and derecruitment of alveoli.

Background

Johnson et al. [1999] conducted a study comparing the lung volume at a given pressure with Zero End Expiratory Pressure (ZEEP) and PEEP. The study showed that the end expiratory volume increased as PEEP was increased. This pattern was apparent even when PEEP was set above LIP. This result indicates recruitment of alveoli continuously occurs through and above LIP. Recruitment of lung alveoli and elements above LIP were also observed in several studies utilising CT scans [e.g. Albaiceta et al., 2004; Gattinoni et al., 2001].

Cheng et al. [1995] used excised rat lungs to determine the role of recruitment and derecruitment in lung inflation. First, the End Inspiratory Pressure (EIP) of the lung was progressively increased from a degassed state to maximum inflation. Second, End Expiratory Pressure (EEP) was progressively decreased from maximum inflation to zero pressure with constant tidal volume. This experiment showed that additional energy is required to recruit collapsed lungs, but that once recruited, it required less energy to re-inflate to the same volume. They also concluded that recruitment and derecruitment is strongly dependent on EEP, as a result.

Crotti et al. [2001] utilised CT scans on ALI/ARDS patients to capture recruitment status of the lungs. They first proved that the PV curve derived from CT images correlates well with a traditional quasi-static super syringe technique. According to the study, recruitment occurs throughout the inflation limb with no correlation to LIP or UIP, and that this recruitment curve parallels that of volume. Pelosi et al. [2001] reached similar conclusions using the same CT technique on dogs with induced respiratory failure.

Carney et al. [1999] used *in vivo* microscopic cameras to capture alveoli dynamics visually during tidal ventilation. This study showed that once recruited, the alveoli showed no significant change in size with increasing pressure. Furthermore, the total lung PV curve also did not correspond to isotropic balloon-like expansion of alveoli, but rather with the number of recruited alveoli. They thus concluded that most of volume change in the lung therefore occurs by recruitment and derecruitment, and not by balloon-like expansion.

Schiller et al. [2003] extended the *in vivo* microscopic studies to include surfactant deactivated injured lungs using pigs. They also observed that normal healthy alveoli do not expand as pressure is increased, and that there is no correlation between recruitment and LIP or UIP. However, surfactant deactivation caused significant change in alveoli characteristics, especially in recruitment and derecruitment timing. They concluded that a normal healthy lung does not expand by isotropic expansion of alveoli. Furthermore, surfactant deactivation significantly altered the recruitment and derecruitment characteristics of alveoli.

New Theory

None of the studies fully explain the entire mechanics of the lung. However, they all lead to similar facts and conclusions:

- Recruitment and derecruitment occurs continuously throughout the breathing cycle and contributes significantly, if not primarily, to the volume change observed/measured in PV curves.
- LIP and UIP do not correspond to points of massive recruitment or derecruitment of alveoli. This result is in counterpoint to the above point.
- Once recruited, healthy alveoli do not change in size as pressure is increased, contributing very little to the volume change. Hence, volume change is not a result of isotropic, balloon-like expansion.

Thus, a summary of the new hypothesised mechanics of the lung under mechanical ventilation, as presented and used in this thesis, is as follows:

1. From atmospheric pressure the air first enters the major airways and the topmost region of the lung, where there is no effect from superimposed pressure. This initial stage yields relatively small volume increase, thus resulting in low compliance.
2. As more air enters the lung, the pressure starts to increase and the alveoli in the dependent region start to "pop" open as the pressure overcomes the superimposed pressure in that region. As pressure increases and overcomes the superimposed pressure in the lower regions, more alveoli are recruited progressively and add a certain volume to the total.

Thus, lung volume keeps increasing until all the recruitable alveoli are opened or maximum pressure in the breathing cycle is reached. Figure 2.4 illustrates a schematic comparison of traditional and new theories on lung mechanics.

The first stage of inflation yields a relatively small volume increase, thus resulting in low apparent compliance on the overall PV curve. As recruitment of

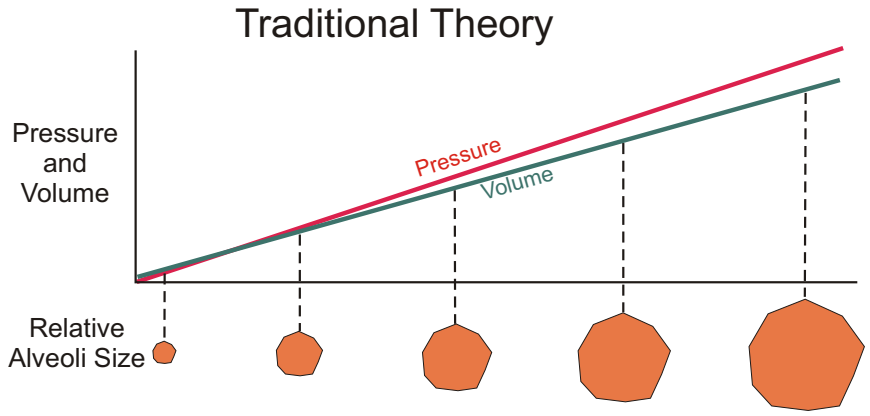

(a) Traditional theory on lung mechanics. No threshold opening pressure.

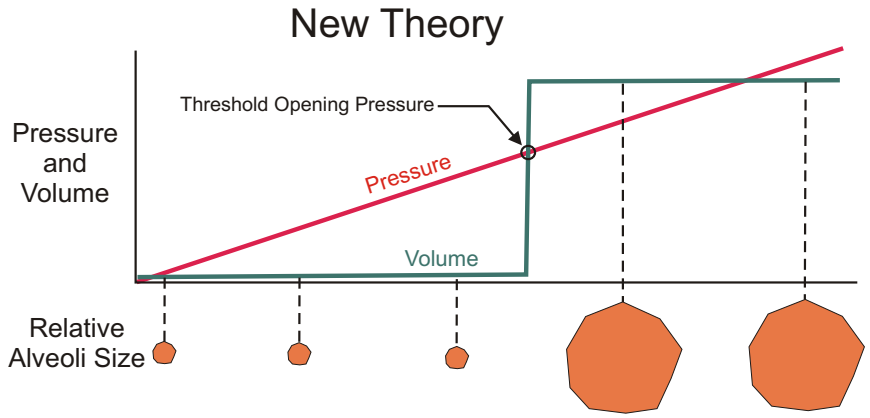

(b) New theory on lung mechanics. Alveoli "pop" open once a threshold pressure is reached.

Figure 2.4 Traditional vs. new theory of lung mechanics. (a) Traditionally, the lung was thought to expand by isotropic expansion of alveoli. As shown on the illustration, the volume increase parallels the pressure increase. (b) New theory suggests that the lung expands by sudden recruitment of alveoli at threshold (opening) pressure. The alveoli is collapsed until the sufficient pressure is reached to recruit the alveoli. Once recruited, the alveoli do not change in size significantly.

alveoli begins, the lung volume increases rapidly and the associated compliance increases. Once all the recruitable alveoli within reasonable breathing cycle pressure are recruited, the rapid volume increase ceases and the effective compliance thus decreases.

The deflation process is the same as inflation, but in reverse. However, the pressures at which the alveoli are derecruited are lower than their recruitment pressure. The result of this difference is the observed hysteresis in the overall lung PV curve.

Limitations

This new theory of recruitment and derecruitment as a primary mechanism is not unchallenged. Martynowicz et al. [1999; 2001] conducted a study using parenchymal marker techniques to measure the regional volume directly. The study found that the regional dimension did not change at end expiration even in the most dependent region of the lung. Based on these findings, they proposed a different mechanism of liquid and foam in airways, rather than recruitment and derecruitment.

This difference in the hypothesised mechanism has not yet been resolved. It is possible that a combination of the 2 mechanisms occurs in the ARDS lung [Mols et al., 2006], and that the results are difficult to distinguish, since both theories produce the same PV curves. However, some evidence of recruitment and derecruitment of lung units, such as the *in vivo* microscopic study with associated video evidence [Schiller et al., 2003] is difficult to ignore.

2.2.3 Recruitment and Derecruitment

All of these recent studies suggest that the recruitment and derecruitment plays a significant role in clinically observed overall lung mechanics. Several studies have shown that most of the volume change occurs by recruitment and derecruitment of lung units. This mechanical understanding is especially important in analysing abnormal lungs, such as in the case of ARDS.

One of the reason ARDS is such a devastating disease is that oedema and inflammation causes lung units to collapse from the additional weight. These collapsed units cannot be recruited within a "normal" clinically applied pressure range. Because the collapsed lung unit cannot transfer gases to blood, this causes a significant reduction in the ability of the body to take up oxygen and release carbon dioxide. This dysfunction thus results in a potentially devastating consequence to the already compromised condition of a critical care patient.

Because of the changed lung physiology from fluid build up and increased weight, ARDS greatly affects the characteristics of recruitment and derecruitment. As a result, overall lung mechanics are skewed from normal. The lung

mechanics are then further altered due to resulting surfactant abnormality, which causes alveolar instability [Halter et al., 2003; McCann et al., 2001] and further inability of the lung to function normally.

The *in vivo* microscopic study by Schiller et al. [2003] not only supported the new hypothesised lung mechanics, and the roles of recruitment and derecruitment, but also showed the fundamental difference between healthy and ARDS lung units. The study concluded that there are 3 types of alveoli depending on the level of injury. Type 1 alveoli do not collapse at the end of expiration and do not change volume significantly during tidal ventilation, and are thus healthy. Type 2 alveoli change volume significantly during tidal ventilation, however they do not collapse at the end of expiration. Type 3 alveoli change volume significantly and collapse completely at the end of expiration. In the normal undamaged lung, all of the alveoli present are healthy, Type 1. However, after surfactant deactivation, all 3 types were present in a single lung indicating that Type 2 and Type 3 alveoli are associated with injured lungs, as in ARDS. This *in vivo* microscopic study thus showed the heterogeneous nature of lung injuries, as well as the differences in injured and healthy lung mechanics at alveoli level.

TOP and TCP

Inflation and deflation of the lung is characterised by the pressure levels at which recruitment and derecruitment occur. The pressure at which a lung unit is recruited is called its Threshold Opening Pressure (TOP). The pressure at which the lung unit is derecruited is called the Threshold Closing Pressure (TCP).

Since recruitment and derecruitment occurs throughout the breathing cycle, the TOP and TCP are widely distributed along pressure, rather than at the LIP and UIP as traditionally assumed. These threshold pressures are influenced by many physical factors, such as superimposed pressure, condition of surfactant, oedema, inflammation, etc. As a result, the distribution of TOP and TCP across or over a range of imposed pressures are unique to a patient and the condition.

Pelosi et al. [2001] conducted an experiment using dog models with induced lung injury using oleic acid. Each dog was ventilated with different combination of PEEP and tidal volume, and the effect of pressures on recruitment and derecruitment were investigated using CT scans. They concluded that recruitment

occurs continuously along the PV curve, and that the superimposed pressure plays a significant role in the timing of regional recruitment. Their estimated opening pressure was normally distributed over pressure, and it was found that the amount of recruited lung units at the end of inspiration and at the end of expiration were highly correlated. This result also suggests that the more units that are recruited at the end of inspiration, the greater the number of units that remain recruited at the end of expiration. Other studies have found similar results to validate these findings [Halter et al., 2003; McCann et al., 2001; Schiller et al., 2003].

Crotti et al. [2001] also reached a similar conclusion in clinical studies with ALI/ARDS patients, and also showed that both TOP and TCP are normally distributed. Figure 2.5 illustrates examples of their results clearly showing normally distributed TOP (right plots) and TCP (left plots) over pressure. Note that the mean of the TOP distribution is higher than that of TCP, indicating the different opening and closing pressures that result in the hysteresis observed in PV loops.

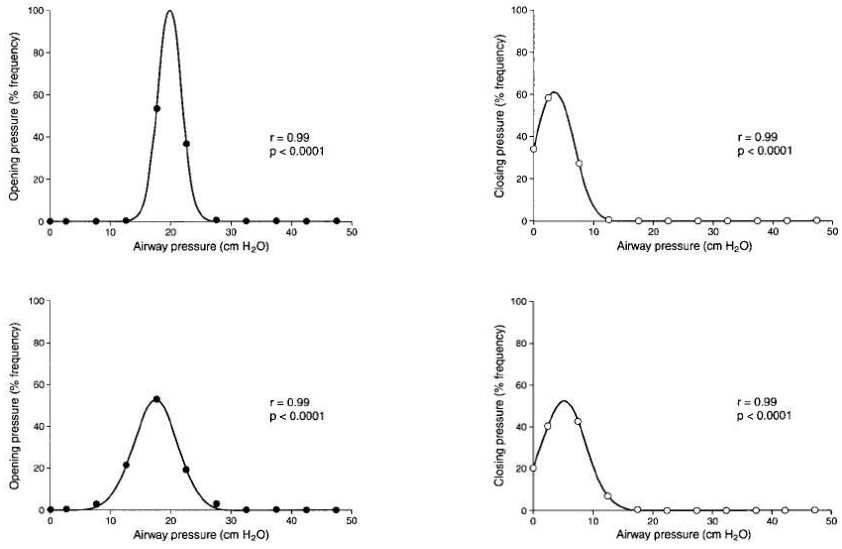

Figure 2.5 Examples of clinical TOP and TCP distributions. The CT scan was used to determine the recruitment status during the breathing cycle and the TOP and TCP distribution was estimated from the result. The left plots show estimated TOP and the right plots show estimated TCP distributions for 2 different clinical data. [Crotti et al., 2001]

Normal vs. ARDS Lungs

Since the distribution of TOP and TCP are a direct result of lung mechanics, they can be used as an indication of the patient's lung condition. The shape and the value of the distribution directly and uniquely reflect the condition and

status of the lung. Because ARDS lungs are affected from many physiological dysfunctions, such as inflammation, oedema and surfactant abnormality, these lungs react differently to pressure changes compared to normal lung. This difference can be clearly captured by the shape of the TOP and TCP distributions.

Due to the increased weight and stiffness of ARDS lungs, the lung units tend to open at higher pressure compared to the normal lungs. This delay in recruitment over pressure, as well as the heterogenous characteristic of ARDS, can be represented by a broader and shifted distribution of TOP, indicating the higher pressure to achieve the same volume, as illustrated by the schematic drawings in Figure 2.6. Similarly, these lung units tend to collapse at higher pressure during expiration, which also shifts the TCP distribution to higher pressure. The heterogeneous nature of the lung disease also contributes to the broadening of the TCP distributions. Because of these significant differences, it may be possible to quantify the severity of lung injury from the threshold pressure distributions, particularly once enough clinical data is collected for a database.

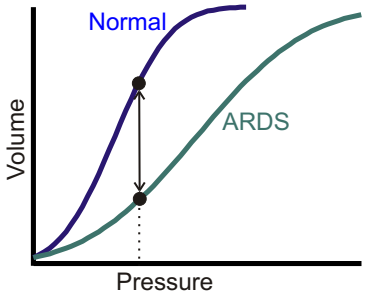

(a) An example of PV inflation curves for normal and ARDS lungs.

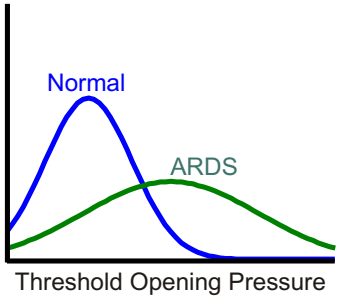

(b) An example of TOP distributions for normal and ARDS lungs.

Figure 2.6 (a) ARDS affected lungs are stiffer than normal lungs, thus the volume is considerably smaller at the same pressure, as indicated by the arrow. (b) The stiffer lung is represented by a broader threshold pressure distribution.

2.2.4 Other Mechanisms and Mechanics

The total respiratory system mechanics are not only those of recruitment and derecruitment, but a combination of many physiological components. Most of them are difficult to distinguish from others, especially with current practice and the equipment readily available in the ICU. However, some consideration on their contribution is required for a more complete model of ventilated lung mechanics.

Visco-Elasticity

Just as other human physiological soft tissues, lung tissues can stretch, especially at the distal airways of the bronchiole where there is no cartilages in the walls [Vander et al., 2001; Sebel et al., 1985]. This elasticity also contributes to the total expansion of lungs, and thus total lung mechanics. The exact amount of its contribution, however, is not known. The stretching of the lung tissue also contains viscose characteristics, where some of the deformation remains after each cycle. This effect is analogous to a balloon, where it is easier to inflate the second time because the material has already been significantly stretched previously.

Chest Wall Compliance

The chest wall consists of the rib cage and other tissues and cartilages that surround the lungs. It is separated from the lung by pleural membranes and a thin layer of fluid, and has its own pressure volume dynamics. This separate mechanism may create difficulty in interpreting the PV curve, because the effect of the chest wall can mask the true lung mechanics.

Several studies have been conducted to quantify the compliance and the effect of the chest wall in ventilated patients [Albaiceta et al., 2004; Karason et al., 1999; Mergoni et al., 1997; Pereira et al., 2003]. The chest wall generally shows higher compliance, compared to the lung. The relative compliance of the chest wall is especially higher in injured lungs because of the increased stiffness of the lung. However, other conditions, such as obesity and external injuries, can also alter the characteristics of chest wall. Such conditions may contribute a significant role in total respiratory mechanics [Pelosi et al., 1996a].

It is therefore essential to determine the effect of the chest wall on the total respiratory system if the true lung mechanics are to be determined. In spite of this issue, measurement of chest wall compliance is not a standard protocol in ICU. One method to determine the chest wall compliance is to estimate the pleural pressure using an oesophageal pressure measurement [Karason et al., 1999]. Measuring oesophageal pressure is easier and less invasive compared to measuring the pleural pressure directly. However, the method still requires additional equipment, and introduces additional invasive measures to the patients, thus it may not be always available. In addition, oesophageal pressure measures only

one pressure point, thus it does not take into account the thoracic pressure gradient. Therefore, the data it provides may not be clinically significant, and the additional clinical burden that it can cause may not be welcome.

2.2.5 Impact of MV

The mechanical ventilator can assist patients to breathe or take over the work of breathing when they are having difficulty achieving the desired results on their own. This treatment is an essential part of a critical care practice, and is widely used in the ICU, particularly for relatively heavily sedated patients. Significant numbers of patients are fully dependent on the ventilator to enable transfer of vital gases [Dasta et al., 2005; Walsh et al., 2004].

The ventilator works to reduce the work of breathing required by the patient by applying positive pressure to the airway. PEEP is applied to maintain the lung volume at the end of expiration, which thus reduces the collapse of lung units and maintains the amount of functional lung units, enabling sufficient gas transfer. However, even optimally controlled ventilators can cause harm to the lungs. There is a fundamental difference in the breathing process between normal active lungs and mechanical ventilation. For a healthy person who is breathing on their own, the lung is inflated by negative pressure, as the chest cavity is expanded by breathing muscles. However, under mechanical ventilation, the lung is inflated by positive pressure applied by the ventilator.

This fundamental difference can cause unnatural iatrogenic complications in the patients' lungs. In normal healthy lungs, the lung units do not experience positive pressure. Breathing under mechanical ventilation, the patient experiences positive pressure, and often does so continuously. An excess of positive pressure can cause further injury to the lung units, or barotrauma [Bersten, 1998; Dreyfuss and Saumon, 1998]. Healthy lung units are relatively compliant and thus can deal with moderately elevated pressure. However, the already injured lung units, such as in ARDS, are more vulnerable to further damage by high pressure due to altered mechanics and physiological factors, such as surfactant depletion [Dreyfuss and Saumon, 1998].

Mechanical ventilation is often life saving. However, sub-optimal ventilator setting can harm the patient. Hence there is a need for careful balance and trade-off. Ideally, the pressure is kept high to maximise the functional lung volume. On the other hand, too much pressure causes over inflation and undesirable further injury to the lung results.

In many cases, the end expiratory collapse and over-inflation occurs in the same breathing cycle as healthy lung units are exposed to too much pressure and damaged units receive too little to be recruited. This difficult situation arises due to the heterogeneous nature of lung injuries where the lung is a mixture of healthy and damaged units. This situation is further hindered by the lack of a clear understanding of the lung mechanics, as well as the lack of a method or ability to determine the exact lung status or condition of an individual patient in critical care.

2.3 The Hickling Model

Hickling [1998; 2001] developed a simple mathematical model based on recruitment and derecruitment using TOP and TCP. The model was developed as an analytical model. However, it uniquely captured the simplified features of lung mechanics as discussed here. Hickling's model effectively showed the relation between the PV curve and recruitment status, as well as the effect of PEEP and Vt, and ventilator strategy. The model used in this research and presented in this theisis was originated in part from Hickling's model.

Hickling's model is based on simplified lung physiology. It mathematically shows that recruitment and derecruitment contribute greatly to the total lung mechanics, supporting the new theory of lung ventilation presented. He went on further and demonstrated the model's ability to simulate different ventilator protocols and showed that end-inspiratory pressure and the resulting end-inspiratory volume have a great effect on lung recruitment and subsequent tidal ventilation.

2.3.1 Description

Hickling's model contains most of the essential elements of lung mechanics described. It is based on the fact that recruitment and derecruitment contribute greatly, if not primarily, to lung inflation and deflation. The lung is modelled as clusters of lung units, which are distributed into compartments of different superimposed pressures. The lung volume at a given pressure is determined by the combination of the unit compliance equation, lung unit TOP or TCP distribution, superimposed pressure, and applied airway pressure.

There are two mechanisms of volume change in this model: 1) individual lung units, or alveoli, compliance and 2) recruitment and derecruitment of lung units. Individual unit compliance is described by a linear pressure-volume relation with a slight modification at high pressure in the initial model [Hickling, 1998], and a Salazar and Knowles equation in the later model [Hickling, 2001]. Recruitment and derecruitment were governed by TOP and TCP distributions. These pressures were uniformly distributed in the initial model, and normally distributed in the later model.

The lung is modelled as a group of lung units, representing alveoli. Each lung unit is associated with an individual compliance. These lung units are divided into compartments with different superimposed pressure, representing horizontal slices of the lung. Superimposed pressure is an additional pressure applied to the lung units by the gravitational force of the lungs above it. Therefore, the upper compartment is affected the least and the bottom compartment is affected the most by the superimposed pressure. The pressure is distributed linearly across these compartments.

Simulation is done by calculating the effective quasi-static volume at each airway pressure increment. For inflation, the model determines whether the applied pressure to each lung unit (airway pressure - superimposed pressure) at each pressure increment is higher than the assigned TOP. If the pressure is higher than the assigned TOP, the unit is recruited and assumes a volume according to the unit compliance equation. For deflation, the applied pressure is checked against TCP, and if the TCP exceeds the applied pressure, the unit is derecruited and assumes a volume of zero. Thus, as a pressure range is traversed up (inspiration) and down (expiration) a lung volume is obtained at each step, creating the overall lung PV curve.

2.3.2 Limitations

The model's simplicity allows clear understanding of the fundamental lung mechanics. However, to keep it simple, the model makes several assumptions that are not fully verified clinically. For example, the values of the TOP and TCP distributions used were selected a priori based on a few studies and reasonable estimates. Thus, it is not particular to or specifically estimated for a given patient in a clinical situation. The model has also ignored other components and effects, such as visco-elastic time dependence and the effect of chest wall compliance. Hence, it does not, for example, fully capture the recruitment effects due to increasing PEEP.

The model was also developed using standard reported values for lung mechanics. Thus, it can be used as an analysis tool, but cannot be applied directly in clinical situations. Clinically, the patients' PV curves are unique to the patient and their specific condition. Thus, the variables and their governing equations need to be flexible and identifiable, which is not the case here. Finally, this model is designed to simulate static PV curves, which are not easily or routinely measured at bedside in critical care.

2.4 Summary

The total mechanisms and mechanics of the lung are a result of the collaboration of several different components. This mechanism is individually unique to each patient and their condition at a given time, and is reflected in these patient specific PV curves. The PV curves can be measured easily at bedside in critical care with modern ventilators. Any model to be used clinically needs to capture and identify these unique characteristics, using fundamental lung mechanics.

The lung mechanics modelled here are based on a newly hypothesised mechanical theory. Traditionally, lung inflation was thought to occur by isotropic balloon-like expansion of alveoli. However, there were mismatches between clinical observation and this theory, and some trends that could not be explained by the traditional theory. Recent studies suggest a new theory, where most of the volume change in lung occurs by recruitment and derecruitment of alveoli and distal airways.

The first evidence of this mechanism was the continuous recruitment of alveoli or lung units. Traditionally, the LIP was thought to be the limit of recruitment. However, various experiments with incremental PEEP [Jonson et al., 1999; Cheng et al., 1995] showed continuous recruitment above LIP. CT scans were also used to capture this continuous recruitment status of the lungs [Albaiceta et al., 2004; Crotti et al., 2001; Gattinoni et al., 2001; Pelosi et al., 2001]. These experiments showed that recruitment occurs throughout the breathing cycle, well above LIP, and the volume increase paralleled the recruitment of lung units, as seen on CT scans.

This new theory was further strengthened by the *in vivo* microscopic experiments by Carney et al. [1999] and Schiller et al. [2003], observing the moments of recruitment and derecruitment of alveoli. These studies also showed that once recruited, the healthy alveoli did not show a significant volume increase with increase in pressure. In other words, the expansion of an alveolus did not correlate with total lung volume change. Instead, once a certain pressure is reached, the alveoli "pop" open to a relatively fixed volume and do not significantly expand further.

The new theory suggests that lung mechanics are governed by the pressures at which the lung units are recruited and derecruited. The pressure at which the lung unit is recruited is called the Threshold Opening Pressure (TOP) and the pressure at which the lung unit is derecruited is called the Threshold Closing Pressure (TCP). Each lung unit is associated with a specific TOP and a TCP. The value of these pressures depends of several different factors, such as superimposed pressure, presence of oedema, inflammation, and condition of lung unit's surfactant.

In the case of acute lung injuries, such as ARDS, the abnormality in the lung unit causes an increase in these threshold pressures, which in turn increases the work of breathing. Mechanical ventilation assists a patient with breathing difficulty by reducing or eliminating the work of breathing required from the patient. However, even when optimally operated, a ventilator can cause harm due to the unnaturally high pressure that may be required to sufficiently ventilate a patient. The evaluation of optimal ventilation is further complicated by the heterogeneity characteristic of the lung injury, leading to heterogeneous mixture of healthy and injured lung units exposed to the same elevated pressure. A final

additional complication is the concomitant lack of a complete understanding of the lung mechanics.

Finally, Hickling [1998; 2001] has developed a simple mathematical model of the lung, utilising a portion of this new theory of lung expansion. His model captures the basic characteristics of lung mechanics using simple components, each representing a physiological component. The model simulated the relationship between pressure, volume, and the recruitment status of the lung units, and demonstrated its ability as an analytical tool for assessing ventilator strategy. However, it has limitations, in particular, an inability to be made patient specific for use in clinical situations.

Part II

Models and Methods

Chapter 3

Physiological Model Components

This chapter presents the lung model elements utilised in this study. Each component is described relative to the basic lung physiology. The physiological and/or clinical significance of the model component parameter is also presented.

3.1 Model Overview

The lung is modelled as a group of individual lung units. A lung unit represents a small cluster of alveoli and/or distal airways. The number of these units in the model can be increased or decreased, depending on the desired resolution. The model can also includes the effect of superimposed pressure in different lung strata. Figure 3.1 provides a schematic overview of the lung model.

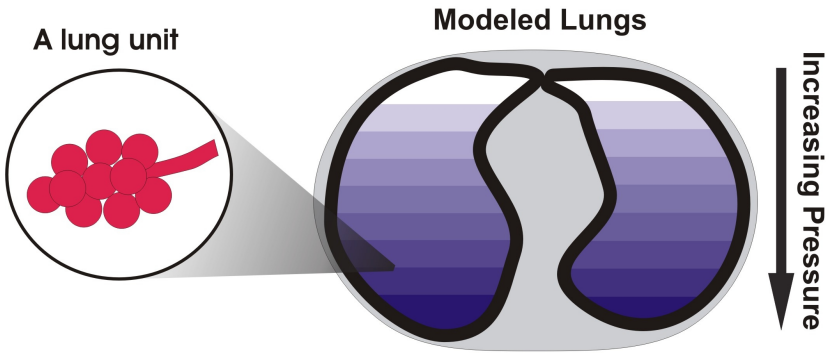

Figure 3.1 An overview of the lung model. The lung is modelled as a group of lung units, which represent distal airways and a cluster of alveoli. The superimposed pressure can be simulated by distributing the lung units into compartments representing horizontal slices of the lung. Each compartment is associated with a different superimposed pressure.

The superimposed pressure is simulated by having several compartments, representing horizontal slices of the lung. Each of the slices, or compartments, is associated with a different superimposed pressure, depending on its relative location. For example, the compartment representing the uppermost region of the lung experiences the least amount of superimposed pressure and the compartment representing the bottommost region experiences the most. Lung units are distributed evenly in all the compartments, and the number of compartments used is based on the model accuracy or resolution required.

Each lung unit has an associated threshold opening pressure (TOP) and a threshold closing pressure (TCP). These critical pressures govern the recruitment status of that lung unit. Once the pressure in the compartment exceeds the TOP of that unit, the unit is recruited. Similarly, on expiration, when the pressure falls below the TCP, the unit collapses or is derecruited. The TOP and TCP can be different for each lung unit. They are thus recruited and derecruited at different pressures. As a result, the threshold pressures can be widely distributed across a wide range of pressures. The difference between TOP and TCP causes hysteresis in the overall PV curve based on the hysteresis in each unit.

The exact values of TOP and TCP for each unit are defined one of two ways. First, they may be identified from measured PV loop data. This approach will be presented in detail in Chapter 5. Second, they can be preassigned based on generic distributions similar to those observed clinically, such as that of Crotti et al. [2001] in Figure 2.5. In either case, these values may be realistically obtained for use in simulation analysis.

The model simulates the lung mechanics by calculating the volume at each pressure point. At each pressure increment, the model determines the amount of recruited lung units from the TOP distribution. The number is then multiplied by the appropriate unit volume according to a unit compliance curve. The result is the volume of the lung at that particular pressure. Similarly, during deflation, the model determines the number of recruited lung units from the TCP distribution, and the appropriate volume is determined.

3.2 Major Components and Parameters

The model consists of 2 different fundamental components: 1) unit compliance, and 2) threshold pressure distribution. Unit compliance describes the compliance of recruited lung units, where each pressure point is associated with a volume. Threshold pressure (TOP and TCP) distributions describe the recruitment status of lung units. Thus, these distributions govern the number of recruited lung units at any given pressure. Each component is described by a governing equation, and the variables of the equation are used to uniquely identify the parameters. These components are combined in calculation and quasi-static simulation to produce total lung mechanics and PV curves.

3.2.1 Unit Compliance

Unit compliance describes the volume of a recruited lung unit. It is essentially the compliance of a single recruited lung unit, and determines the volume of that unit at any given pressure. The unit compliance is only applicable to recruited units, because derecruited lung units have a volume of zero based on the recruitment mechanics theory presented in Chapter 2. However, when the pressure reaches a specific unit's TOP, the unit is recruited and the unit compliance then determines the volume that the newly recruited unit assumes for all pressures above TOP, and back down, during expiration, to its TCP.

Physiologically, the unit compliance represents the elastic component of modelled lung unit mechanism. The curve is described by a basic sigmoid shape, where it inflates in three phases: low slope at a low and high pressure and high slope in the middle. The shape is analogous to inflating a balloon, where initially the pressure increases without much increase in volume. Once the pressure reaches a sufficient level, the balloon suddenly increases in volume with relatively small additional pressure. This phase is associated with the middle, high slope phase. Once the volume reaches near its maximum, the elastic material is fully stretched and will appear less compliant, and increases in volume cease rapidly with any increase in pressure, resulting in a second low slope phase.

In lung units, the elasticity is governed by surface tension, surfactant, and the mechanical characteristics of lung tissues. Since the lung unit consists of soft tissues, it has an elastic aspect. However, this model is based on the hypothesis that recruitment and derecruitment are the main mechanism of lung volume change. Therefore, the unit compliance has a very small contribution to the total volume change.

The compliance curve employed is described by 4 parameters: minimum (min), maximum (max), curvature, and mean. Min and max describe the initial and final volume within the total possible pressure range. Curvature governs the slope of the middle section, and the mean governs where the maximum slope occurs. Physiologically, the minimum value is the smallest possible volume, or Functional Residual Capacity (FRC), for a recruited lung unit. The maximum is the largest possible volume for a recruited lung unit at any pressure over TOP. This maximum value, thus, also determines the maximum possible total lung volume. The curvature determines the rate of inflation and the mean determines the pressure range of the high compliance section, where the majority of volume change occurs in recruited units.

The basic shape of the curve can be described using a sigmoid equation. However, the actual equation used in this model is slightly different depending on the version of the model. The sigmoid equation is defined:

$$V(p) = \frac{a}{1 + e^{[b(-p+c)]}} + d \tag{3.1}$$

where V is volume, p is pressure, d is the min, a is difference between min and max, thus $a + d$ is max, b is the power for the curvature, and c is the mean. Figure 3.2 shows an example of a unit compliance curve and its features.

Although it takes 4 parameters to describe the unit compliance, these parameters do not need to be varied in most simulations in order to fit the clinical data. It is unlikely that the unit compliance at alveolar level varies significantly, physiologically. Furthermore, because unit compliance plays a minor role in the total lung mechanics in this model, as compared to recruitment alone, the influence on the simulated result from the unit compliance is small. This point can be represented by the fact that, physiologically, the variable d is significantly larger

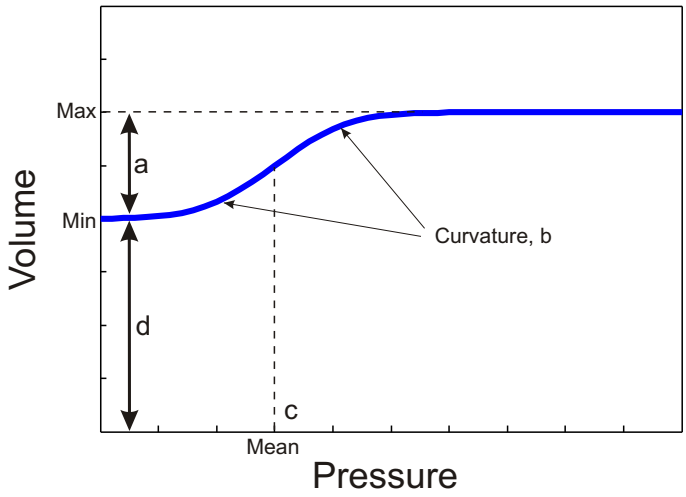

Figure 3.2 The unit compliance is described by the basic sigmoid shape having 4 basic parameters: Min, Max, Mean and Curvature. Each parameters describes a unique feature of the curve. The unit compliance represents elastic component of the lung mechanism.

than a, suggesting that, as presented in Chapter 2, most of the volume change occurs due to the recruitment of lung units. Therefore, these parameters can often be fixed to a predetermined global population constant for all patients, or fixed for a patient after an initial fitting to clinical data.

3.2.2 TOP and TCP

Each unit in this model has only two possible states: 1) recruited and 2) derecruited. This recruitment status is described and governed by the unit specific TOP and TCP. When applied pressure during inflation reaches TOP, the unit "pops" open and stays recruited as long as the applied pressure is above TOP. When applied pressure falls below TCP during deflation, the unit collapses and assumes a volume of zero. Thus, if the maximum applied pressure during inflation is lower than TOP, the unit is not recruited during the tidal ventilation, and thus does not contribute to volume change. Similarly, if the TCP of the unit is lower than the pressure at the end of expiration (PEEP) the unit does not collapse and its volume only changes according to the unit compliance curve during subsequent tidal ventilation.

Figure 3.3 shows a schematic plot of single unit mechanics. At the beginning of inflation, the unit is derecruited, and has a volume of zero. As the pressure

increases during inflation, the unit is derecruited until the pressure reaches TOP. At TOP the unit is recruited and assumes a volume according to the unit compliance curve. It then follows the compliance curve until the end of the inflation limb. On the deflation limb, the unit volume follows the unit compliance curve as pressure decreases. At TCP, the unit is derecruited and the volume becomes zero, and remains derecruited.

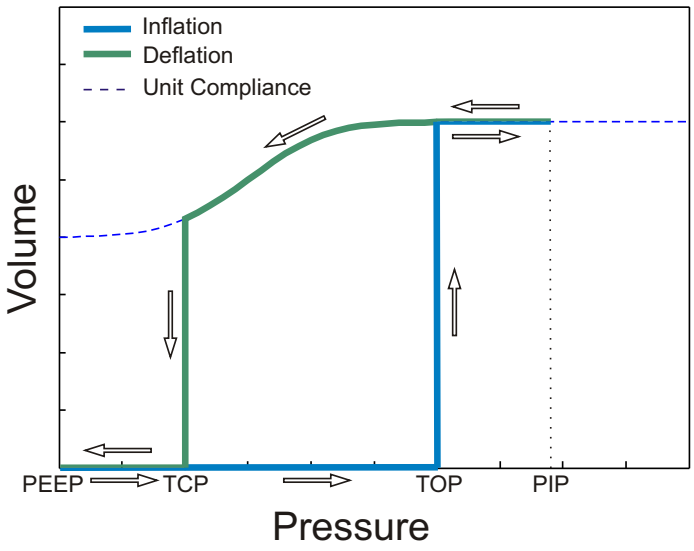

Figure 3.3 An example of a single unit PV mechanism from zero to PIP. The unit is derecruited at the beginning of inflation. When pressure reaches TOP, the unit is recruited, and inflates to a volume determined by the unit compliance. The unit volume follows the compliance until PIP. During deflation, the unit follows the compliance until the pressure reaches TCP. At that point, the unit is derecruited, and the volume becomes zero.

There are many physiological factors upon which TOP and TCP depend. These factors include: surface tension, inflammation, oedema, and surfactant condition. Physiologically, each lung unit may thus react differently to an applied pressure, especially in ARDS. This behaviour is clearly seen in the *in vivo* microscopic study, showing different alveoli types heterogeneously distributed in a single lung [Schiller et al., 2003]. Accordingly, each lung unit has unique TOP and TCP values, and the severity of the lung disease, such as ARDS, greatly affects these values.

TOP describes inflation and TCP describes deflation. During mechanical ventilation, the inflation process is performed by applying pressure in a controlled manner until a desired volume or pressure is reached. In contrast, during the deflation process the ventilator simply reduces the pressure to PEEP all at once, releasing the air passively from the lung.

The phase change between inflation and deflation is rapid, and each phase uses separate mechanics. These phases can thus be viewed as completely separate processes and treated as such. This separation also simplifies model simulation by having entirely separate calculations for the inflation and deflation portions, which are governed by the TOP and TCP, respectively.

3.2.2.1 Threshold Pressure (TP) Distributions

The recruitment of lung units do not occur at once, rather it is widely distributed over a pressure range. There are several factors that contribute to this distribution, such as varying superimposed pressure within the lung and heterogeneous characteristics of lung units. This distribution essentially determines the overall characteristics and the mechanics of the lung, and thus the shape and values defining the distribution uniquely reflect the lung condition.

One of the major determinants for the shape and values of threshold pressure distributions is the superimposed pressure. It accounts for the additional pressure within the lung caused by the weight of the lung itself. Thus, the applied airway pressure must be sufficiently high to overcome this additional pressure, as well as the TOP for a lung unit to be recruited. This additional pressure can be simplified using the concept of hydrostatic pressure, which increases linearly with height. This simplification is valid as long as the density is relatively uniform throughout the lung [Gattinoni et al., 2001], which is the case assumed here.

The superimposed pressure increases linearly from top to bottom. Thus, the pressure required to overcome the superimposed pressure is also linear. Therefore, the TP distributions resulting from the superimposed pressure alone is uniform for both TOP and TCP. However, the actual distribution is not uniform due to other factors, such as heterogeneous lung units. As Schiller et al. [2003] have shown in their *in vivo* microscopic study, a lung consists of different unit types even within the same lung region. This effect is especially prominent in the ARDS affected lung. Thus, the individual lung units have a different recruitment and derecruitment timing, even when they experience the same superimposed pressure. This heterogeneous behaviour also contributes to the wide distribution of threshold pressures in a lung region.

Over an entire lung, the typical PV curve can be seen as a cumulative density distribution function for the TOP and TCP distributions. Therefore, the TP distributions can be seen as normal probability density distributions. Physiologically, this distribution has been validated in clinical studies using CT scans [Crotti et al., 2001; Pelosi et al., 2001].

Therefore, this model uses normal probability density (Gaussian) distributions to describe the threshold pressure distributions for TOP and TCP. This distribution is well known and the equation is simple to use. Hence, it is easy to manipulate and adapt to most desired shapes and values without significant computational or mathematical complication. The equation for the Gaussian distribution is

$$N(P) = \frac{1}{SD\sqrt{2\pi}} e^{-\frac{(P-\mu)^2}{2SD^2}} \tag{3.2}$$

Where N is the number of units, P is pressure, μ is the mean, and SD is standard deviation. An example plot of the distribution is shown in Figure 3.4, indicating the two main parameters that determine its shape over the range of pressure.

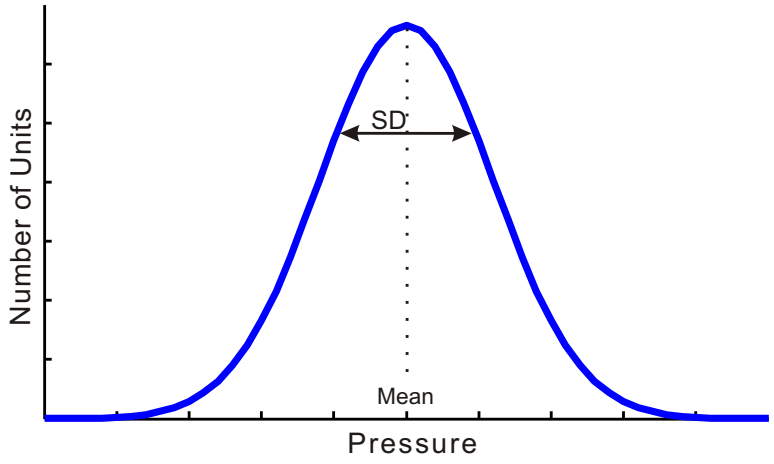

Figure 3.4 An example of normal (Gaussian) distribution of threshold pressure. The distribution is described by Equation 3.2, basically using 2 variables: μ, mean, and SD, standard deviation. It describes the number of units recruited and derecruited at each pressure for TOP and TCP, respectively.

3.2.2.2 Parameters

The normal probability density distribution in Equation (3.2) requires 2 parameters to describe its shape: mean and standard deviation.

Mean

The mean in the Gaussian distribution is simply where the maximum value occurs. In the TOP distribution, the mean indicates the pressure at which the maximum rate of recruitment occurs during inflation. Thus, this pressure yields the maximum compliance. Similarly, in the TCP distribution, the mean indicates the maximum rate of derecruitment during the passive expiration cycle of the ventilated patient.

Mean: Healthy vs. ARDS - Physiological Meaning

ARDS affected lungs are stiffer overall, and require higher pressure to inflate to the same volume compared to a healthy lung. This difference in pressure can be represented in the TOP distribution by shifting the mean toward higher pressure. The resulting PV curve is thus also shifted towards higher pressure. In terms of the total lung mechanics, this shift results in reduced volume at a given pressure compared to a healthy lung.

Figure 3.5 shows the effect of shifting the mean on the PV curve, simulating a stiffer lung or ARDS lung. The resulting PV curve also shifts towards higher pressure, reducing the volume at any given pressure. The net result is that aerated or recruited lung volume is reduced in the pressure range in which healthy lung units are recruited. Note that, as discussed in Chapter 2, simply increasing the pressure to recruit more ARDS or injured lung units could also damage the healthy units that were already recruited at much lower pressure.

Standard Deviation (SD)

The standard deviation (SD) describes the shape or tightness of the distribution. Lower SD values result in distributions with higher more prominent peaks and narrower width. Higher SD values result in broader distributions. Mathematically, SD represents the spread of the lung units population for TOP and TCP.

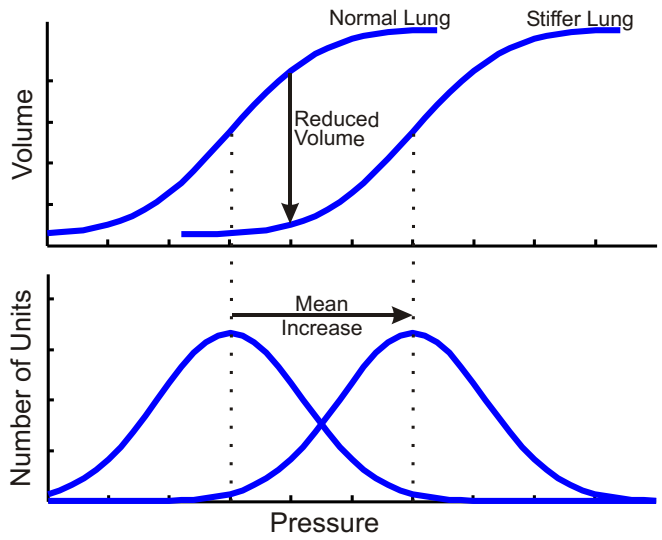

Figure 3.5 An example of the effect of increasing mean. The stiffer lungs can be represented by increasing the mean of the distribution. This increase results in the shift of entire PV curve towards higher pressure. The overall effect on the total lung mechanics is the reduced volume at the same pressure.

In a normal distribution, about 68% of the population is within one standard deviation of the mean and 99.7% is within 3 standard deviations.

In terms of the TOP distribution and the PV curve that results, low SD yields a higher maximum compliance, and a high SD yields low maximum compliance. More specifically, a low SD and tight distribution indicate rapid recruitment with pressure, resulting in higher compliance. A large SD yields the opposite result. Hence, SD will also reflect the patient condition, or vice versa.

SD: Healthy vs. ARDS - Physiological Meaning

ALI, such as ARDS, does not affect the entire lung the same way. As the study by Schiller et al. [2003] showed, alveoli with various levels of injury appear in the same region of the lung, and even in the same microscopic field. However, the injured lung units are recruited at higher pressure, while the healthy units are recruited at a normal pressure. The resulting PV curve has lower overall compliance and broader TP distributions as a result of the injured lung units. Thus, this heterogeneous characteristic of lung disease is represented in this model by larger SD values.

Figure 3.6 shows an example of the effect on the PV curve of an increased SD in TOP distribution. In this case, the mean is also shifted to account for the fact that no recruitment will occur at a pressure lower than that of a normal lung distribution, a change that also represents lung injury. The increase in SD causes significant reduction in resulting lung compliance, and a loss of volume at given pressure values. Thus, this result also matches clinical observation and expected behaviours in the ARDS or injured lung.

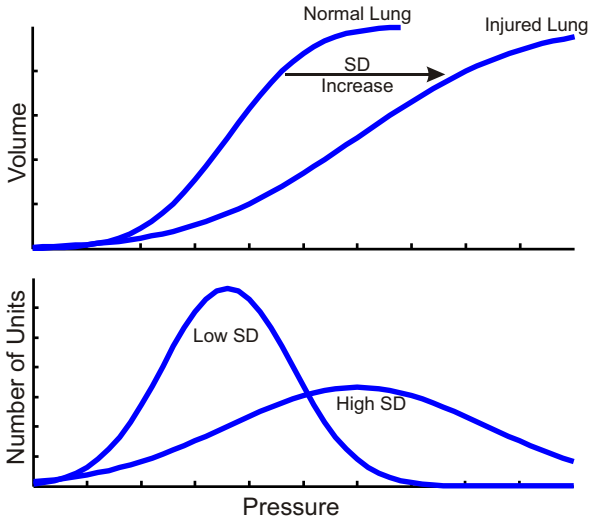

Figure 3.6 An example of the effect of increasing SD. The stiffer lungs can be represented by increasing the SD of the distribution. This increase results in reduced compliance of the lung. In this example, the mean of the distribution is also shifted. The overall effect on the total lung mechanics is the reduced volume at the same pressure.

3.2.2.3 PEEP and Mean Shift

Another parameter that is required to capture the fundamental mechanics of the ventilated lung is the shift in the PV curve that is present between different PEEP levels during ventilation. More specifically, clinical PV curves show a shift towards higher pressure as well as higher volume, as PEEP is increased. This shift cannot be explained by a single set of TP distributions. With a single set of TOP and TCP distributions, the inflation limbs would merge at higher pressures and the deflation limbs would merge at lower pressures. Instead, the limbs were distinguishably separate between different PEEPs. An example of this behaviour is observed in the clinical data from the study of Bersten et al. [1998] that is shown in Figure 3.7. As illustrated, the PV curves for each PEEP level is distinguishably separate from the others.

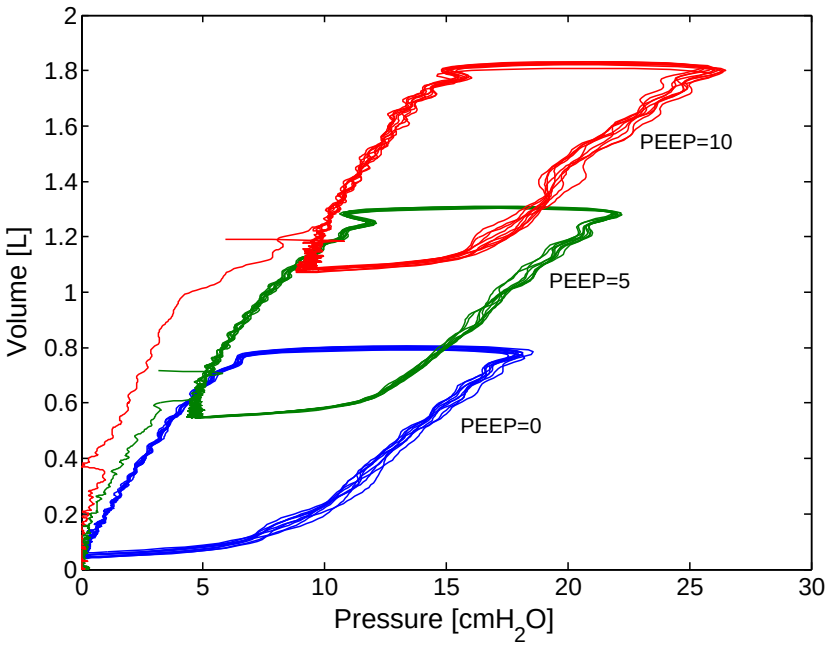

Figure 3.7 An example clinical PV data [Bersten, 1998]. The data shows PV curves for PEEP=0, 5, and 10 cmH_2O. As PEEP increases, the volume at a given pressure also increases, producing distinguishably separate curves.

In this model, this shift in the PV curve is captured by shifting the mean of the TP distributions while fixing all other parameters. Varying just a single parameter for different PEEP values simplifies the parameter identification, while capturing this shifting trend. Physiologically, this shift represents the change in recruitment of lung units. It is thought that, once a unit is recruited, it is easier to re-recruit during subsequent inflation. Thus, increasing the PEEP not only increases the lung volume by keeping additional lung units open at the end expiration, but also by bringing more recruitable units within the tidal ventilation pressure range.

In other words, by increasing PEEP, the TOP distribution shifts toward a lower pressure, closer to the "healthy" distribution range. This mechanism is consistent with several clinical studies showing that PEEP increases the total amount of recruitment at a given pressure [Cheng et al., 1995; Halter et al., 2003; McCann et al., 2001]. Figure 3.8 shows an example of the effect of shifting the mean on lung unit recruitment. By shifting the mean slightly towards lower pressure, the amount of lung units recruited at a given pressure can increase significantly.

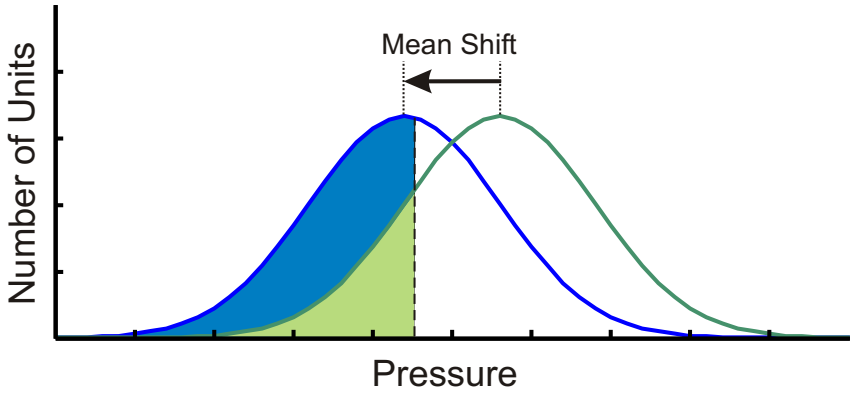

Figure 3.8 An example of additional recruitment with a mean shift. Clinical data shows an additional volume increase at a given pressure with increase in PEEP. This trend is modelled by the shifting the mean of threshold pressure distribution. At a higher PEEP, the mean of distribution shifts towards lower pressure (blue line) compared to the original (green line). As a result, the number of recruited units increases at a given pressure, as shown in green shaded area with original mean and blue + green shaded area for shifted mean. The increased recruitment leads directly to an increase in total lung volume.

The net effect can be simply described as bringing the TOP of more lung units into lower pressure values. Thus, compared to a TOP distribution before changing to a higher value, more units will be recruited at a given pressure than before the change. As further validation, this behaviour is regularly observed in clinical recruitment maneuvers and PEEP studies [Borges et al., 2006; Foti et al., 2000; Halter et al., 2003; Henzler et al., 2005; Lim et al., 2003; Richard et al., 2001].

Recruitment maneuvers performed during ventilator treatment are employed to take advantage of this behaviour to recruit additional lung units and increase the total lung volume, thus enhancing gas transfer. Because this model and the mean shift parameter are directly based on the recruitment status of the lung units, the model can be used to capture the lung mechanics resulting from recruitment maneuvers, as well as the overall effect of the maneuver. Therefore, this model can capture the mechanics and effect of standard ventilator operation, such as changing PEEP, as well as additional typical but non-linear therapies, such as recruitment maneuvers.

3.3 Calculation / Simulation

The model simulates the lung by calculating the volume at each pressure increment over a pre-defined range. It determines the volume of each individual lung unit and sums them up as a total volume at that pressure. At each pressure increment during inflation, the model determines if the applied unit pressure exceeds the TOP of the unit. If the pressure exceeds TOP, then the unit is recruited and assumes an appropriate volume determined by the unit compliance curve. If superimposed pressure is used, the pressure value for a compartment is subtracted from the applied airway pressure and used as a unit pressure. At the same time, previously recruited units also increase in volume according to the unit compliance curve, which is the same for all units.

Therefore, there are two ways that lung volume increases at each pressure increment: 1) expansion of already recruited lung units, and 2) recruitment of new lung units. The second mechanism is the principal factor in lung volume change with increasing pressure. The total volume of the lung is thus the sum of all recruited lung unit volumes at that pressure.

Similarly, during deflation, the volume is calculated at each pressure decrement. If the unit TCP exceeds the applied pressure, then the unit is derecruited and assumes a volume of zero. At the same time, the volume of recruited lung units is reduced according to the unit compliance curve. The overall process is effectively quasi-static and computationally simple.

3.4 Summary

The lung is modelled as a group of individual lung units. Each lung unit is associated with a TOP and TCP as part of overall TP distributions, and a unit compliance curve. Thus, each lung unit has its own pressure volume relationship. TOP and TCP govern the timing of recruitment and derecruitment, respectively, and are either identified from data or predefined from generic curves. The unit compliance curve determines the volume of recruited units. The derecruited lung units have a volume of zero. These components are functions of pressure, thus volume is calculated at each pressure point.

The model is based on the hypothesis presented in Chapter 2 that most of the volume change in the lung occurs by recruitment and derecruitment. Therefore, TOP and TCP are the components that dictate the majority of volume change in the lungs. In turn, the TOP and TCP distributions are defined by 2 unique parameters and can be treated individually for inspiration and expiration, respectively.

The TOP and TCP of individual units are unique, as they are recruited and derecruited at different pressures. This difference results in wide distributions of TOP and TCP over applied pressure. One of the major elements causing the distribution is the superimposed pressure, which is caused by the weight of the lung itself. The lung thus inflates progressively from top to bottom as applied pressure overcomes this superimposed pressure, and as observed clinically [Gattinoni et al., 2001; Puybasset et al., 1998, 2000].

A second major element contributing to the TP distributions is the heterogeneous characteristic of lung units within a region. Each lung unit reacts differently to an applied pressure, especially in ARDS affected lungs. Some units are recruited at lower pressures and some are recruited at higher pressures, depending on their condition or level of injuries. As a result, the threshold pressures are distributed widely over a range of pressure, even within a region of the same superimposed pressure.

Threshold pressure is described in this model by normal Gaussian distributions. The equation is well known and simple to manipulate, and requires just 2 parameters to determine the shape and values of the distribution. These parameters can also be associated directly with the accepted and observed physiological mechanics of the lung.

Unit compliance curves determine the volume of recruited lung units and represent the elastic component of lung unit mechanics. The curve follows a basic sigmoid shape. However, because this model uses recruitment and derecruitment as the major mechanism for volume change, the unit compliance curve has only a small contribution to the overall volume change compared to the threshold pressures. For this reason, the unit compliance curve may be fixed to a predefined global constant or generic function for a patient.

The model is created based on the fundamental clinically observed mechanics of the lung. Each component and their parameter can be directly related to physiological components or mechanisms. In addition, the relationship with other components is clear and easy to understand. The calculation and simulation is also done in logical steps, rather than by computationally heavy mathematics. Therefore, the entire system should be intuitively clear and physiologically relevant, and the overall concept of how they are put together to create a model should therefore be easy to grasp.

Chapter 4

System Models

The model components discussed in the Chapter 3 describe the mechanics of individual lung units. The system model defined in detail in this chapter integrates these mechanics into a full model of lung mechanics. Depending on the severity of the disease, the affected lung units exhibit different pressure and volume mechanics. Since these units have different unit compliance and threshold pressures they can be considered to be specifically different types of units with their own associated, type specific unit compliance and threshold pressures.

A computational program, MATLAB, is used for development of all models. Three different system models are developed, each one succeeding the previous. The differences are primarily a function of the number of different unit types and direct physiological analogy.

The first model, being the full model, accounts for every unit type described in the clinical study by Schiller et al. [2003]. The unit compliance curve is also represented by the most flexible of equations utilised. The second model is simplified to contain 2 different unit types and a simpler unit compliance and is thus easier to identify. This approach compromises some direct physiological accuracy to enhance the potential clinical usefulness.

The third and final model is designed and developed specifically for clinical use. This model consists of just a single flexible unit type. This simplification allows direct parameter identification. The model is thus designed to be simple enough for easy parameter identification, while capturing the fundamental lung mechanics to be useful at the bedside in clinical situations. Thus, all subsequent model validation is done on this final model.

Parameters identifying the patient's unique lung mechanics are determined by fitting the model to clinical PV data. The model parameters in the system model equations describe the unique features of the lung unit mechanism. Varying these parameters can thus reproduce the unique characteristics of the lung. The parameters are back calculated from the best fit to a clinical data. The fitting method is described in full detail in Chapter 5, prior to model validation.

4.1 Full Physiological Model

The first model developed is the most detailed and fully incorporates lung unit physiology based on the study by Schiller et al. [2003]. As the study described, there are 3 different types of alveoli in ARDS affected lungs, denoted Type 1, 2, and 3. Severity of injury is different for each type and they thus exhibit different pressure-volume relations.

This first model accounts for the presence of all three types of alveoli and treats them as separate unit types. In addition, the distal airways, which also exhibit unique pressure-volume relations different to alveoli, are also considered as a different unit type. Thus, the model consists of effectively 4 different types of lung units. Each unit type is associated with its own unique unit compliance and threshold pressures. This model is the most physiologically accurate and representative of the types of units present in ARDS lungs. The model then individually incorporates the unique biomechanical characteristics of each type into the full system model.

4.1.1 Unit Types

Schiller et al.'s *in vivo* microscopic study [2003] found that the alveoli in ARDS affected lungs have significantly different characteristics in both compliance and recruitment. Some alveoli showed a very small change in size throughout a fixed breathing cycle, while others showed significant expansion and contraction. Some alveoli collapsed at the end of expiration and were recruited again during the next inspiration, while others did not collapse at all. These results showed that the injuries to the lung affect each alveolus differently and that a variety of measur-

ably different alveoli characteristics are heterogeneously distributed through an injured lung.

The study by Schiller et al. microscopically examined lung tissue in mechanically ventilated pigs. These pigs were ventilated with 10 ml/kg tidal volume and 3 cmH_2O PEEP. Images of alveoli were then examined for both normal healthy lungs and the surfactant deactivated lungs. They summarised their findings into 3 basic alveoli types:

Type 1 alveoli are the most healthy and normal alveoli. In a healthy lung, all of the alveoli observed were of this type. These alveoli are already recruited at the beginning of inflation due to the PEEP levels used and show very small size change during tidal ventilation. This behaviour results in an almost flat uniform unit compliance curve. The TOP and TCP for this unit type are thus concentrated around zero or relatively low pressures. These mechanics are summarised in Figure 4.1.

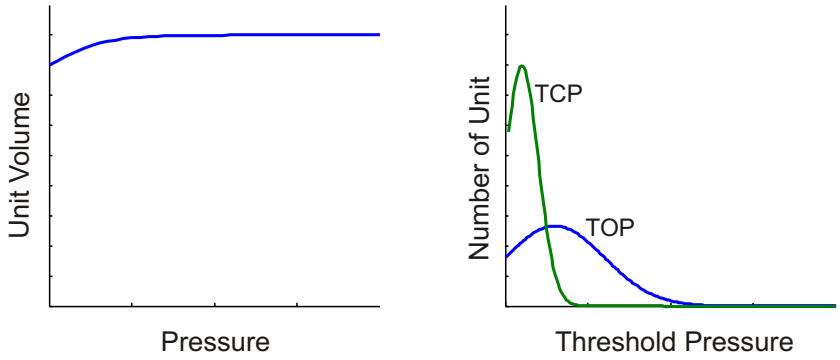

Figure 4.1 Schematic of the typical features of Type 1 alveoli. The alveoli exhibits almost no expansion as pressure increases, resulting in a flat unit compliance curve as illustrated in the left plot. The Type 1 alveoli generally have low TOP and TCP, thus the distribution is concentrated at lower pressures, as illustrated in the distribution plot on the right.

Type 2 alveoli are defined as slightly to moderately affected by the disease and only present in injured lungs. The sizes of these alveoli change slightly, but significantly during tidal ventilation, and generally to a measurably larger final size than Type 1 alveoli. These alveoli also may not collapse at the end of expiration. The size change of this unit type is represented by a slightly greater difference in minimum and maximum values in the unit compliance curve. Its TOP and TCP are also concentrated at a lower pressure. Note that the level of impact of the disease or injury will affect the exact distributions and recruitment at a given PEEP level. These results are summarised schematically in Figure 4.2.

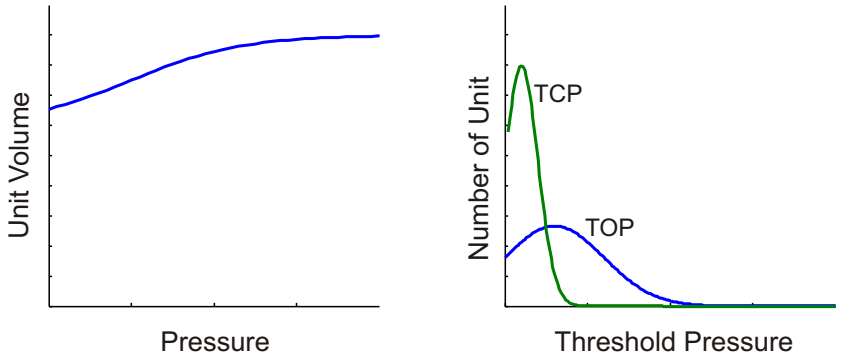

Figure 4.2 Schematic of the typical features of Type 2 alveoli. The alveoli exhibits slight expansion compared to Type 1, as pressure increases, resulting in a slight increase in the unit compliance curve as illustrated in the left plot. Similar to Type 1 alveoli, the Type 2 alveoli generally have relatively lower TOP and TCP, thus the distribution is also concentrated at lower pressure as illustrated in the distribution plot on the right.

Type 3 alveoli are those most affected by the injury. These units collapse at the end of expiration, and are gradually recruited again during subsequent inflation. Once recruited, these alveoli exhibit a significant expansion as pressure is increased. Furthermore, these alveoli are recruited at several different pressures over the inflation range. Note that in the most damaged cases, some units may not be recruited with any clinically reasonable pressure applied, and remain collapsed for the entire breathing cycle. The significant expansion compared to the healthy Type 1 alveoli is represented by a large difference between minimum and maximum relative volumes in the unit compliance curve. As a result, there is a wide range of recruiting pressures, as represented by the much more broadly distributed TOP and TCP distributions, as illustrated in Figure 4.3.

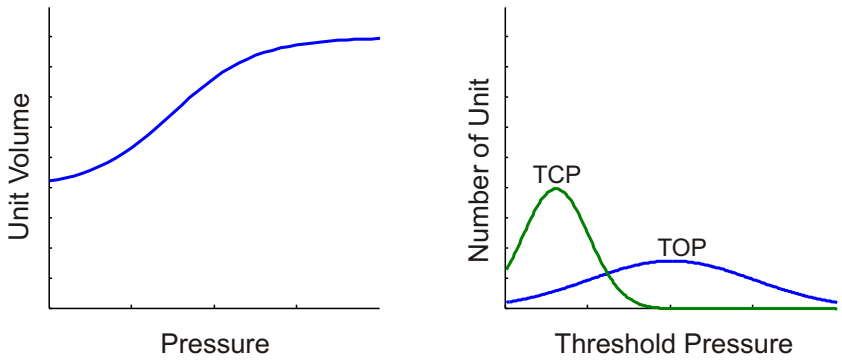

Figure 4.3 Schematic of the typical features of Type 3 alveoli. The Type 3 alveoli exhibit a significant expansion as pressure increases, resulting in large volume changes as illustrated in the plot on the left. The Type 3 alveoli collapse completely at the end of expiration, and have wide range of threshold pressures, resulting in a broader distribution as illustrated in the plot on the right.

Finally, the distal airways are also considered as a separate lung unit. These airways consist of soft tissues. Thus, they exhibit expansion and contraction, as well as recruitment and derecruitment. Movement of these distal airways also contributes to the total lung volume change. However, the pressure-volume relation of the distal airways has not been fully studied and reported, thus its actual mechanics are not known. Therefore, assumptions are made based on physiological features of lung tissues, namely the visco-elastic property of the soft tissues.

4.1.2 Model Parameters

Unit Compliance

This full model utilises a specially developed equation to describe unit compliance curve. It consists of 2 separate equations, each uniquely and independently describing the upper and lower curvatures separately. This separation allows maximum control over the shape of the curve, and is thus fully flexible to match a wide variety of clinical data.

The first equation is defined:

$$P_1 = \frac{V_{max} - (V - V_{min})}{V_{max}}(1 - e^{-a_1(V - V_{min})})S_1 \tag{4.1}$$

The second equation is defined:

$$P_2 = \frac{V_{max}}{V - V_{min}}[(e^{a_2((V - V_{min}) - V_{max})})(1 - S_2) + S_2] \tag{4.2}$$

where P_1 and P_2 are normalised pressures, V is volume, V_{max} is the maximum unit volume, V_{min} is the minimum unit volume, a_1 and a_2 are the power of curvature for P_1 and P_2, respectively, and S_1 and S_2 are the location of the centre of curvature for P_1 and P_2, respectively. Finally, these equations are added and multiplied by

a maximum defined pressure, P_{max} to produce the final unit compliance curve.

$$P = P_{max}(P_1 + P_2) \tag{4.3}$$

Note that the direct solution of this equation is the inverse of the actual unit compliance used in the model. Figure 4.4 illustrates the 2 curves from the Equations (4.1) and (4.2), and the final curve produced by Equation (4.3).

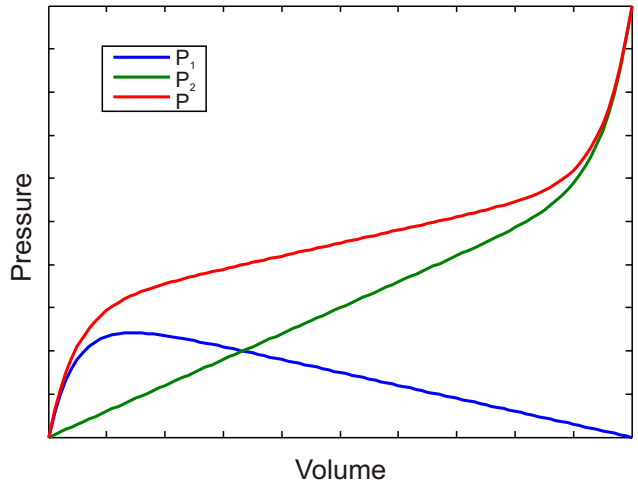

Figure 4.4 Unit compliance curve for the full model. The curve, P, is derived from 2 separate curves, P_1 and P_2. Each curve is described by a separate equation, thus each curvature is defined separately. This arrangement provides the model with the flexibility to fit a variety of data. Note that the direct result of these equations, shown in the plot, is the inverse of the actual unit compliance used.

Finally, the unit compliance in this full model includes separate inflation and deflation curves to account for the hysteresis in individual lung units. Thus, the inflation and deflation limbs of ventilation have separate unique unit compliance curves and the associated parameters.

Threshold Pressures

Threshold pressure distributions require 2 parameters each, as discussed in Chapter 3 for TOP and TCP: mean and SD. Other parameters, such as the total number of units, minimum and maximum pressure, and Total Lung Capacity (TLC) are also variable and can be adjusted. However, these latter values can be determined or estimated from reasonable clinical values.

4.1.3 Model Summary

This full physiological model is described by a total of 12 parameters per unit type per respiration limb. These parameters are summarised in Table 4.1. Note that the $*$ marked parameters are the ones that can potentially be determined or estimated from clinical studies and/or reports.

Table 4.1 Summary of the full model parameters. The parameters shown here are for one unit type and for one respiratory limb only.

Unit Compliance Curve	Threshold Pressure Distribution
$V_{max}*$	SD
$V_{min}*$	mean
a_1	number of units/ratio
a_2	$P_{min}*$
S_1	$P_{max}*$
S_2	
$P_{max}*$	

Figure 4.5 shows an example of all the model components for the full model. Since the full model consists of 4 unit types, there are 4 unit compliance curves and 4 sets of threshold pressure distributions, each uniquely reflecting the mechanism of a specific lung unit types. The figure illustrates components for the inflation limb only for clarity. The full system model also requires a similar set of components for the deflation limb.

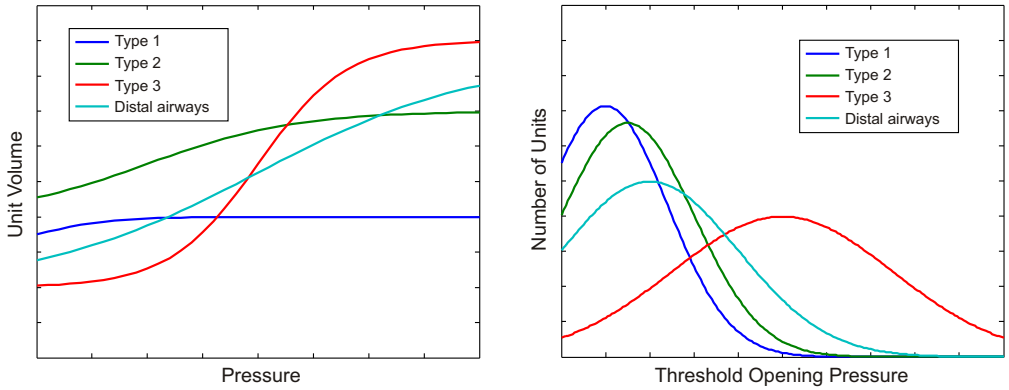

(a) Unit compliance curves. (b) TOP distributions.

Figure 4.5 An example of system model components for the full model. The full model utilises 4 unit types, thus there are 4 separate model components. Plot (a) illustrates an example of the unit compliance curve for the full model. Each type of unit has a unique compliance curve, reflecting its own mechanics. For an example, the Type 1 alveoli shows very small expansion, while Type 3 alveoli shows a significant volume change. Plot (b) illustrates example TOP distribution for the full model. Note that only components for the inflation limb are shown.

4.1.4 Model Limitations

This model represents the true physiology in the most detailed manner. It accounts for all different types of alveoli reported in literature, as well as distal airways, and considers them as separate unit types. Furthermore, it is designed to fit a variety of clinical data by utilising the most flexible governing equations for lung unit mechanics. However, the large number of details included in this model requires at least the same number of parameters to describe them. Thus, it has limited use in clinical situations.

Specifically, the major limitation of this model is the large number of parameters that need to be identified. The unit compliance curve requires 7 parameters and each threshold pressure distribution requires as many as 5 parameters including the number of units and pressure limits. Thus, the model requires 12 parameters per unit type per respiration limb. Since the model consists of 4 different unit types, it requires a total of 48 parameters. Even if some parameters are estimated or predetermined using reasonable values from clinical studies [Yuta et al., 2004], the model still requires close to 30 total parameters to be simultaneously identified for a single limb of ventilation.

Therefore, this model, while physiologically the most detailed and flexible, is clearly not practical in clinical situations for several fundamental reasons. All of these reasons are build around the need to identify the model clinically for it to be relevant to treating a specific patient. In particular:

1. It is impossible to uniquely identify each parameter from a single PV curve or very short series of PV curves.
2. Each type of unit in this model has slight differences in pressure-volume characteristics, however the overall behaviour is similar. Furthermore, the parameters for the governing equations also influence the curve in a similar manner. Therefore, it is practically impossible to separate the unique behaviour or contribution of a single unit type from another using only PV curves. More succinctly, the trade-off between parameters is such that the model is not uniquely identifiable from readily available clinical data.
3. Some parameters in this model cannot be identified uniquely from the clinical PV curves and may require additional tests to measure them directly.

Most of these direct measurements may be invasive, such as esophageal pressure measurement. Therefore, identifying this model may pose additional risk to the patient, as well as additional cost. Finally, some parameters may not be possible to measure with current technology, such as the ratio of different unit types in a lung.

4. Even if all of the parameters were identified, the information obtained from them are not all necessary, or useful, at the bedside in clinical situations. Current ventilators can only control the pressure and volume applied to the entire respiratory system, and obviously cannot control each lung unit differently. Thus, information on individual lung unit types will most likely not aid the process of optimising the ventilator for a given patient.

5. Even if all the parameters were identifiable, the time to obtain all the required data, especially on regular or daily basis, would render the model clinically ineffective.

4.2 Two Unit Type Model

To address some of the issues with the first model, the second model utilises just 2 unit types. These units are categorised as healthy and ARDS affected. This simplification of unit types reduces physiological accuracy. However, it also reduces the number of parameters by half. Furthermore, the unit compliance curve was modified to use a simpler equation, further reducing the number of parameters. The overall model therefore has reduced physiological accuracy and flexibility in unit compliance, however it still contains the fundamental mechanics and the total number of parameters is potentially more manageable for clinical use.

4.2.1 Unit Types: Healthy and ARDS

This model utilises only 2 different unit types, instead of the 4 used in the previous model. These unit types are categorised as healthy and ARDS affected unit types. The essential reasoning for still including two different unit types is that not all lung units react the same way. The reduction in the number of diseased unit

types may not be as physiologically accurate, however the fundamental mechanics of the lung are still captured. Healthy units are recruited at lower pressure and exhibit very small or almost no expansion as pressure is further increased. Injured or ARDS units are recruited at relatively higher pressures and exhibit some expansion as pressure is increased. The 2 unit type model thus captures these essential heterogeneous features of the injured lung and incorporates them into the model.

More importantly, it may be possible to measure and differentiate between healthy and injured unit types using available equipment, unlike the case with the 4 parameter model. Medical instruments, such as the portable CT scan, may be used to make an estimate of the ratio of healthy and ARDS affected lung units to differentiate their contribution to the model. Such equipment is less invasive and more widely available in modern hospitals. However, direct measurement is still difficult, and the cost associated with the additional testing will not be practical for every patient.

Outside of the reorganisation to 2 unit types, there is no difference in the unit mechanics. Each unit type has threshold pressures and their number must be identified as a percentage of the total number of lung units. Each type still also has a unique compliance curve.

4.2.2 Unit Compliance

The unit compliance curve of this model was also modified to reduce the number of parameters. Rather than having complex equation of Equation (4.3), a simpler more well known and identifiable equation was chosen. Furthermore, because the major mechanism of volume change in this model is recruitment and derecruitment, the unit compliance curve has only a very small effect in the overall lung mechanics. Thus, simplifying the governing equation of the curve should have a negligible or small influence. The new unit compliance curve is based on a sigmoid function with a few additional parameters to allow adjustment of the shape and the values. The curve is described with equation:

$$V(p) = \frac{a}{1 + e^{[b(-p+c)]}} + d \tag{4.4}$$

where V is volume, p is pressure, d is the minimum volume, a is difference between minimum and maximum volume, thus $a+d$ is the maximum volume, b is the power for the curvature, and c is the mean. An example plot is shown in Figure 3.2 in Chapter 3

Equation (4.4) is not as versatile as Equation (4.3), which is used in the full model. However, it still describes the basic shape of compliance [Venegas et al., 1998]. The effect of switching to a simpler equation is minimal, because it still produces a reasonable curve and the previous model could not fully identify or utilise the previous equation. Finally, for this equation, generic parameters could be chosen for each type using the data from the clinical study by Schiller et al. [2003].

4.2.3 Model Parameters

This model drastically reduced the number of parameters that requires identification. The unit compliance curve is described with 5 parameters per unit type per respiration limb. The threshold pressure distribution requires the same number of parameters as before. However, because the total number of unit types is now just 2, the ratio of unit types are directly related. Thus, this ratio can be determined directly by assessing the percentage of healthy or ARDS unit types using a CT scan, for example.

Therefore, each limb of respiration can now be described by a total of 20 parameters. Furthermore, many of the parameters, such as the minimum and maximum volume for Equation (4.4), can be estimated from reasonable clinical values, further reducing the number of parameters to be simultaneously solved. Table 4.2 summarises the 2 unit type model parameters. Note that the $*$ marked parameters are those that can potentially be determined or estimated from clinical studies and/or reports.

Figure 4.6 illustrates an example of the system model components for the 2 unit type model. The unit compliance curve for each unit type, illustrated in Figure 4.6(a), includes hysteresis for the difference between inflation and deflation. The threshold pressure distributions, both TOP and TCP, for both unit types are shown in Figure 4.6(b).

Table 4.2 Summary of the 2 unit type model parameters. The parameters shown here are for one unit type and for one respiratory limb only, thus only 1/4 of the total parameter is shown.

Unit Compliance Curve	Threshold Pressure Distribution
V_{max}*	SD
V_{min}*	mean
curvature	number of units/ratio
mean	P_{min}*
P_{max}*	P_{max}*

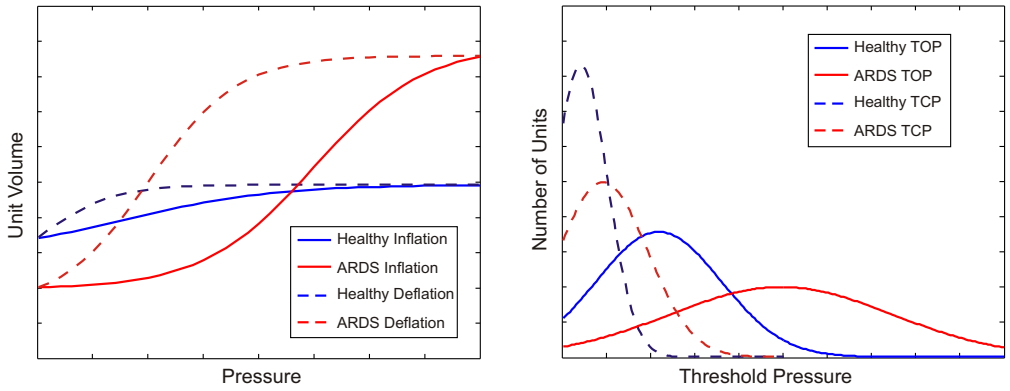

(a) Unit compliance curves.

(b) TP distributions.

Figure 4.6 An example of the system model components for the 2 unit type model. This model utilises 2 unit types, thus there are 2 separate sets of model components. Plot (a) illustrates an example of the unit compliance curve for the healthy and the ARDS types. The curve for healthy unit type reflect healthy normal lung units, and ARDS unit type reflect the key features of the injured lung units. Plot (b) illustrates example TOP and TCP distributions. The broad distribution of the ARDS unit type reflects the stiffer, heavier lung of ARDS.

4.2.4 Model Limitations and Summary

Even though this model dramatically reduced the number of parameters by more than 50%, the number is still too high for most clinical use. The model still requires as many as 17 parameters to be solved simultaneously, which would require at least that many PV curves to uniquely identify each parameters. This level of required data would introduce too great a burden on the patient and/or staff and might still require regular additional tests beyond normal treatment, such as CT scans.

One of the other major difficulties is to differentiate the 2 unit types in a single PV curve, as with the previous model. Both unit types are governed by

the same equation and parameters, and can produce similar PV curves. Thus, uniquely identifying the mechanics of each unit type requires predefined values, or some other measurement or constant (potentially theoretical) to obtain the values directly. A CT scan might offer such a measurement but is not typically used on such a regular basis.

It may be possible to measure certain parameters directly with modern medical equipment. However, the methods may require invasive protocols and/or expose the patient to additional unnecessary risk, as well as the additional cost of treatment. Furthermore, the ventilator can only treat or measure the entire respiratory system as a whole. Thus, having the knowledge of the specific number and distribution of different types of lung units may be useful in analytical studies, but it may not be as directly useful for routine optimisation of ventilator therapy in critical care.

4.3 Single Unit Type Model

The difficulty with the previous, more physiologically accurate models was that they required too many parameters to be uniquely identified. These parameters were difficult to distinguish from others because they were all part of the same governing equation. The only difference between unit types was in the specific parameter value ranges and not their mechanics. However, even if the parameters were identified, the information obtained from those uniquely identified parameters may not be useful in clinical situations because the current ventilator cannot differentiate the treatment given to different unit types, as it has to treat the entire respiratory system as a whole.

This final model was developed with a focus on clinical usefulness. It consists of a single lung unit type for direct comparison to ventilator treatment and what the ventilator "sees" with its sensors. The unit compliance curve is further simplified, and most of the remaining parameters are defined so that they can be readily predetermined from clinical values and reasonable estimates. The single unit type further simplifies the parameter identification by allowing some parameters to be calculated directly from clinical data. The resulting model lacks the physiological details and resolution of the previous models, however it may be more appropriate for the intended clinical application.

4.3.1 Modifications Made to Prior Model

The final model was developed to be the most useful in clinical situations, specifically in the optimisation of ventilator treatment. Hence, the number of unit types is reduced to just one. This change allows a direct relationship between the model and the ventilator. Furthermore, the single unit model no longer requires differentiation between unit types. Thus, this model can uniquely identify all parameters from PV curves and requires no additional tests, further enhancing the potential clinical usefulness.

The unit compliance curve was also modified to have the same curve for both inflation and deflation. Thus, the unit compliance no longer exhibits the individual unit hysteresis, as in prior models. The elastic component of the lung mechanics, especially at lung unit level, has very little hysteresis [Cheng et al., 1995]. The majority of total lung hysteresis is therefore caused in this model by the difference between TOP and TCP distributions. Furthermore, the influence of the unit compliance on the total lung mechanics is considered small compared to the recruitment and derecruitment of the lung units in this study, thus the effect of modifying the compliance curve should also be minimal.

However, this simplification of the lung model also further reduces the physiological detail. Considering the entire lung as a collection of a single type of lung unit reduces the specific resolution of the modelled lung, and the individual effect of different unit types is no longer directly available. The reduction in the number of unit types and a simplified unit compliance curve also means that the model is less flexible. Thus, it may not be able to achieve as good a fit to clinical data as previous models.

4.3.2 Model Parameters

The unit compliance of this model uses same governing equation as the previous 2 unit type model, and can be described with 4 parameters for both inflation and deflation. However, most of these parameters can be determined from clinical studies, and can thus be predefined as population constants for all patients. Alternatively, patient specific parameters can be determined, using patient specific

data and then fixed for the rest of the simulation. The flexibility of the model to fit the data should not be compromised by this global constant due to the relatively small influence of the unit compliance on total lung volume mechanics.

The TP distributions require a total of 5 parameters. However, some parameters are directly related to clinical observations, such as the total number of units directly relates to total lung volume and the maximum unit volume being determined by the unit compliance. Thus, these parameters can be calculated or closely estimated directly from the patient data. Minimum and maximum pressures can be fixed at a reasonable values based on clinical observation and experience, as well as reported data.

Table 4.3 summarises the parameters for this single unit type model. Note that the $*$ marked parameters are those that can potentially be determined or estimated from clinical studies and/or reports. Therefore, all parameters except for the SD and the mean of the threshold pressure distributions can be constant or determined specifically for a patient.

Table 4.3 Summary of a single unit type model parameters.

Unit Compliance Curve	**Threshold Pressure Distribution**
$V_{max}*$	SD
$V_{min}*$	mean
curvature$*$	number of units$*$
mean$*$	$P_{min}*$
$P_{max}*$	$P_{max}*$

The resulting system model requires just 4 parameters to uniquely describe the entire PV curve. In particular, 2 parameters, mean and SD, for each of the inflation and deflation limbs. These parameters describe unique, potentially patient specific features of the data, and can thus be easily identified from clinical PV data. Figure 4.7 illustrates the system model components for the single unit type model. The unit compliance curves now have a single curve for both inflation and deflation, as illustrated in Figure 4.7(a), and one pair of TOP and TCP distributions for the entire lung model, as illustrated in Figure 4.7(b).

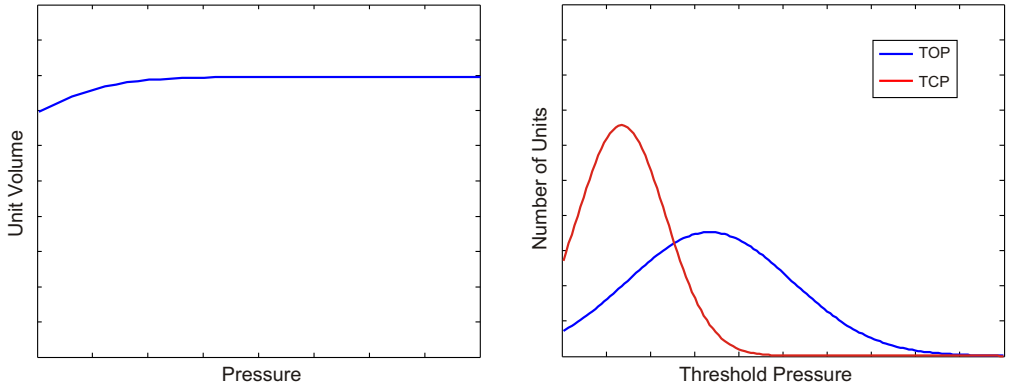

(a) An example of unit compliance curve. (b) An example of TP distributions.

Figure 4.7 An example system model components of the final single unit type model. This final model utilises just a single unit type. Plot (a) illustrates an example of unit compliance curve for the full model and plot (b) illustrates example TOP and TCP distribution. The single unit type representing all lung units matches the actual operation of the ventilator and greatly improves the parameter identification due to the reduced number of parameters.

4.3.3 Model Limitations and Summary

One major concern that might arise is the use of a single TOP and TCP distribution to describe the impact of all alveoli types observed by Schiller et al [2003]. While they are now uniquely identifiable, these TP distributions can also capture a wide range of behaviour in their shape. Specifically, the recruitment of these units and the number of each type are represented by the width (SD) and location (mean) of the distributions. Hence, an ARDS affected lung would have its TOP distribution shifted primarily to higher pressure, indicating the stiffer lung requiring additional pressure for similar recruitment status. The width of the TOP distribution for ARDS lungs would also be wider indicating the presence of heterogeneous distribution of injured lung units. However, validation of this model with clinical data will be required to ensure that a single threshold pressure distribution can capture all the clinically observed and relevant responses.

Finally, this model was developed to overcome limitations with identifiability associated with prior models. In this task, it has succeeded. Physiologically, the impact appears to be small. However, further studies are required to validate the clinical relevance and abilities of this model. Preliminary validation using a mechanical simulator and clinical data are presented in Chapter 6 and 7 in this thesis respectively.

4.4 Summary

The model components described in Chapter 3 are combined in a system model to enable simulation of the lung as a whole. Each component essentially describes a feature of one unit type. Overall, 3 different models are developed in succession, with each one improving aspects of the previous model. The major difference is the number of unit types utilised. The more units the model utilised, the more accurate and directly relevant the physiological detail. However, it also increases the number of parameters that need to be identified to unreasonable and non-unique levels.

The first model is directly based on the microscopic study conducted by Schiller et al. [2003], who summarises their findings into 3 types of alveoli based on the level of injury or damages. The first model, thus, has 4 different unit types, representing 3 different types of alveoli and distal airways. This model reflects the physiological details most accurately and has the finest resolution of the severity of the lung injury. It also has most flexible governing equations. However, the number of parameters required is too large, and it is practically impossible to uniquely identify the parameters.

The second model slightly simplified the first model, and consisted of 2 unit types: healthy and injured. The model is also modified to use a simpler unit compliance equation to further reduce the number of parameters. The reduction in number of unit types and simplified unit compliance sacrificed some physiological details and resolution of the severity of lung injury. The model has significantly less parameters to be identified, however the number is still too large for a unique solution without making additional assumptions or invasive measurements.

The final model is designed specifically for ventilator optimisation in clinical situations. This goal requires further simplification and reduction of parameters, and thus the number of unit types is reduced to just one. The ventilator can only treat the respiratory system as a whole and cannot differentiate between different types of lung units. Thus, the number of unit types now matches the way in which the ventilator affects patients. Using predetermined and directly calculated values, this model requires just 4 parameters to uniquely identify patient specific lung mechanics for clinical use. The remaining tasks for this third model are to present the identification methods and fully validate its mechanics with respect to clinical observations, data expectations, and experience.

Chapter 5

Parameter Fitting and Identification Methods

The model has to be fitted to a variety of clinical data for validation and/or use. The parameters of the governing equations that produce the best fit to the data are identified as the unique patient and condition specific parameters. Some parameters are kept constant as predefined global values, such as the arbitrary number of units and associated maximum unit volume. Unit compliance curve values are also kept constant at population values, since they have a less significant contribution to the main lung volume mechanics.

Different fitting methods were considered, due to the different types of PV data available. More specifically, the same clinical data can be presented differently, depending on the additional available data and the methods used to collect the data. A typical ventilator records data of tidal ventilation. Accordingly, the resulting PV curves range from PEEP to PIP and from End Expiratory Volume (EEV) to End Inspiratory Volume (EIV). Thus, the EEV is often considered to be the zero volume point because it is the minimum volume measured during tidal ventilation, and the ventilators do not often deflate down to the lung's Functional Residual Capacity (FRC). A fitting process using this data is simple, because all the values are known and no additional intervention is required to obtain the data.

A second type of clinical PV data does contain deflation to FRC. This type of data enables direct calculation of EEV and thus includes information about the operating volume relative to the inspiratory capacity. However, the data acquisition is slightly more complex, as it requires additional intervention from ICU staff. Overall, as discussed later in this chapter and in Chapter 7, data including

EEV is clinically more relevant and the information that can be obtained is potentially more useful in many clinical situations. However, because this data is not always available, both methods of fitting are presented.

5.1 General Parameter Fitting Method

In either approach, fitting the model to a given set of clinical PV data is relatively straightforward. Each key feature of the clinical data is described by a parameter, or a combinations of parameters. For example, the maximum lung volume is defined by the fixed maximum unit volume and the total number of units. Thus, each shape or value of the clinical data indicate, or at least estimate, a model parameter. A general fitting process can therefore be defined:

1. **Set minimum and maximum volume:**

   For data without deflation to FRC measurement, the minimum and maximum volumes are simply the EEV and EIV, respectively. For data with deflation to FRC, the minimum is set to FRC and the maximum is set to the measured or estimated inspiratory capacity. These values essentially determine the maximum unit volume and the number of units.

2. **Set minimum and maximum pressure:**

   For data without deflation to FRC, the minimum and maximum pressures are simply set at PEEP and PIP, respectively. For data with deflation to FRC, the minimum is set to absolute zero and the maximum is set to a measured or estimated plateau pressure. These values determine the range of threshold pressures.

3. **Set Unit Compliance (UC) parameters:**

   The parameters for the unit compliance curve are fixed to a set of clinically reasonable generic values. Alternatively, these values may also be fit by grid search, as discussed later in this section. The unit compliance has a relatively small influence on the total lung mechanics, thus keeping the parameters generic simplifies the identification process without significantly sacrificing flexibility or accuracy.

4. **Set TP SD to match the slopes of the PV curve:**

   The standard deviation of a threshold pressure distribution essentially determines the maximum slope of the resulting PV curve. Thus, by varying the SD to match the slope of the PV curve determines, or at least provides a good estimate of, this parameter. Note that these slopes are also effectively a measure of lung compliance. Inflation and deflation curves are fitted separately. Thus, the TOP SD is matched to the inflation limb and the TCP SD is matched to the deflation limb.

5. **Set the TP mean values to match location of maximum slope:**

   The mean of the TP distributions determines the location where the maximum slope occurs on each limb. Thus, by matching the location, or pressure, the mean can be determined or estimated. Inflation and deflation curves are fitted separately. Thus, the TOP mean is matched to the inflation limb and the TCP mean is matched to the deflation limb.

However, after this process, all parameters may still require fine tuning to achieve a best fit. For example, different combinations of SD and mean produce different slopes at different volume levels. Thus, simply placing them according to these values and shapes does not necessarily produce the best fit. However, it does provide a very good estimate, and thus a good starting point. From this point, a grid search of surrounding physiologically reasonable points finds the optimal values, and is computationally simple given a good starting point.

Overall, the parameter identification method is basically a simulation process where clinical data is used to identify TOP and TCP distribution parameters to create a patient specific curve. The two basic data types and the fitting methods are also related. However, different ways of presenting the data and fitting the result necessitate the slightly different fitting methods. The data with deflation to FRC uses, what is called here, a **Min-to-Max** range approach. For data without deflation to FRC, a method defined here as, the **PEEP-to-PIP** method is used.

5.2 PEEP to PIP Method

Clinical PV data without deflation to FRC can be fitted by using a pressure range from PEEP to PIP. This method allows model fits over an entire curve of tidal ventilation. The minimum and maximum pressure of the threshold pressure distributions are set to PEEP and PIP, respectively, and the maximum volume is set to the tidal volume. Because these values are set by the ICU staff, they can be obtained directly from the ventilator or extracted directly from the data.

The data is fitted simply by setting the model to the known values and varying the unknown TP distribution mean and SD for both the inflation (TOP) and deflation (TCP) limb data. Figure 5.1 illustrates an example of the PEEP-to-PIP fitting method using a clinically measured PV curve [Bersten, 1998]. The volume data goes from zero to tidal volume and the model is fitted over that range.

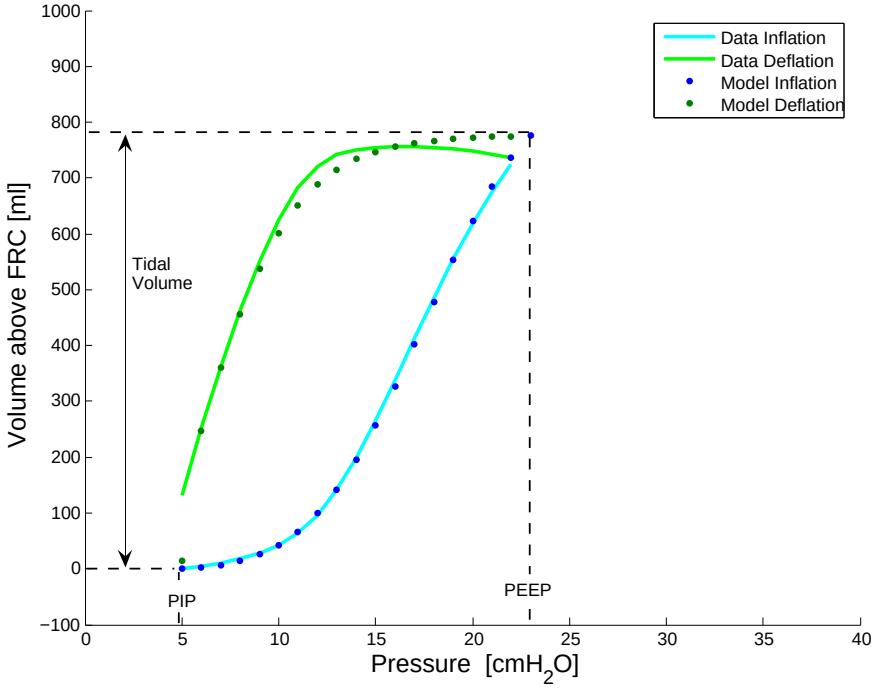

Figure 5.1 An example of PEEP-to-PIP fitting. The plot shows data for inflation (solid blue), data for deflation (solid green), modelled inflation (dotted blue), and modelled deflation (dotted green). This method fits the entire PV curve, and most of the parameters can be directly obtained from the data.

Another advantage of using PEEP to PIP data fitting is the ease of data collection. Many modern ventilators have their own data acquisition systems built into the machine [e.g. Hamilton Medical, 2006; Maquet Medical Systems,

2006]. The majority of them automatically adjust the pressure and the flow. Thus, these data are already measured and analysed in real time. Because these data are measured at each breath, the data recorded is from PEEP to PIP. Therefore, this particular data can be obtained directly from these ventilators without manipulation of the machine or interrupting the treatment.

Limitations

The PEEP to PIP PV curve contains the transition period between inflation and deflation. As discussed in Chapter 2, these sections are highly dynamic as the mode of ventilation changes between active inflation and passive deflation. The measured values are thus strongly influenced by other non-lung mechanics in this region, such as the establishment of flow. They are also prone to measurement errors as flow and pressure changes are very small. Therefore, these sections of the data may not accurately reflect the true lung mechanics. More importantly, these variations can easily mask the actual mechanism and trends that the model is designed to capture for use in optimising therapy. The model fit over this section is thus difficult to interpret and not necessarily clinically relevant.

The simple breath-to-breath data may be advantageous in terms of data collection, however it may be a drawback in terms of clinical usefulness. In the PEEP-to-PIP PV data, the information on End Expiratory Volume (EEV) is absent. EEV indicates the volume level at which the lung is ventilated within total lung capacity. This information is closely related the recruitment status of the lung units [Malbouisson et al., 2001; Rylander et al., 2004]. It is thus clinically very useful for analysing the entire lung mechanics and predicting disease state [Guyton and Hall, 2000; Puybasset et al., 2000; Rylander et al., 2004].

More specifically, the combination of EEV and the associated compliance is directly related to total Inspiratory Capacity (IC), which essentially determines the maximum amount of air a person can inspire with a single breath. The more air that enters the lung, the more rapidly or likely the gas change can occur. Clinically, one of the symptoms of ARDS is markedly decreased IC [Gattinoni et al., 2001; Pelosi et al., 1996b; Puybasset et al., 1998]. Thus, FRC and the resulting EEV essentially indicates this volume of functional lung, and the associated disease state, providing data that has significant potential clinical use with this model.

The lack of information and uncertainty in lung mechanics also makes it more difficult to make predictions of lung behaviour in response to changes in ventilator therapy. More specifically, because the PEEP-to-PIP PV data is a complete loop on its own, the data is essentially seen as individual data. Therefore, the relationship between different PV loops from the same lung is more difficult to determine. This difficulty may be further exaggerated by the uncertain mechanics caused by dynamic effects during the transition between active inflation and passive deflation.

5.3 Min to Max Method

Another approach to fit the model to clinical data is by simulating the entire inspiratory capacity of the lung. This approach allows the model to capture the entire lung mechanics, rather than just those seen for tidal ventilation. It can therefore show the relative ventilated volume within the entire relevant lung mechanism PV range. Thus, relevant information, such as EEV, is clearly displayed and easily obtained. However, EEV must be known or measured to perform this task.

Figure 5.2 shows an example of the Min-to-Max fitting method using the same clinical data as in Figure 5.1. In this case, the pressure ranges from zero to the maximum, or plateau, pressure. The volume ranges from FRC to the total inspiratory capacity. This method therefore considers the entire inspiratory capacity, and clearly shows the level at which the lung is operating. Finally, note that this approach minimises exposure to the uncertain and dynamic portions of the PV curve at the transition between inspiration and expiration.

More specifically, by fitting the entire inspiratory capacity, the dynamic portion of the PV curve can be avoided. The model and fitting thus focuses on the more certain steady portion of the data, where it most strongly reflects the actual underlying lung mechanics. This approach is potentially much more robust to variations that are unrelated to the true lung mechanics.

This fitting method utilises the relation between tidal volume and the entire lung. Therefore, the trend set by changing ventilator treatments, such as PEEP and tidal volume can be readily captured by the model. This trend can then be used by the model to predict and simulate other ventilator settings. Thus,

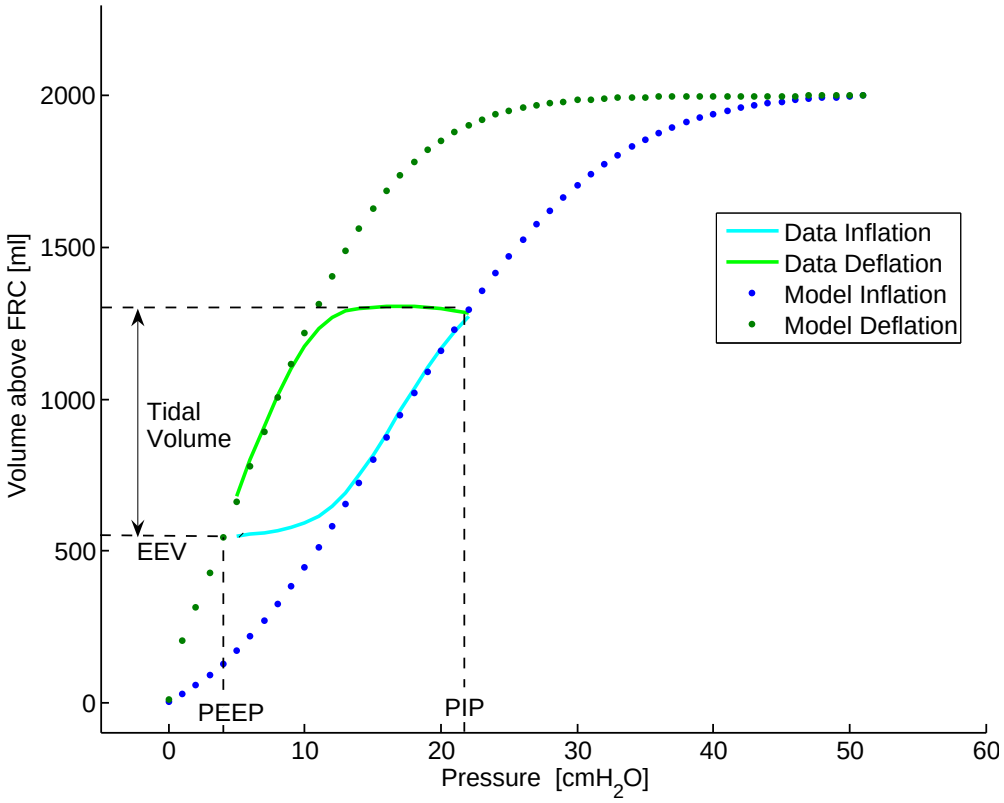

Figure 5.2 An example of Min-to-Max fitting method. The plot shows data for inflation (solid blue), data for deflation (solid green), modelled inflation (dotted blue), and modelled deflation (dotted green). This method fits the entire lung capacity as one, and shows information more relevant in clinical situations.

this approach is potentially more flexible and useful clinically. More specifically, the information it provides is likely to be more directly relevant and valuable in clinical situations. It is also more flexible in its ability to consider different forms of ventilation and more drastic changes in therapy.

Limitations

A major limitation for this fitting method is that it requires data with deflation to FRC. This data is not normally obtained during current protocols for ventilator treatment [Rylander et al., 2004; Stenqvist et al., 2002; Bersten and Soni, 2003]. The measurement can be done simply by deflating the lung to atmospheric pressure. Once the airway is opened to atmospheric pressure, the lung assumes FRC rapidly, and the entire measuring process can be completed in a matter of seconds [Bersten, 1998].

However, this process requires intervention from ICU staff and interruption of the patient's breathing pattern, both of which may be clinically unavailable or undesirable. Furthermore, a typical ventilator is only designed to record data on tidal ventilation, so that recording the deflation to FRC would require either a specialised ventilator or a separate data acquisition system. As a result, inclusion of FRC in PV data has been primarily for a research purpose to date.

This approach uses pressure and volume at maximal possible or likely inspiration to set the maximum pressure and volume for the TP distributions and unit compliance. However, these values are not easily obtainable with any ethically reasonable ventilation protocol. More specifically, the measurement requires the lung to be inflated to maximum capacity. This intervention is most likely to cause further injury to the already damaged lung, and devastating consequences to the patient's condition.

This fitting method therefore uses individually assumed values for maximum pressure and volume within a reasonable range seen in typical clinical observation [Guyton and Hall, 2000; Albaiceta et al., 2003; Lee et al., 2002; Ochs et al., 2004]. A patient specific value may be computed using obtained PV data and a specifically designed program, but it may be computationally intense and time consuming. However, ventilators in normal circumstances will not be operating at these extreme values so that exact values for these peak pressures and volumes may not be necessary in most, if not all, clinical situations.

5.4 Summary

Two different fitting methods were considered due to the different types of PV data usually available in clinical situations. The advantages and limitations of both methods are detailed. Both methods are very similar in the basic approach and use the same generic compliance curve parameters. While the Min-to-Max method utilising EEV is potentially better clinically, this data is not always readily available and requires interruption in ventilator treatment. Subsequent chapters will use both of these methods to validate the overall model mechanics.

Part III

Model Validation and Clinical Use

Chapter 6

Initial Validation Using a Mechanical Simulator

A mechanical lung simulator was developed to demonstrate all the fundamental mechanics in a controlled fashion. Data measured from this system is used to validate the model. The simulator was built using simple equipment and was ventilated through an Endotracheal (ET) tube to include and measure the effect of its resistance.

The simulator was ventilated at several different settings to validate the model and methods for a wide range of compliance, PEEP, and flow rate. The pressure and the flow data were measured and recorded in all cases at every possible combination - many of which would not be feasible clinically - to best validate all the modelled mechanics. Results are analysed to validate the mechanical simulator behavior versus expected and reported physiological behavior in similar conditions. The model was then fitted to the resulting PV data for its validation. This overall approach enables a much more comprehensive initial evaluation and validation against accepted physiological responses.

6.1 Mechanical Simulator Description

The simulator was designed to produce realistic pressure and volume data mimicing the fundamental mechanics of a ventilated patient. The compliance of the simulator can be continuously adjusted for a wide range of lung conditions. Hence, it can more than adequately represent a majority of the fundamental clinically observed dynamics.

The main lung mechanism of the simulator is a Continuous Positive Airway Pressure (CPAP) device (LV300, LifeVent Medical Ltd. Dunedin, New Zealand). This device provides a constant pressure at any volume and allows a continuous adjustment of the pressure by a pneumatic system. Rather than a standard bellows, a rubber anaesthetic bag (APM 50261, Parker Healthcare Pty Ltd, Mitcham, VIC, Australia) was used to simulate the elastic mechanism of the lung. Thus, this device consists of two mechanisms contributing to the total lung compliance. Both mechanisms are inflated and deflated completely by the ventilator, simulating the sedated patient who has no spontaneous breathing.

Figure 6.1 illustrates an overview of the lung mechanism portion of the simulator. The photo shows the rubber bag at close to maximum inflation. The device is ventilated using a standard ICU ventilator (Series 7200, Puritan Bennett, Pleasanton, CA).

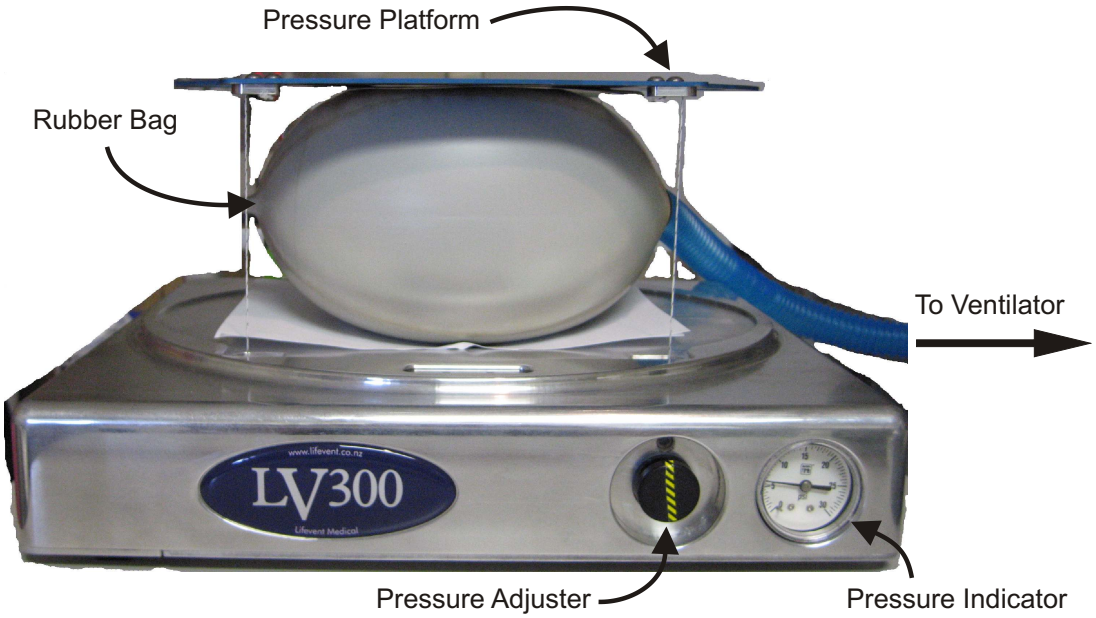

Figure 6.1 An illustration of the mechanical lung simulator. The main mechanism of the simulator was a CPAP device, which applies a constant pressure. A rubber anaesthetic bag was used to include elastic effect of the lung. The device allowed a continuous adjustment of applied pressure, which represent the compliance of the simulated lung.

The device was ventilated through an 8 mm inner diameter Endotracheal (ET) tube (Blue Line®Cuffed Endotracheal Tubes, Portex Ltd. Hythe, Kent, UK) to simulate a realistic patient under mechanical ventilation. It thus offers the opportunity to measure the effect of the ET tube and its resistance, which

is often not available clinically. Pressure was measured before and after the ET tube, representing proximal and carina pressure, respectively. The proximal pressure was measured at the Y-piece of the ventilator connector. The carina measurement was taken using a closed suction system (Ballard TRACH CARE-72, Ballard Medical Products, Draper, Utah), with its tip placed at the end of ET tube. This sensor tube was left in the ET tube for the entire experiment for consistency. Figure 6.2 illustrates the connecting tubes for the simulator.

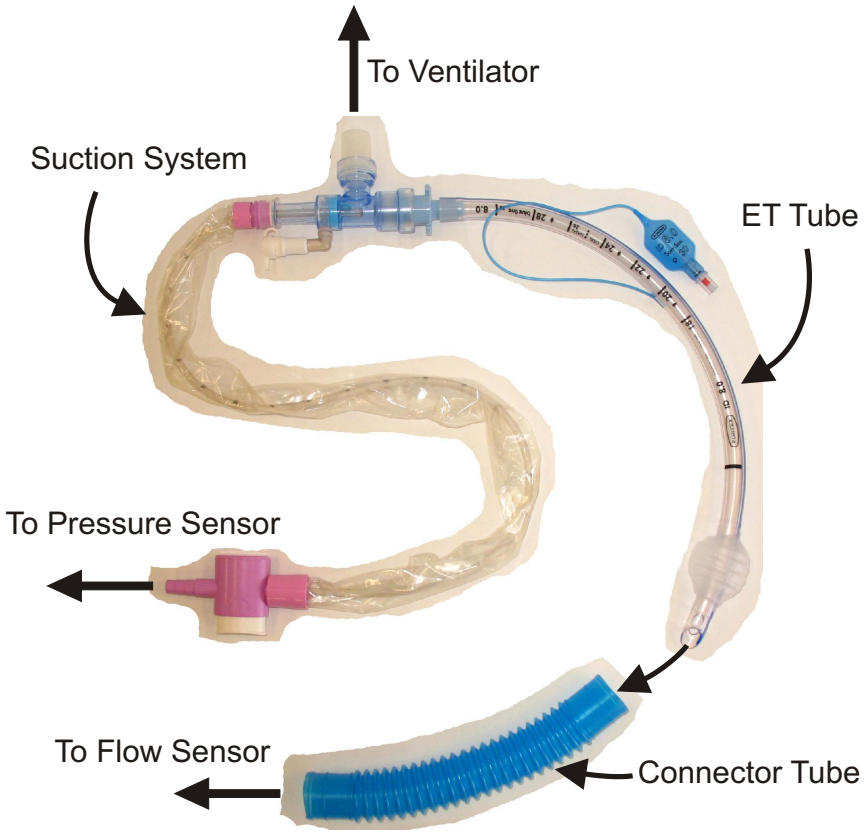

Figure 6.2 An illustration of connectors for the mechanical lung simulator. The ET tube was connected to the closed suction system and the suction tube was inserted to the tip. The carina pressure was measured through the suction tube. The tip of ET tube was inserted and sealed in the connector tube, representing the trachea. The connector tube was then attached to the flow sensor of the calibration analyser.

The ET tube was inserted and sealed in the connector tube, and tested for leaks. The connector tube was then attached to the flow sensor. Pressure and flow data were measured and recorded using a ventilator calibration analyser (RT300, Allied Health Care Products, St. Louis, MO). The analyser consists of a flow sensor and a separate pressure sensor. Thus, when proximal pressure is being measured, the pressure tube from the Y-piece is connected to the sensor and the

connector from suction tube is sealed. For carina measurement, the position of the tube is reversed. All data was downloaded in realtime to a laptop computer (Dell Inspiron 6400, Dell Computers, Austin, TX).

6.1.1 Physiological and Clinical Relevance

Each component in this simulator is designed to represent physiological mechanics, behaviours, or components to closely reproduce the actual lung mechanics. It also includes the airway system from the ventilator to the lung. Thus, this simulator system not only represent the lung, but the entire system of a ventilated patient, as would be seen in most clinical data and situations. Major components and mechanics represented by this simulator include:

Recruitment and derecruitment: The linear compliance produced by the CPAP device fundamentally describes the continuous recruitment and derecruitment of lung units. Several clinical studies have found that the recruitment occurs throughout the inflation matching this appraoch [i.e. Carney et al., 1999; Crotti et al., 2001; Schiller et al., 2003]. Over a normal respiratory pressure range, lung units are recruited as soon as the applied pressure overcomes the superimposed pressure [Gattinoni et al., 2001; Hickling, 1998]. Thus, the rate of inflation due to recruitment is relatively constant. In terms of threshold pressures, this CPAP device, which would closely represent clinical carina data, essentially simulates or provides a nearly uniform distribution of TOP and TCP values.

Elastance: The elastance of lung units are represented by the rubber anesthetic bag. It takes relatively small effort to initially inflate this bag due to its size and shape, and the material itself is not yet being stretched. During this stage, the compliance is essentially governed by the CPAP device. However, once a certain volume is reached, the rubber material starts to stretch and the compliance of the material starts to decrease the overall compliance. Near a maximum size or inflation, where all available units are effectively recruited, the additional pressure starts to stretch the lung units. This behaviour is represented by the increasing stiffness of the bag near maximum size. Thus, the rubber bag describes the compliance of recruited lung units, as well as the decreased compliance at the end of recruitment.

Airway Resistance: Every airway has some level of resistance, including the physiological airways, such as the trachea. Essentially, every airway that is between the ventilator and the actual lung is accounted for in this simulator. The ventilator connector tube is attached to the suction system and to an ET tube, just as in a real clinical situation. An ET tube represents a major resistance in the entire ventilated airway system. Thus, its inclusion is essential given that most clinical PV data is measured proximally. The ET tube is connected to the rubber bag by the connector tube, representing the trachea. The ET tube is sealed inside the connector tube using its own soft seal cuff as it seals a trachea in a real patient.

Variable Compliance: The compliance of a lung depends on patients' individual lung mechanics and their disease condition. Thus, the compliance of a lung varies greatly between patients. The compliance of this simulator is controlled by a continuously variable pneumatic adjuster in the CPAP device. Thus, this device can represent a wide range of compliance with precision. Because the CPAP device represents the recruitment and derecruitment of lung units, adjusting the CPAP device essentially signifies altering the TOP and TCP distribution of the lung for different disease states. This mechanism also conforms to the hypothesis of lung mechanics described in Chapter 2 upon which this model is based.

6.1.2 Experimental Protocol

The ventilator was set to volume controlled mode with a square wave inspiratory flow pattern. The tidal volume was set to a reasonably typical value of 750 ml. These values were kept for the entire experiment for consistency and only PEEP, compliance, and flow rate were varied. These variables were chosen to mimic clinical experience as disease state (compliance) and/or therapy (PEEP and flow rate) evolves.

The lung was simulated at different PEEP levels and compliances to produce a broad variety of data across expected clinical usage. More specifically, three different PEEP levels, 5, 10 and 15 cmH_2O, were simulated and recorded. At

each PEEP, the pressure of the CPAP device was adjusted to produce a realistic compliance and thus a realistic PV curve. The pressures examined and used for the CPAP device were 5, 15 and 25 PSI for PEEP levels of 5, 10 and 15, respectively.

The pressure applied at a PEEP of 15 is considerably higher than at a PEEP of 5, indicating that additional pressure was required to inflate the lung to a similar volume. Physiologically, this represents a stiffer, less compliant lung being treated with higher PEEP, which is one of the prominent features of ARDS [Atabai and Matthay, 2002]. Thus, 3 compliances covering a range from healthy to stiff ARDS lungs were simulated at appropriate or therapeutically relevant PEEP levels.

Four different peak flow rates of 10, 20 40 and 60 litres per minute (LPM), were used and recorded for each set of PEEP. Inspiratory patterns, which result in different flow rates, are often varied as part of evolving ventilation therapy in critical care as clinicians seek to find optimal solutions to maximise recruitment [Edibam et al., 2003]. The respiration rate was set to 10 seconds (6 breaths/min) to allow complete deflation for all flow rates. These experimental input data are summarised in Table 6.1.

Table 6.1 Summary of simulator protocol inputs.

		PEEP [cmH_2O]		
		5	10	15
CPAP pressure [PSI]		5	15	25
Flow Rate [LPM]	10	Proximal Carina	Proximal Carina	Proximal Carina
	20	Proximal Carina	Proximal Carina	Proximal Carina
	40	Proximal Carina	Proximal Carina	Proximal Carina
	60	Proximal Carina	Proximal Carina	Proximal Carina

At each input set, the simulator was ventilated for at least 5 breathing cycles until pressure and volume were stabilised. Two complete breathing cycles were recorded for each input setting. The entire experiment thus produced 24 sets of PV data, including both carina and proximal PV loops for each input.

Volume was calculated by integrating the flow data over time for each data set. A specialised program was written using MATLAB to discretise the PV data at each pressure. The 2 PV loops from each set are then combined into a single loop by taking an average at each pressure point. Finally, the data was smoothed using a 3 point moving average method to eliminate the low level of noise.

Note that the overall process of ventilating, gathering, and analysing the data is designed to mimic, as closely as possible, what might or could occur clinically. Hence, a second goal is to ensure the clinical reality of the conditions and thus the clinical robustness of the methods.

6.2 Simulation Results and Physiological Relevance

Figure 6.3 illustrates an example of raw pressure and flow data. This data is for a data set with PEEP of 5 cmH_2O and flow rate of 10 LPM. The red line shows the pressure and blue line shows flow. The data captures 2 complete cycles of ventilation. Figure 6.4 illustrates the resulting volume, as calculated from the data in Figure 6.3. The resulting PV curve is illustrated in Figure 6.5. The black solid line shows the original raw data and blue and green dashed lines shows processed inflation and deflation data, respectively.

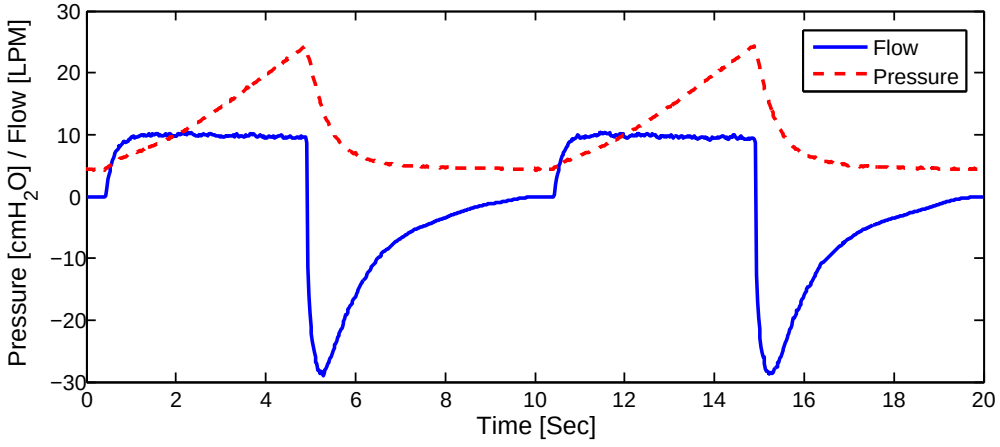

Figure 6.3 An example of raw pressure and flow data. Pressure and flow are measured and recorded for each set of data. These plot shows data set for carina measurement at PEEP=5 cmH_2O and flow rate=10 LPM.

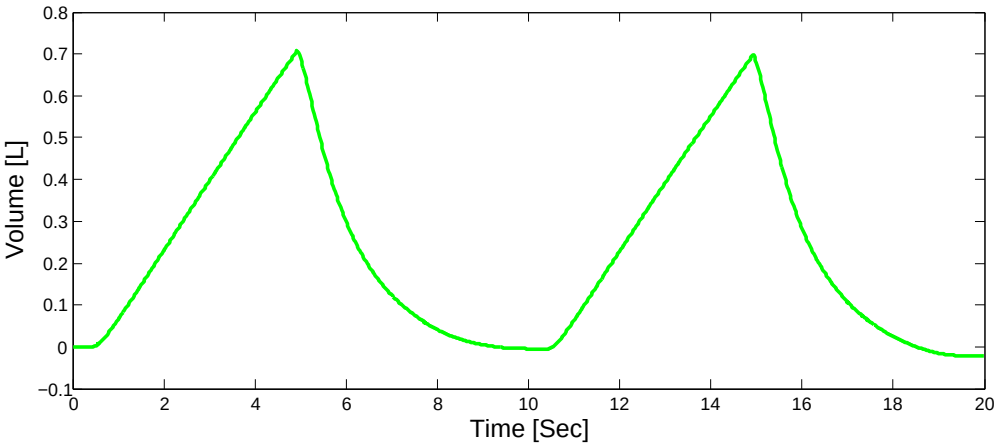

Figure 6.4 An example of calculated volume data. The volume is calculated by integrating the flow. The plot shows data set for carina measurement at PEEP=5 cmH_2O and flow rate=10 LPM. The volume is thus a result of integrating the data shown in Figure 6.3.

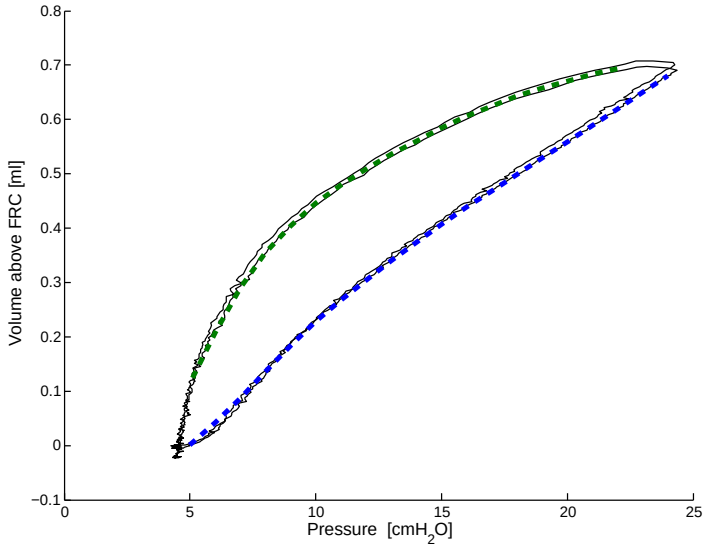

Figure 6.5 An example of resulting raw and processed PV data. The pressure and volume data were discretised, combined into a single loop, and smoothed for ease of fitting process. The black solid line shows the original raw data and blue and green dashed lines show processed inflation and deflation data, respectively. This plot shows the data set for PEEP=5 cmH_2O and flow rate=10 LPM.

The relatively high noise level at lower volume in the raw PV data is caused by the concentration of sampled points and the diminishing sensitivity of the flow sensor at low values. Due to the nature of inflation and deflation mechanics, and the relationship between pressure and volume, there are more data points at lower volume in the PV loop for data with a constant sample rate. Furthermore, the sensitivity of the flow sensor decreases at a low flow causing the noise level to increase, especially at the end of deflation, where the flow nears zero. This effect

is noticeable even in this near perfect simulator environment, as compared to a real clinical situation where greater noise might be encountered.

Effect of ET Tube Resistance

The effect of ET tube resistance was analysed using the multiple measurements available from the mechanical simulator. Pressure measurements were taken before and after the ET tube, representing the proximal and carina pressures, respectively. The proximal pressure includes the effect of ET tube resistance, however this data is often the only data available for a mechanically ventilated ICU patient. In contrast, the carina measurement at the tracheal end of the ET tube reflects the more accurate true lung mechanics, especially at higher flow rates [Karason et al., 2001]. However, in most cases, this measurement requires additional invasive sensors and equipment. Thus, this measurement is only taken in special circumstances or for research purposes [Karason et al., 2000; Sondergaard et al., 2002; Stenqvist, 2003].

Figure 6.6 illustrates the pressure and flow measurements at the carina of the mechanical simulator for the data set with PEEP of 5 cmH_2O and a flow rate of 60 LPM. Compared to the 10 LPM flow rate in Figure 6.3, the inspiratory time is significantly shorter because the target volume is reached more quickly due to the increased flow rate. Figure 6.7 illustrates proximal pressure and flow data from the same data set. The inspiratory pressure in Figure 6.7 is almost twice as high as the carina measurement in Figure 6.6, indicating the significant contribution of the resistive effect at this higher flow rate.

Finally, the effect of the resistance is also clearly illustrated in the PV loops in Figure 6.8, where the outer loops are the proximal measurements and the inner loops are the carina measurements for each plot. The figure includes PV loops for all 4 flow rates. The proximal PV loops were similarly and significantly different for other flow rates. For example, the data for 10 LPM illustrated in the top left plot, shows minimal differences in PV data during inflation as the lower flow rate induces lower flow resistance based on standard fluid mechanics [Zamir, 2000]. This lesser difference during the inflation limb increased as the flow rate increased, as illustrated in the top right plot for 20 LPM, the bottom left plot for 40 LPM, and the bottom right plot for 60 LPM in Figure 6.8. This trend clearly indicates the strong dependence of resistance on the flow rate.

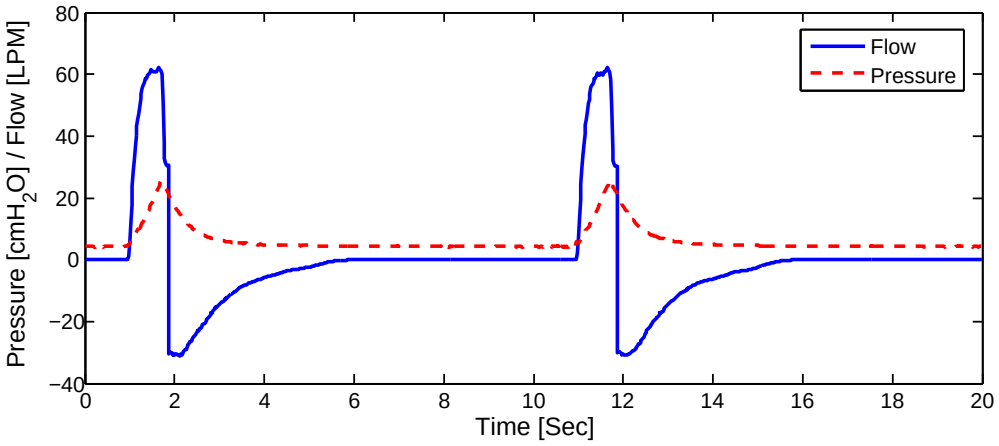

Figure 6.6 An example of raw pressure and flow data at carina. This plot shows the data set for PEEP=5 cmH_2O and flow rate=60 LPM.

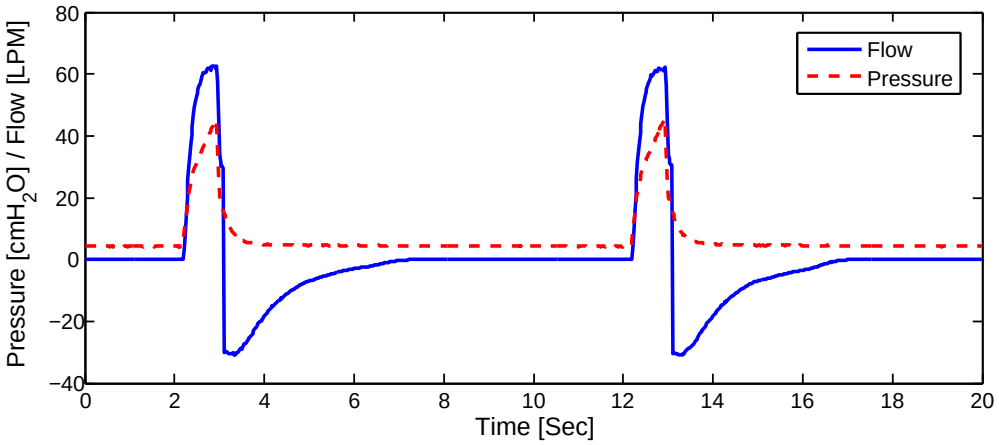

Figure 6.7 An example of raw pressure and flow data at proximal. This plot shows the data set for PEEP=5 cmH_2O and flow rate=60 LPM.

In contrast, the deflation limbs essentially do not vary for different flow rates, as illustrated in Figure 6.9. This lack of difference is caused by the uncontrolled passive nature of the deflation process. The varying flow rates only control the flow rate for the inflation portion. During deflation, the applied pressure is simply reduced to PEEP at the beginning of deflation and the air flows out passively. Since the volume inside the simulator and the carina pressure is similar at the end of inflation for all flow rates, the deflation proceeds at the same rate for all flow rates as a function primarily of the outlet size and pressure. However, there are significant differences between proximal and carina deflation measurements, especially at the beginning of deflation where the flow is the highest, as best illustrated in Figure 6.8.

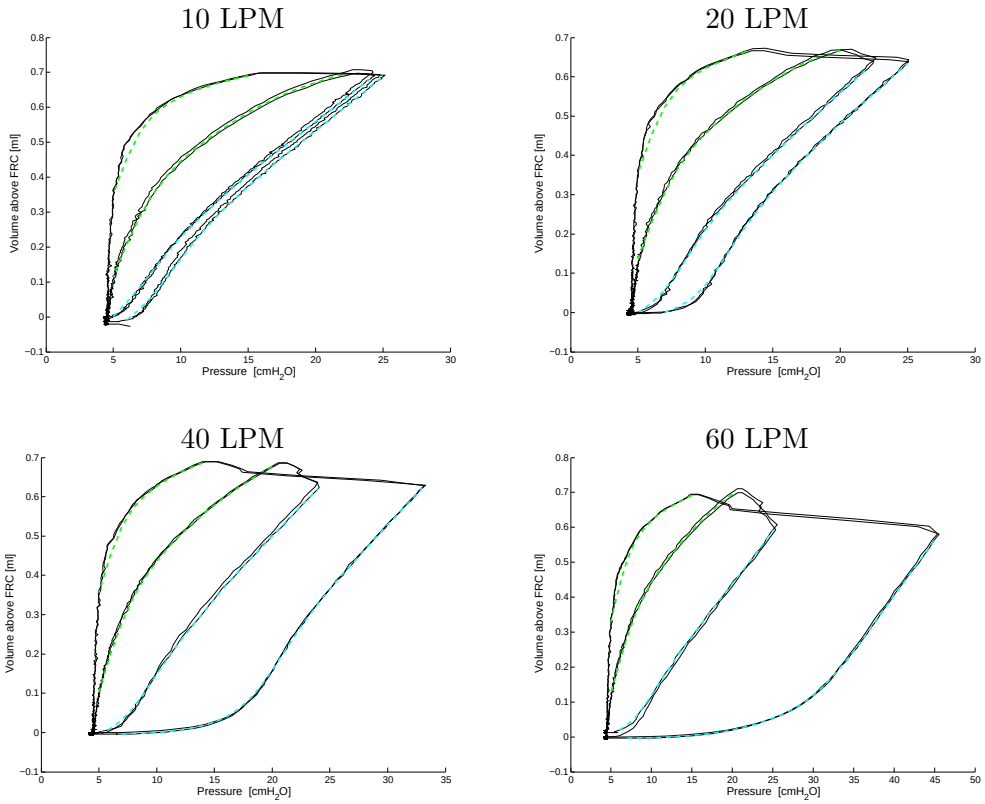

Figure 6.8 The resistive effect of the ET tube. These plots illustrate the differences between carina and proximal measurement for all flow rates. The outer PV loop is the proximal and the inner loop is from the carina measurement. The significant difference in pressure between the data are a direct result of the resistance in the ET tube.

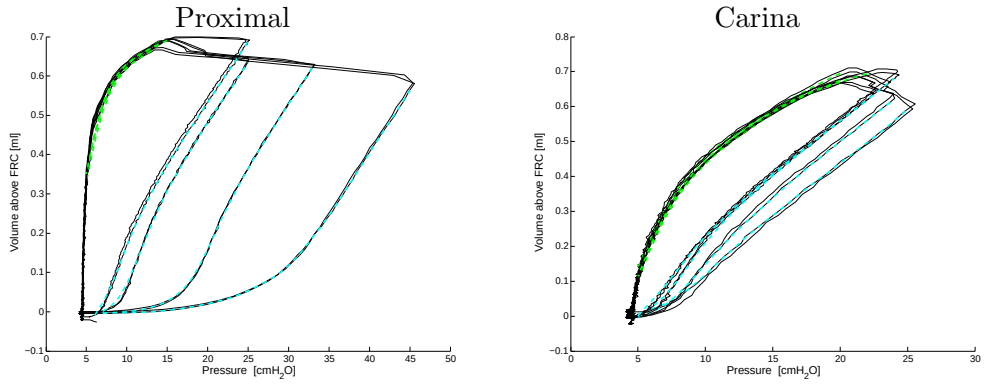

Figure 6.9 Carina and proximal PV data for all 4 flow rates. In contrast to proximal PV data in the left plot, the carina PV data on the right show significantly less differences between different flow rates.

Karason et al. [2000] have conducted a similar experiment on both a mechanical lung model and actual patients. They reported similar results and conclusions on flow and resistance through an ET tube. Figure 6.10 illustrates an example of the resulting plots from the study. These plots show PV data for a patient who is ventilated at 20 breaths/min, PEEP of 8 cmH_2O, I:E ratio of 1:2, and

the ventilator is volume controlled. Different tidal volumes of 4, 8, and 12 ml/kg were used in this particular data set. Because the respiration rate and the I:E ratio is kept constant, higher tidal volume leads to a higher flow. Thus, this result is comparable to the CPAP simulator results where different flow rates were simulated.

The plot for 4 ml/kg shows a relatively small difference between the proximal Y-piece and tracheal carina loops during inflation, while at 12 ml/kg, the difference is significant. On the deflation limb, the overall relative shape between proximal and carina loops is unchanged. These features are closely matched by the CPAP model, as illustrated in Figure 6.8. Thus, this comparison further demonstrates the model's validity to simulate realistic lung mechanics.

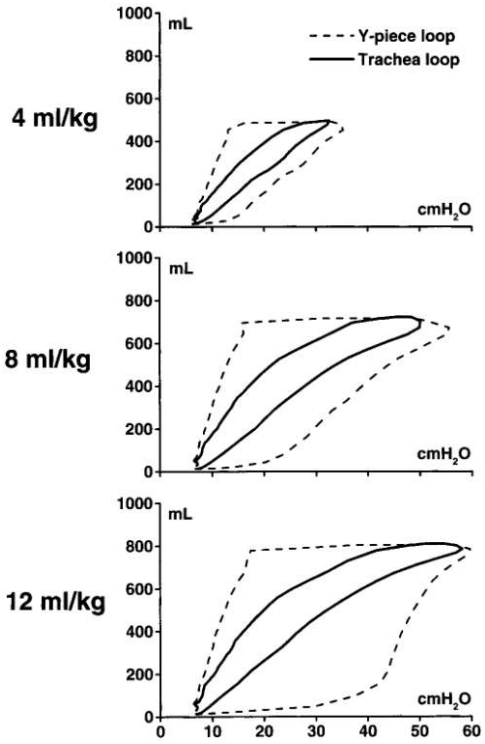

Figure 6.10 An example result from study conducted by Karason et al. [2000]. The plot shows PV loops for Y-piece and tracheal measurement for different tidal volumes. Because respiratory rate was kept constant, the flow rates were changed between different tidal volumes. The CPAP model closely matches this clinical data.

The carina PV data shows very small differences between different flow rates compared to the proximal PV data. Figure 6.9 clearly illustrates this minimal difference. This similarity in carina PV data suggests that the mechanism of the simulator is relatively stable. It can also be concluded that, in this experiment, most of the differences are caused by the resistive force in the ET tube.

6.3 Lung Model Fitting Results and Clinical Relevance

The results of Section 6.2 indicate that the mechanical simulator is a clinically valid representation of the major lung mechanics. In this section, it is used to initially validate the lung model by fitting it to the same measured mechanical simulator data and analysing the result. The model was fitted to each set of data. PEEP-to-PIP fitting of Section 5.2 was used because the data did not include the deflation to FRC, and thus no EEV measurement.

The number of modelled units was fixed to 100,000. This number was chosen partially to simplify the identification of the unit compliance curve. The maximum volume for unit compliance was determined from the maximum volume of the simulator, which for this case is equal to a tidal volume of 750 ml. The maximum unit volume was thus, determined to be 0.0075 ml. This number multiplied by the total number of units equals the maximum volume of the lung. However, for some data, the maximum volume was slightly reduced, by about 7% on average, because the lung volume did not reach the target 750 ml in the simulation. This loss of volume is caused by the differences in the data measured at the simulator and the ventilator sensors due to the flexible and compliant tubes of the ventilator circuits.

Two different fitting errors were calculated for each data set. The first error is the pressure point error, where the absolute difference in volume was determined at each pressure point between the mechanical simulator data and the fitted model. The average absolute error was calculated for inflation and deflation separately. The second error is the Work of Breathing (WOB) error. The area inside the PV curve represents the work of breathing done by the ventilator and is a clinically useful metric [Straus et al., 1998; Kallet et al., 2006; Maeda et al., 2003]. The difference in the area between the simulator PV and the model PV is presented as a percentage of the mechanical simulator "clinical" data.

Fitting Results

The model was able to fit all the data well. The average inflation pressure point error for proximal measurement was approximately 13 ml (1.8%) and approximately 18 ml (2.4%) for deflation. The carina average error was approximately 12 ml (1.6%) and 11 ml (1.5%) for inflation and deflation, respectively.

The average work of breathing error was about 11% for proximal measurement and 5% for carina measurements. This error data is summarised in Table 6.2.

Table 6.2 Summary of model fitting error for simulator data. Inf=Inflation; Def=Deflation; WOB=Work of Breathing.

		Proximal			Carina		
PEEP	LPM	Inf [ml]	Def [ml]	WOB [%]	Inf [ml]	Def [ml]	WOB [%]
5	10	19.07	12.30	5.25	6.59	16.10	0.36
	20	18.59	5.91	10.52	8.55	11.14	5.08
	40	18.48	13.57	5.90	14.62	11.91	10.40
	60	5.18	15.42	9.10	11.45	16.70	4.33
10	10	25.79	32.74	22.97	16.65	9.47	5.74
	20	16.79	13.73	5.45	15.29	10.27	11.33
	40	12.60	24.83	28.29	15.12	13.24	7.43
	60	6.04	27.25	3.37	17.82	17.43	7.36
15	10	7.39	13.64	5.01	6.83	7.86	3.04
	20	13.80	13.53	12.74	6.13	4.81	2.22
	40	9.62	21.23	18.32	8.99	5.95	4.00
	60	4.99	18.22	3.64	12.54	6.58	2.13
Average		13.19	17.70	10.88	11.71	10.95	5.29

The top plots in Figure 6.11 illustrate the model fit (left) to the carina data with PEEP of 5 cmH_2O and a flow rate of 10 LPM and its associated TOP and TCP distribution (right). The bottom plots illustrates the same data at 60 LPM. The only significant difference is the 10 LPM inflation data shows a slight shift towards lower pressure, which is also evident in the lower TOP mean.

Clinically, these shifts in TOP and changes in recruitment over pressure are typical and provide PV slopes like those in Figure 6.11. In addition, these differences over flow rate match the results of clinical studies where faster flow and inflation rates lead to lower compliance [e.g. Edibam et al., 2003] and thus recruitment. Hence, these results in Figure 6.11 are validated clinically, as well as the model's ability to capture these relevant trend in terms of recruitment status.

Figure 6.12 illustrates the model fit to the proximal data for PEEP of 5 cmH_2O and flow rates of 10 and 60 LPM with associated TOP and TCP distributions. The top plots show the fitting results for the 10 LPM data and the bottom plots show the same results for 60 LPM data. There is much more significant difference in the proximal TOP distributions, where the majority of TOP

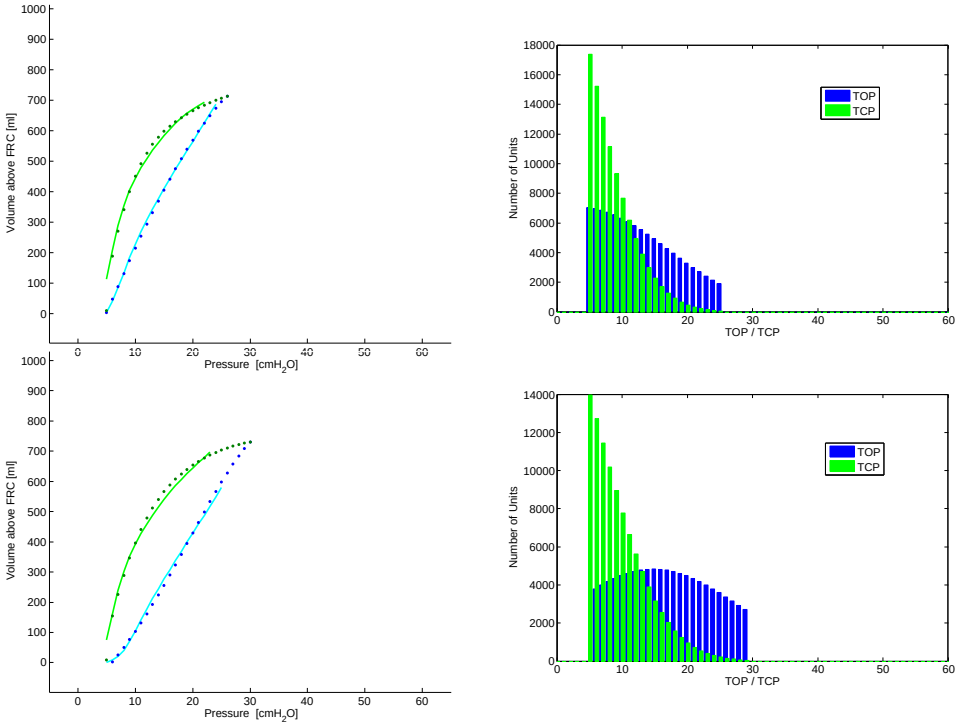

Figure 6.11 Carina data model fit for PEEP: 5 cmH_2O, Flow rate: 10 and 60 LPM. The plots on left show the model fit to the simulator data with 10 LPM (top) and 60 LPM (bottom). Solid lines represent the simulator data and the dotted lines are the resulting fitted model. The associated threshold pressure distributions are shown on the right.

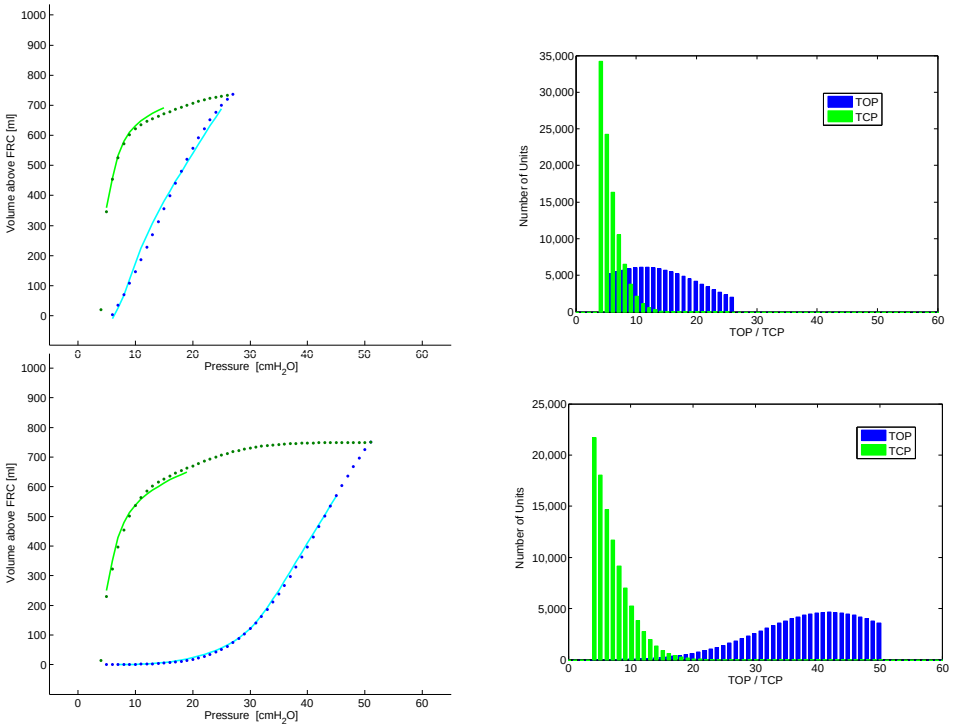

Figure 6.12 Proximal data model fit for PEEP: 5 cmH_2O, Flow rate: 10 and 60 LPM. The plots on left show the model fit to the simulator data with 10 LPM (top) and 60 LPM (bottom). Solid lines represent the simulator data and the dotted lines are the resulting fitted model. The associated threshold pressure distributions are shown on the right.

for data with 60 LPM are located at much higher pressures compared to the 10 LPM case. This significant difference is caused by the higher proximal resistance associated with the higher flow. The TCP, however, shows only slight differences between 10 and 60 LPM indicating the uncontrolled, passively deflating lungs. Finally, this model clearly captures the essential features of each data set and the clinically significant recruitment features associated with each case.

Similar results are seen for all the other cases, as illustrated in Figures 6.13 - 6.15. In these figures, only the fitted model results are shown. However, all the cases show very small errors in the same order as the sensor error. Hence, the model is able to accurately match the full range of data provided by the simulator and with the same clinically expected recruitment features in the TOP and TCP distributions.

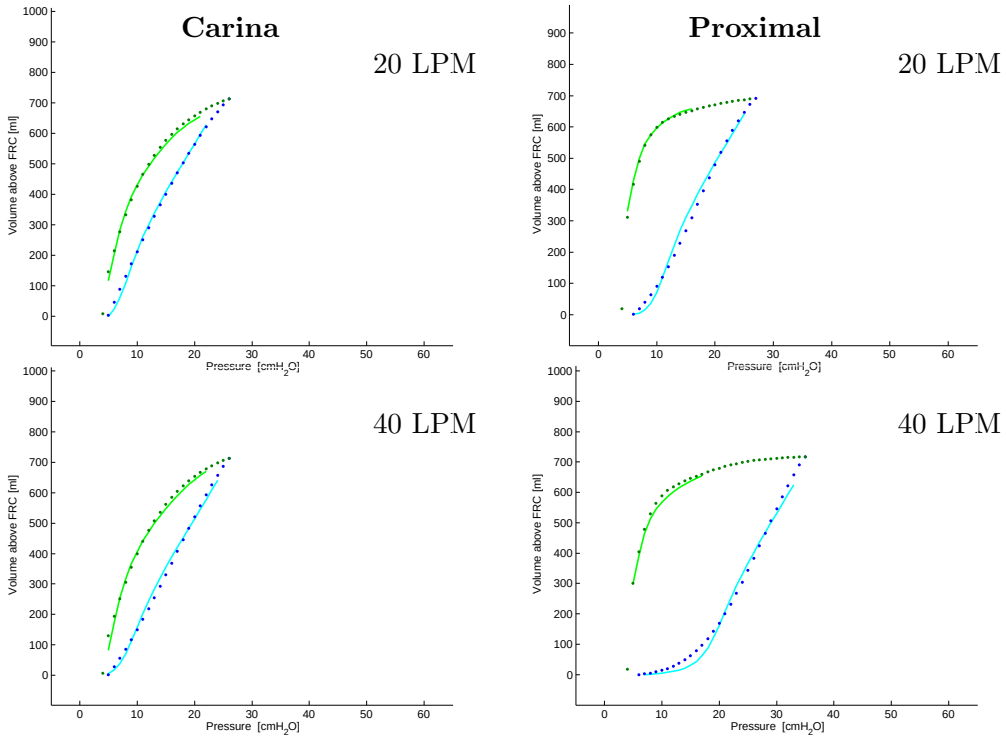

Figure 6.13 Model fit for PEEP: 5 cmH_2O, Flow rate: 20 and 40 LPM. Carina and proximal measurements are illustrated on the left and the right column, respectively. The top row shows data with 20 LPM and the bottom row shows 40 LPM.

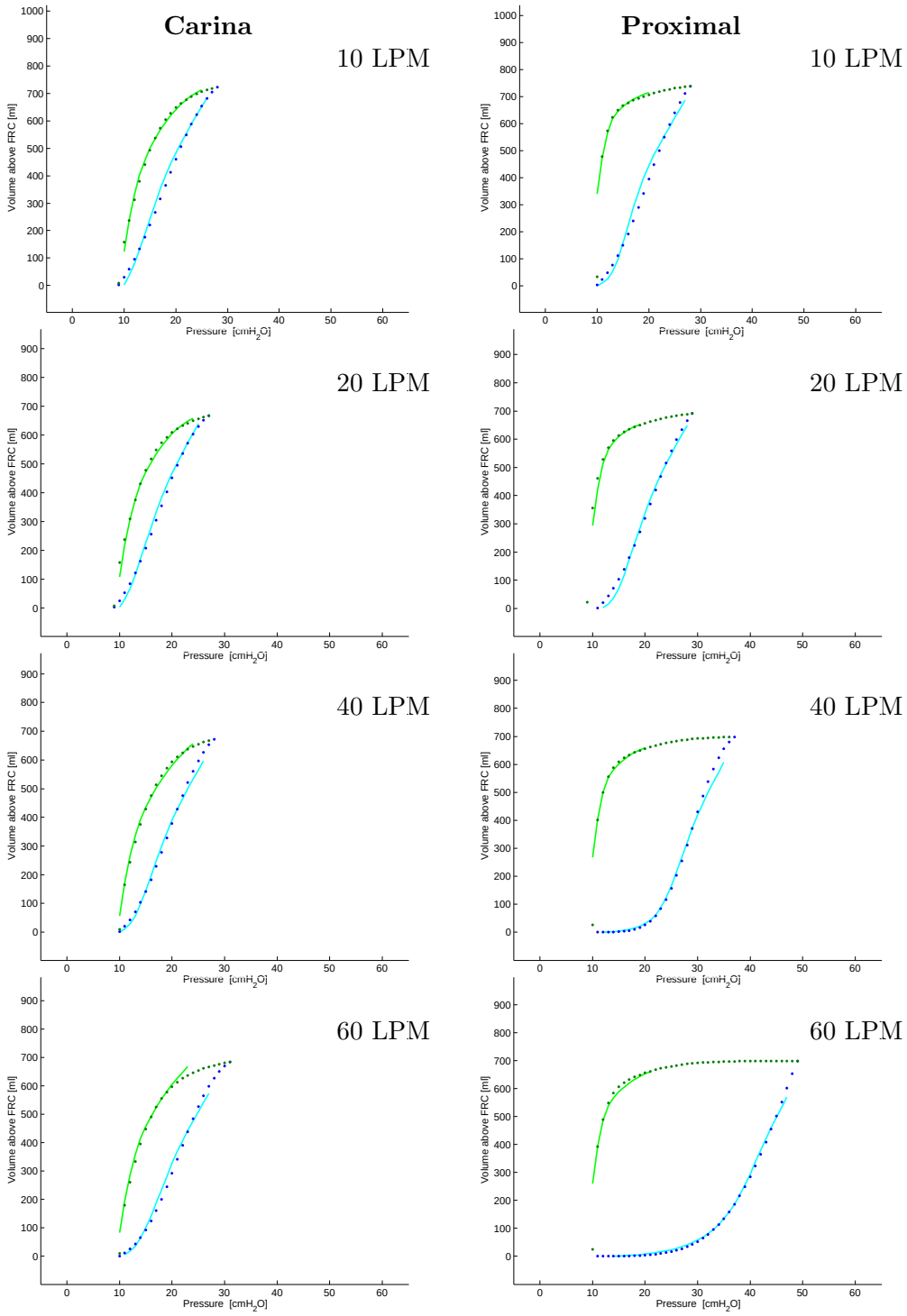

Figure 6.14 Model fit for PEEP=10 cmH_2O. Carina and proximal measurements are illustrated on the left and the right column, respectively. The data with a flow rate of 10, 20, 40, and 60 LPM are shown on first, second, third, and fourth row, respectively.

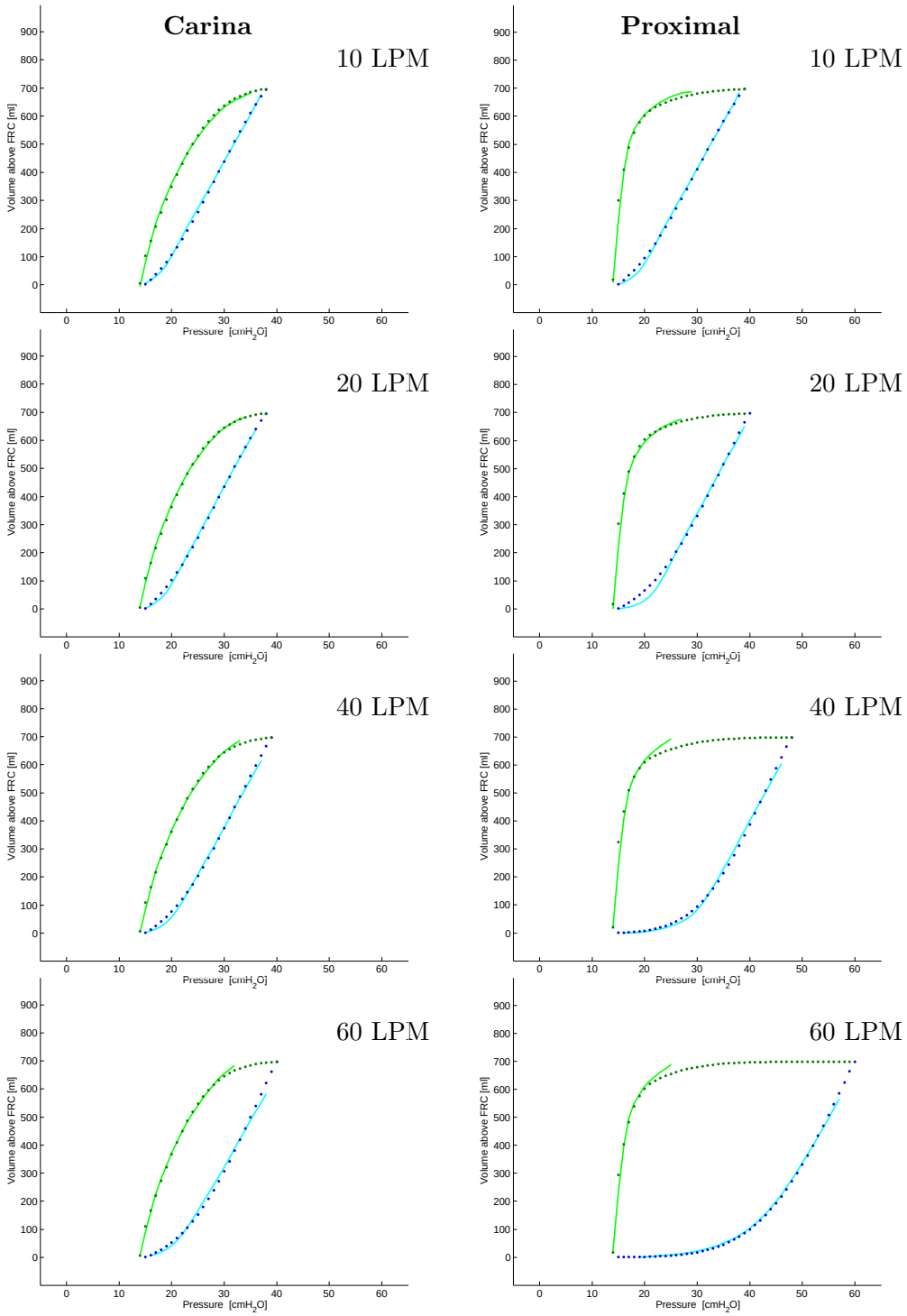

Figure 6.15 Model fit for PEEP: 15 cmH_2O. Carina and proximal measurements are illustrated on the left and the right column, respectively. The data with a flow rate of 10, 20, 40, and 60 LPM are shown on the first, second, third, and fourth row, respectively.

6.4 Discussion and Limitations

The simple mechanical lung simulator developed using the CPAP machine produces realistic data that matches fundamental clinical observations in terms of pressure, volume, and their relationship. Because it is ventilated by a standard ventilator, the result is directly comparable to the actual patient situation seen in the ICU. Furthermore, the simulator was able to clearly show the effect of the ET tube resistance and thus how it might be readily approximated or estimated for clinical use where carina measurements are not typically available. This latter result is also valuable for validating the versatility of the lung model in its ability to fit both proximal and carina data sets. Overall, the results showed that the lung model can be applied to a variety of different clinically relevant situations.

The model was able to fit all data sets well. The maximum average pressure point error was about 18 ml, or less than 3% of the tidal volume. The average WOB error was about 11% of the original data. The model was also able to capture the key clinical features of the PV curve, such as the LIP and compliance. This validation clearly showed the model's ability to fit a variety of different PV data. Furthermore, the model was able to fit the data both with (proximal) and without (carina) ET tube resistance. Thus, the model can be used for further clinical validation on clinical lung mechanics using data directly from the ventilator. This versatility could also broaden the application of the lung model from the clinical bedside decision support tool to medical research applications.

There are a few limitations to the mechanical simulator and these results. Due to the size of the rubber balloon, the volume range for which the simulator can produce clinically reasonable values is small. It cannot be used, for example, to simulate the entire inspiratory capacity of the human lungs. This limitation also implies that it cannot simulate the same lung with significantly different PEEP or tidal volume, because simulating the same lung requires keeping the compliance of the CPAP machine at the same value. Thus, increasing PEEP or the tidal volume also increases the total volume of the simulator, reaching the volume limit in this case.

However, this problem may be solved by using a larger specialised balloon, or multiple devices connected to a single ventilator [e.g. Chase et al., 2006]. In addition, it was not the goal of this simulator to simulate the same patient mul-

tiple ways. More specifically, the goal was to simulate clinically reasonable PV loops across a broad range of compliance, PEEP, and flow rate. In this latter task, it was successful, but would require some added design to be a more specific patient model.

The resistive force in the ET tube derived in this experiment is not the exact resistive force of a clinically typical ET tube. This experiment used a closed suction system to measure the pressure at the carina. Thus, the suction tube was inside the ET tube throughout the experiment, which would not be the case during normal ventilation clinically. More specifically, the diameter of the suction tube was about 4 mm and the ET tube used had an inner diameter of 8 mm. The presence of the suction tube reduced the effective cross sectional area, thus increasing the resistance in the simulated airway. Therefore, the values obtained are only valid in this, or a similar, configuration for clinical tracheal measurements at the carina. However, similar configurations to this method have been used in clinical studies [e.g. Karason et al., 2000, 2001].

The most significant limitation of using simulated data for validating the model is, simply, that the data is not actual clinical data. Mechanical simulation data has the advantage that it is easy to obtain and closely match that of actual clinical data and expectations. Furthermore, the simulator can be adjusted to produce a variety of different data sets over a clinically reasonable range, thus it is suitable for initially validating the versatility of the model. However, for this model to be clinically applied and useful, the actual clinical data and analysis are essential to fully validate the model.

6.5 Summary

A mechanical lung simulator was developed to initially validate the model. The simulator was ventilated using a standard ventilator and produced realistic values, closely matching clinical observations. It also clearly illustrated the effect of flow resistance due to the ET tube for cases using proximal measurement. The model was fitted to the simulator data using the PEEP-to-PIP fitting method because the deflation to FRC was not included in the data matching the more typical clinical scenario. The model was able to fit all the data with minimal error. It

captured the key features of each data set, both proximally and at the carina. These results clearly demonstrate the model's versatility to fit different types of clinical data, and capture clinically relevant trends and features. However, the simulator results cannot be a substitute for actual clinical data and validation.

Chapter 7

Validation on Basic Clinical Data

Following the mechanical simulator validation of fundamental mechanics, this chapter further validates the lung model using clinical data from the over-inflation study of Bersten [1998]. The clinical data in this study were taken at different PEEP settings for each patient, and each measurement included an EEV measurement. The model is thus further validated by fitting the patient and their clinical trends over change in therapy, rather than fitting individual PV loops.

Trends produced by different PEEP values are modelled by shifting the mean of the identified threshold pressure distribution, as discussed in more detail in Section 7.2 and previously in Chapter 3. All other patient specific parameters, such as number of units, were fixed. Hence, only the TP distributions are identified. The model was able to fit the data well, and the expected clinical trends produced by changing PEEP are also closely captured in comparison to reports in the medical literature.

7.1 Patient Data

There are a total of 12 patient data sets. All come from different patients with various levels of lung injury. All of the data sets include at least 3 different PEEP levels with an associated deflation to FRC measurement. Data was sampled for 60 sec at 100 Hz for each PEEP level, with the last 15 to 20 sec used for the FRC measurement. Figure 7.1 illustrates an example of the raw clinical data. Further details of the experimental methods are in the report by Bersten [1998].

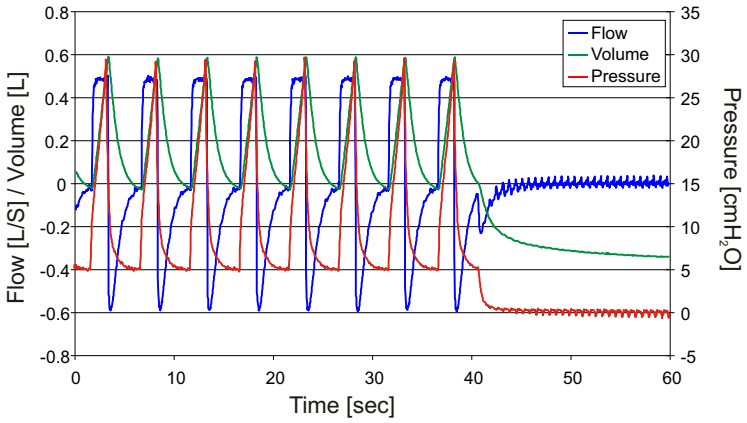

Figure 7.1 An example of raw pressure, flow, and volume data. The data is taken for a total of 60 sec at 100 Hz. THe last 15 to 20 sec are used for deflation to FRC measurement.

While the deflation to FRC measurement was included in these data sets, a typical ventilator does not measure this absolute lung volume because it only monitors the flow. Hence, the volume is calculated from the flow and only the tidal lung volume is available. Therefore, a specific intervention is necessary for this lung capacity measurement. For this data, after about 40 sec of tidal ventilation, the ventilator pressure was reduced to zero, or atmospheric for the patient. The lung then deflates, and settles at FRC in about 10 to 15 seconds. FRC is thus essentially the relaxed lung volume at atmospheric pressure.

As a result, the non-zero volume at the end of expiration (EEV) that is caused by PEEP can be calculated by deflating the lung to the FRC. Hence, this maneuver does not determine the actual value of FRC, but it provides the value required to determine EEV, creating a more mechanically accurate PV loop. Note that some studies report the EEV at a given PEEP, instead of atmospheric, as FRC, causing some potential confusion [e.g. Rylander et al., 2004].

This information on EEV can lead to a better understanding of the overall lung mechanics. Figure 7.2 illustrates the last 25 seconds of a measured data. The FRC measurement starts after 40 seconds, at which point the pressure is decreased to atmospheric pressure, and the volume gradually assumes FRC. It is clear that in this example a steady state FRC is approximately 0.5 litre below EEV. Thus, a total lung PV loop of this data would start with EEV of 0.5 litre.

The clinical data were all processed in the same manner as the mechanical simulator data in Chapter 6. First, the PV data were separated into inflation and

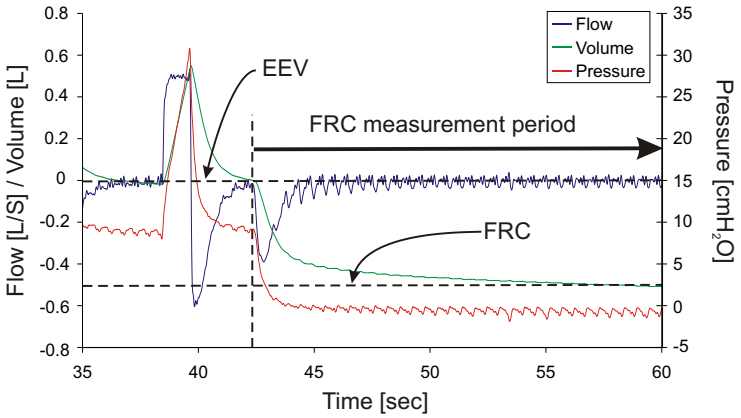

Figure 7.2 An example of illustrating deflation to FRC measurement. After about 40 sec of tidal ventilation, the airway pressure is decreased to atmospheric pressure. The lung is, then, deflated and settles at FRC.

deflation limbs. This separation allows the model to treat them separately and avoids continuous processing of the highly dynamic transition area. The PV data were discretised by pressure for all recorded breaths at a given PEEP level, and then combined into a single curve by averaging. Finally, the data were smoothed using a 3 point moving average method.

Figure 7.3 illustrates the PV loops obtained from the raw data with the superimposed processed data. The "tail" portion of the raw data is the result of the EEV measurement. Table 7.1 summarises the data according to PEEP levels with associated tidal volume and EEV. Note that while each patient is treated similarly, there is also typical clinical variation between patients.

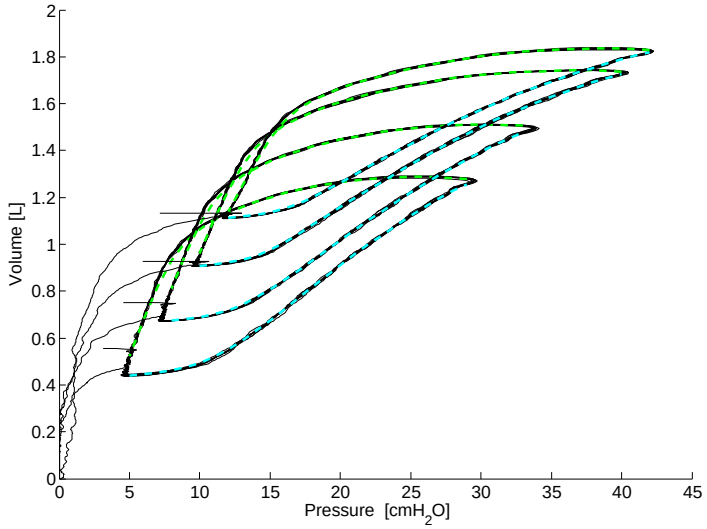

Figure 7.3 An example of a set of PV data and processed data. The plot shows a set of PV data from Data Set 10 (solid black line) with processed inflation (blue dash line) and deflation (green dash line) data. This data includes 4 different PEEP settings and the non-zero EEV, determined from FRC measurement.

Table 7.1 Summary of key values of clinical data.

		PEEP [cmH_2O]					
Data Set		0	5	7	10	12	15
1	Vt [L]		0.846	0.836		0.722	
	EEV [L]		0.441	0.674		1.113	
2	Vt [L]	0.748	0.756		0.739		
	EEV [L]	0.050	0.549		1.085		
3	Vt [L]		0.664	0.664	0.653		
	EEV [L]		0.358	0.467	0.651		
4	Vt [L]		0.803	0.777	0.781		
	EEV [L]		0.243	0.430	0.655		
5	Vt [L]		0.827	0.822	0.800	0.773	
	EEV [L]		0.253	0.344	0.464	0.623	
6	Vt [L]		0.578	0.579	0.566	0.565	
	EEV [L]		0.152	0.263	0.498	0.659	
7	Vt [L]		0.749	0.746	0.762	0.760	
	EEV [L]		0.738	1.070	1.561	1.889	
8	Vt [L]		0.794	0.788		0.771	
	EEV [L]		0.400	0.721		1.307	
9	Vt [L]				0.711	0.789	0.773
	EEV [L]				1.003	1.231	1.501
10	Vt [L]		0.846	0.836	0.833	0.722	
	EEV [L]		0.441	0.674	0.909	1.113	
11	Vt [L]		0.853	0.847	0.846		
	EEV [L]		0.499	0.772	1.149		
12	Vt [L]		0.800		0.817		0.853
	EEV [L]		0.116		0.330		0.596

7.2 Parameter Identification

Because the data include the deflation to FRC, the Min-to-Max fitting method of Section 5.3 is used. This fitting method allows modelling of the entire range of lung operation. It also contains information on the EEV level of the tidal ventilation for each PEEP setting. Thus, it can illustrate the effect of PEEP more clearly.

The model was fitted only to the non-dynamic section of the data on each limb of the breathing cycle as discussed above. Accordingly, the fitting error was also calculated only for the region where the model was fitted. The error was

calculated for each pressure point and the difference between the clinical data and the model fit is presented as both an absolute value and as an absolute percentage of the clinical data.

Unit Compliance and Number of Lung Units

The maximum volume of a unit was fixed to a predefined value for all data sets. Physiologically, the individual size of alveoli does not vary significantly between different sized lungs. Instead, the volume of the lung simply depends on the number of alveoli [Ochs et al., 2004]. Thus, the maximum unit volume was fixed, since it represents the individual size of generic lung units.

However, not all lungs have the same total volume. Therefore, the number of lung units was adjusted to match the total inspiratory capacity (IC). The value of the IC can be estimated from clinical studies, however in this validation study the number of units were varied as one of the model parameters. This arrangement makes the fitting process simpler, and physiologically more accurate. For this model validation, the maximum unit volume was fixed to 0.01 ml, which provides sufficient resolution and simplicity of calculation.

The unit compliance curve for this validation study was described using a cumulative distribution function. The function can produce the identical shape of Equation 4.4 and is still described with the same 4 parameters as the sigmoid function. However, the curvature is now described by a standard deviation instead of the power of the curvature. These choices are, as noted, mathematically interchangeable.

The overall lung mechanics are thus described by 2 distribution functions over pressure. Specifically, a redefined lung unit compliance curve, and the TOP and TCP distributions describing the total lung behaviour. This switch enables a simpler operation for the grid search identification methods, while having no effect on the overall role of unit compliance or model behaviour. For this clinical validation study, all parameters for the unit compliance curve were kept constant for all data sets.

Several clinical studies hypothesised that the primary mechanism describing lung mechanics is recruitment and derecruitment, rather than expansion and contraction of lung units [e.g. Carney et al., 1999; Schiller et al., 2003]. This is

also discussed in Chapter 2. This model is designed to conform to this hypothesis. Furthermore, prior to using fixed unit compliance curves, a grid search was performed for all parameters, including unit compliance parameters. The results showed that the unit compliance parameters have significantly less effect on the overall fit compared to the threshold pressure distributions.

More specifically, Figure 7.4 shows the effect of unit compliance standard deviation and threshold pressure standard deviation on the total fitting error for inflation limb of Data Set 1. The threshold pressure parameters show a clear minimum value within the range, while the unit compliance parameters show almost no effect on the error. These results indicate that the overall error is insensitive to the unit compliance parameters, and varying these parameters does not result in a clearly distinguishable better fit. Figure 7.5 illustrates the comparison between threshold pressure SD and unit compliance mean, with similar results. Finally, Figure 7.6 illustrates the comparison between unit compliance mean and the total number of lung units. The total number of units has a clearly distinguished minimum error, indicating the importance of this parameter on total lung mechanics.

Overall, it can be seen that the unit compliance curve has very small influence on the model fit. Hence, it is held at generic values. For this validation, the mean of the curve was fixed to 0 cmH_2O, the standard deviation was fixed to 2, and the maximum volume was fixed to 0.01 ml, as stated previously. In addition, from Figure 7.6, the total number of lung units is fixed to an identified patient specific values. This approach leaves only the TOP and TCP distribution parameters to be identified for each PEEP level.

Threshold Pressures

Clinically for a given patient, a PV loop with higher PEEP shows an upward shift in volume, as well as pressure, from curves at lower PEEP as illustrated in Figure 7.3. Thus, the data shows a significantly higher volume at a given pressure for a higher PEEP compared to a lower PEEP value. This trend cannot be modelled by a single set of TP distribution parameters, because a single set can only produce a single set of inflation and deflation curves and any tidal ventilation modelled is superimposed on these curves.

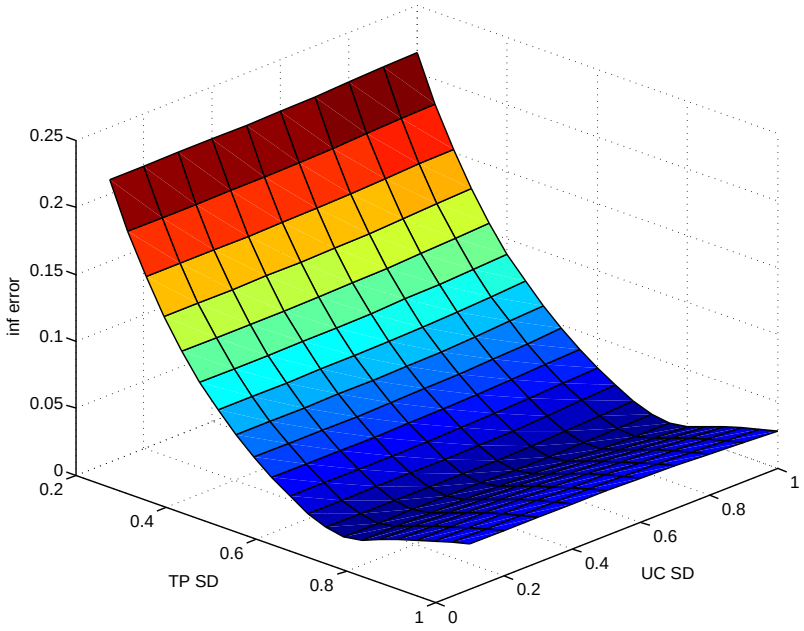

Figure 7.4 Comparison between unit compliance and threshold pressure parameters on model fit. The plot illustrates the direct comparison between threshold pressure standard deviation (TP SD) and unit compliance standard deviation (UC SD) on model fit error on inflation limb (inf error). TP SD clearly indicates the minimum error, while UC SD shows almost no change over the range. Note: all values shown are normalised against the maximum values.

This shifting trend can be explained by how PEEP changes the characteristics of unit TOP and TCP. It is thought that once any lung unit is recruited, it can be re-recruited at a lower pressure than its original recruitment, thus effectively changing the TOP of the unit. This change in the threshold pressures are accounted for in this model by shifting the mean of the distribution, while other parameters, such as standard deviation of the distribution, are kept constant. Relating the amount of shift and the level of PEEP allows the model to capture the lung mechanics at a variety of different PEEP settings. Specifically, a correctly chosen PEEP level increases the amount of recruited lung units [Halter et al., 2003; McCann et al., 2001] as discussed in detail in Chapter 2.

Incorporating the mean shift allows the model to capture the lung mechanics of a patient as a whole. However, because it requires fitting both individual PV data and the mean shift trend, the fitting process is slightly more complicated. More specifically, the best fit must be achieved with all the parameters kept constant for all PEEP levels except for the means values of the TOP and TCP distributions.

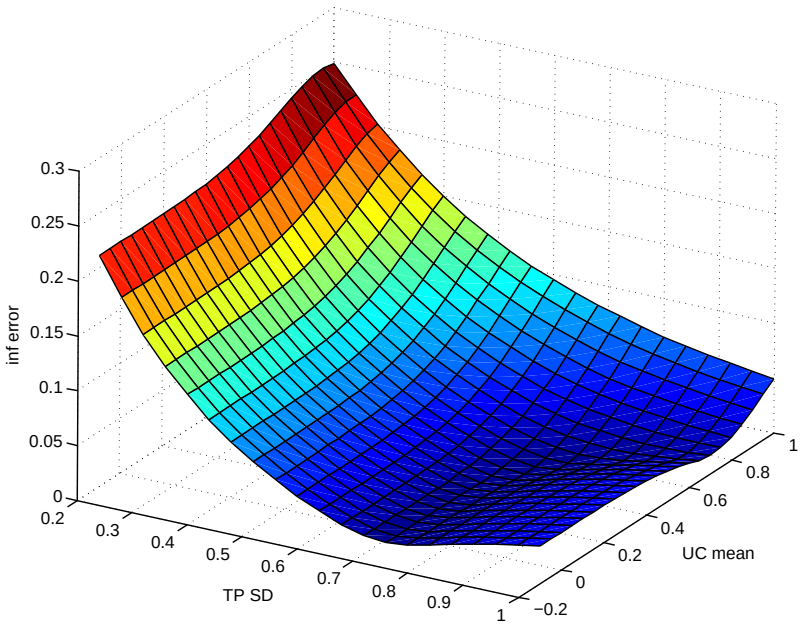

Figure 7.5 Comparison between unit compliance and threshold pressure parameters on model fit. The plot illustrates the direct comparison between threshold pressure standard deviation (TP SD) and unit compliance mean (UC mean) on model fit error on inflation limb (inf error). TP SD indicates distinguishable minimum error, while UC mean shows small change over the range. Note: all values shown are normalised against the maximum values.

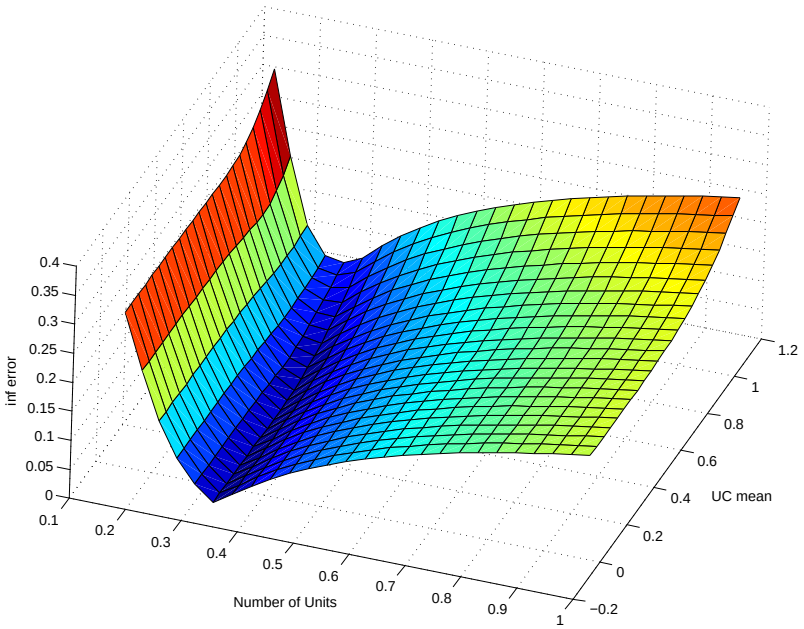

Figure 7.6 Comparison between unit compliance and number of units on model fit. The plot illustrates the direct comparison between number of units and unit compliance mean (UC mean) on model fit error on inflation limb (inf error). The number of units clearly indicates a minimum error value, while UC mean shows small change over the range. Note: all values shown are normalised against the maximum values.

Therefore, the PV loops were fit initially by the method described in Chapter 5, however a specially developed grid search program in MATLAB was used to fine tune the fit. The program runs through every combination of parameters except for the mean values. For each combination, TP distribution means that produced the best fit for each PEEP level are determined using the built-in curve fitting algorithm in MATLAB with initially determined values as a starting point. Finally, the set of parameters that produced the minimum overall average error were then recorded as uniquely identified parameters.

It should be noted here that originally, the threshold pressures are designed to represent the opening and closing pressures of individual lung units. However, determination of actual opening and closing pressures, as well as all the resistive forces between proximal airway and individual lung units required to utilise the true lung unit TP is clinically impossible. Therefore, the TOP and TCP presented here represents the opening and closing of "lung units" at the proximal pressure. The original concept is thus adopted for the clinically oriented approach.

7.3 Results

The model was able to fit to the clinical data well. The overall average absolute pressure point error for inflation was 10.76 ml, or 1.62%. The average absolute error for deflation was 28.04 ml or 4.42%. The number of lung units varied from 152,000 to 304,000, which resulted in inspiratory capacities of approximately 1.5 to 3 litres.

The standard deviation and the mean were significantly higher for the TOP distribution than the TCP distribution, as expected. The average mean for the TOP distribution was 19.8 cmH_2O, while the TCP distribution averaged 10.4 cmH_2O. The average SD for the TOP distribution was 17 cmH_2O and for TCP it was 7.25 cmH_2O. Most of the data showed a mean shift trend very close to a linear relation relative to PEEP, which is a surprising new result for this type of clinical data. The TOP distribution mean shifts were significantly larger than those for the TCP distribution. In general, the mean of TOP distribution decreased and the mean of TCP distribution increased, as PEEP increased.

Table 7.2 summarises the best fit TP distribution parameters and the average absolute fitting errors for all 12 cases. In each case, the TP distribution standard deviations are constant over all PEEP levels for each patient. However, as described, the TP mean shifts as PEEP changes. The fitting errors are presented as average absolute volume fitting errors and as a percentage.

Table 7.2 Summary of model fitting error for clinical data.

Data Set 1			Number of Units	180000
			Inflation SD	18
			Deflation SD	7

	Inflation			Deflation		
PEEP	Mean	Error [ml]	Error [%]	Mean	Error [ml]	Error [%]
5	21.1	11.87	1.46	7.7	85.61	12.38
7	18.5	6.78	0.54	8.6	44.14	4.46
12	12.7	5.34	0.32	10.0	10.75	0.82

Data Set 2			Number of Units	220000
			Inflation SD	12
			Deflation SD	7

	Inflation			Deflation		
PEEP	Mean	Error [ml]	Error [%]	Mean	Error [ml]	Error [%]
0	23.18	44.92	20.81	9.16	38.76	31.21
5	18.95	15.28	1.84	8.54	11.37	1.32
10	15.23	11.36	0.81	8.84	3.85	0.28

Data Set 3			Number of Units	152000
			Inflation SD	18
			Deflation SD	8

	Inflation			Deflation		
PEEP	Mean	Error [ml]	Error [%]	Mean	Error [ml]	Error [%]
5	24.46	9.01	1.39	8.29	23.87	3.93
7	22.55	2.72	0.36	9.58	20.98	2.59
10	19.13	4.71	0.47	9.67	21.07	2.36

Data Set 4			Number of Units	171000
			Inflation SD	12
			Deflation SD	6

	Inflation			Deflation		
PEEP	Mean	Error [ml]	Error [%]	Mean	Error [ml]	Error [%]
5	23.55	6.70	1.27	10.63	12.98	2.62
7	22.77	17.59	2.53	12.58	11.05	1.99
10	15.54	15.11	1.34	12.00	19.17	2.48

Data Set 5			Number of Units	171000
			Inflation SD	14
			Deflation SD	6

	Inflation			Deflation		
PEEP	Mean	Error [ml]	Error [%]	Mean	Error [ml]	Error [%]
5	22.49	15.69	2.90	9.03	53.40	10.00
7	21.89	5.51	0.83	10.53	43.17	7.47
10	20.82	4.50	0.58	11.67	35.26	5.52
12	19.70	7.01	0.67	12.96	26.02	3.05

Table 7.2 Contd. Summary of model fitting error for clinical data.

Data Set 6			Number of Units			152000
			Inflation SD			18
			Deflation SD			8
	Inflation			Deflation		
PEEP	Mean	Error [ml]	Error [%]	Mean	Error [ml]	Error [%]
5	31.19	13.71	3.56	12.39	21.41	9.52
7	28.57	6.28	1.03	13.22	9.70	2.49
10	21.04	7.07	0.87	11.81	7.25	1.13
12	17.78	3.98	0.42	11.85	6.00	0.75

Data Set 7			Number of Units			304000
			Inflation SD			20
			Deflation SD			9
	Inflation			Deflation		
PEEP	Mean	Error [ml]	Error [%]	Mean	Error [ml]	Error [%]
5	20.06	17.44	1.61	9.55	69.09	7.05
7	16.98	9.28	0.57	9.79	35.41	2.91
10	10.80	9.20	0.43	8.68	9.90	0.51
12	7.45	6.38	0.28	8.35	4.92	0.24

Data Set 8			Number of Units			240000
			Inflation SD			16
			Deflation SD			6
	Inflation			Deflation		
PEEP	Mean	Error [ml]	Error [%]	Mean	Error [ml]	Error [%]
5	25.69	16.51	2.28	9.96	31.78	5.08
7	21.45	6.07	0.67	10.07	20.62	1.86
12	17.16	9.37	0.59	11.56	17.59	1.02

Data Set 9			Number of Units			240000
			Inflation SD			25
			Deflation SD			10
	Inflation			Deflation		
PEEP	Mean	Error [ml]	Error [%]	Mean	Error [ml]	Error [%]
10	19.92	9.64	0.68	11.43	14.83	1.18
12	18.15	6.99	0.40	12.71	12.06	0.78
15	11.59	19.89	0.98	12.45	13.86	0.82

Data Set 10			Number of Units			190000
			Inflation SD			19
			Deflation SD			7
	Inflation			Deflation		
PEEP	Mean	Error [ml]	Error [%]	Mean	Error [ml]	Error [%]
5	21.13	17.70	2.23	7.91	62.55	9.32
7	18.21	5.20	0.47	8.62	40.28	4.08
10	14.69	0.66	0.05	9.32	24.56	2.20
12	11.82	9.01	0.55	9.97	14.34	1.09

Table 7.2 Contd. Summary of model fitting error for clinical data.

Data Set 11			Number of Units			240000
			Inflation SD			17
			Deflation SD			7
	Inflation			Deflation		
PEEP	Mean	Error [ml]	Error [%]	Mean	Error [ml]	Error [%]
5	18.82	10.63	1.16	8.40	84.81	10.44
7	16.09	14.91	1.10	8.83	56.34	5.38
10	11.70	8.77	0.54	8.45	34.19	2.52

Data Set 12			Number of Units			180000
			Inflation SD			15
			Deflation SD			6
	Inflation			Deflation		
PEEP	Mean	Error [ml]	Error [%]	Mean	Error [ml]	Error [%]
5	32.43	9.06	2.25	11.09	32.40	8.01
10	28.99	22.40	3.13	13.83	23.55	4.37
15	25.96	6.04	0.65	15.84	12.88	1.60

The median for the number of units was 185,000 and the interquartile range was 171,000 to 240,000. The inflation standard deviation median was 17.5 cmH_2O and the inter quartile range was 14.75 to 18.25 cmH_2O. The deflation standard deviation median was 7 cmH_2O and the inter quartile range was 6 to 8 cmH_2O. Table 7.3 shows the interquartile range of TP mean and percentage fitting errors for each PEEP value, as summaised over the entire set of fitted patient data. Data for PEEP of 0 and 15 cmH_2O were omitted because there was only 1 data with PEEP of 0 and 2 for PEEP of 15.

Table 7.3 Model fitting error and distribution mean inter quartile ranges.

	Inflation		Deflation	
PEEP	Mean	Error [%]	Mean	Error [%]
5	20.6 - 25.1	1.4 - 2.3	8.3 - 10.3	4.5 - 9.8
7	18.2 - 22.5	0.5 - 1.0	8.8 - 10.5	2.5 - 4.5
10	14.8 - 20.6	0.5 - 0.9	9.0 - 11.8	1.1 - 2.5
12	12.3 - 18.0	0.4 - 0.6	10.0 - 12.3	0.8 - 1.1

Figures 7.7 - 7.18 illustrate the fitting results for all data sets. The main plot illustrates the clinical PV data and the fitted model. The bottom left illustrates the patient specific TOP and TCP distributions. The bottom right plot illustrates the mean shift of the TOP and TCP distributions against PEEP.

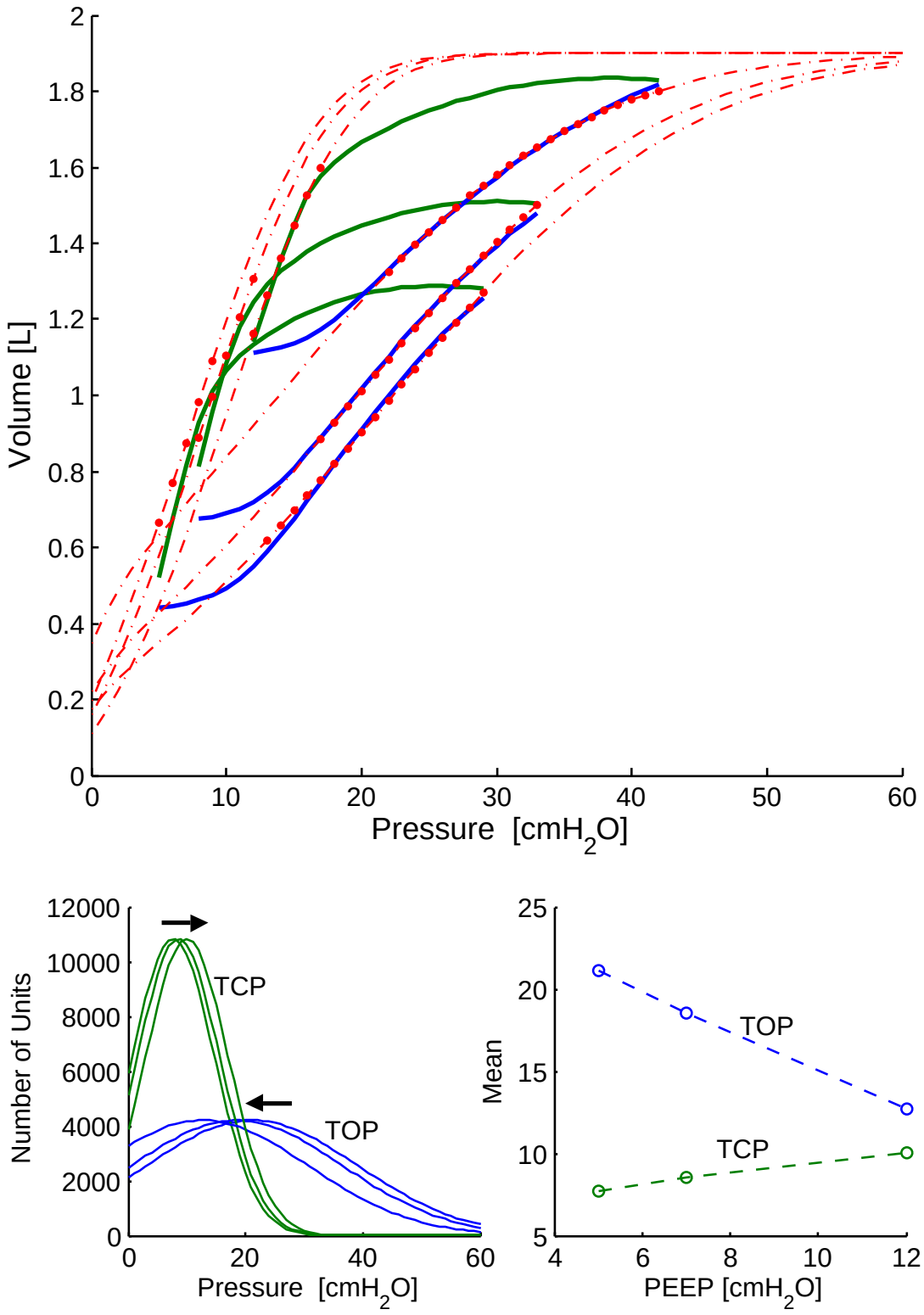

Figure 7.7 A model fit and the parameter for Data Set 1. The main plot shows clinical data (solid lines), fitted model (red dash lines), and fitted regions (red dots). Plot on the bottom left shows resulting TP distributions. Arrows indicate the movement of TP distribution mean with increasing PEEP. The plot on the bottom right shows the TP mean shifts.

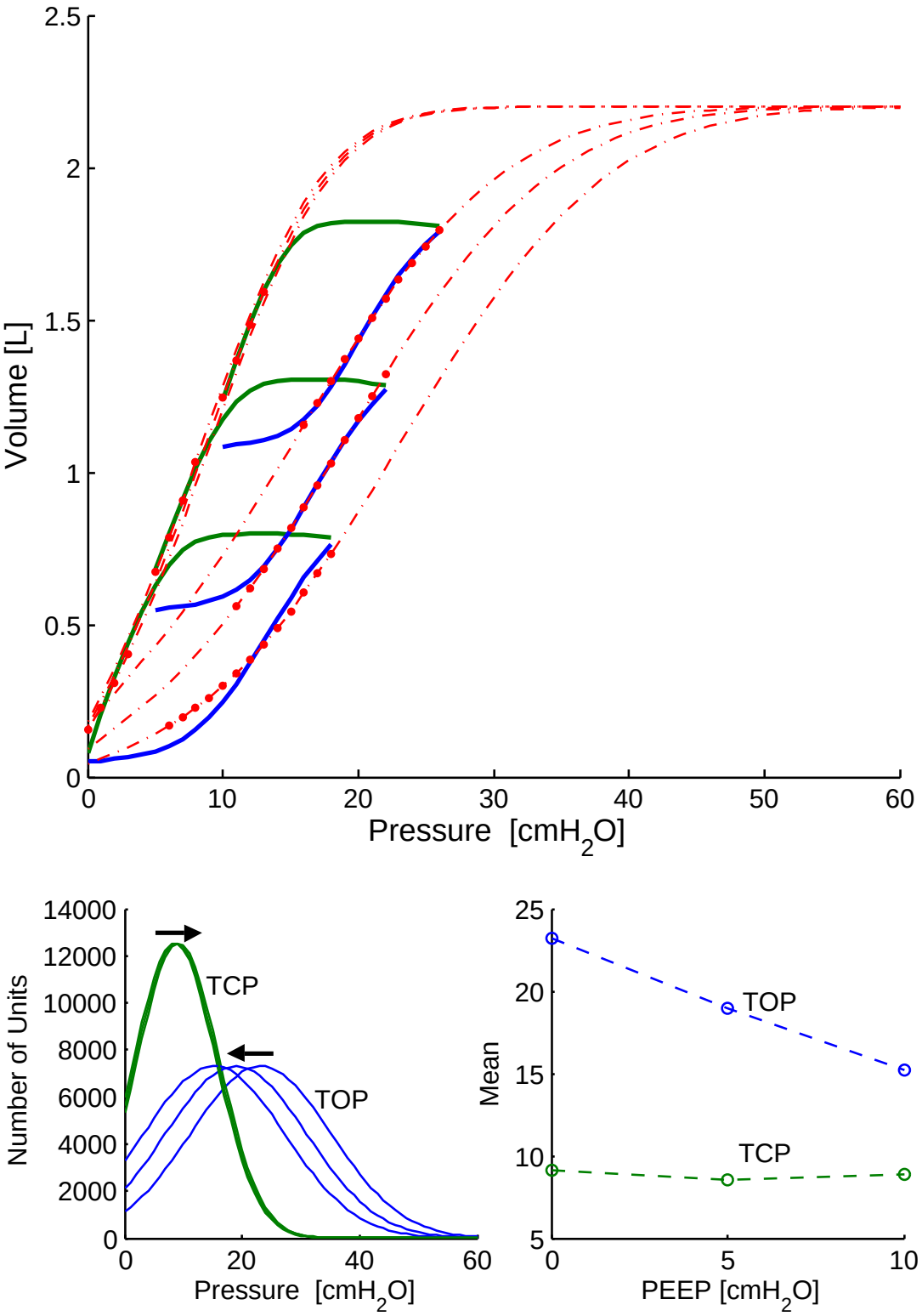

Figure 7.8 A model fit and the parameter for Data Set 2. The main plot shows clinical data (solid lines), fitted model (red dash lines), and fitted regions (red dots). Plot on the bottom left shows resulting TP distributions. Arrows indicate the movement of TP distribution mean with increasing PEEP. The plot on the bottom right shows the TP mean shifts.

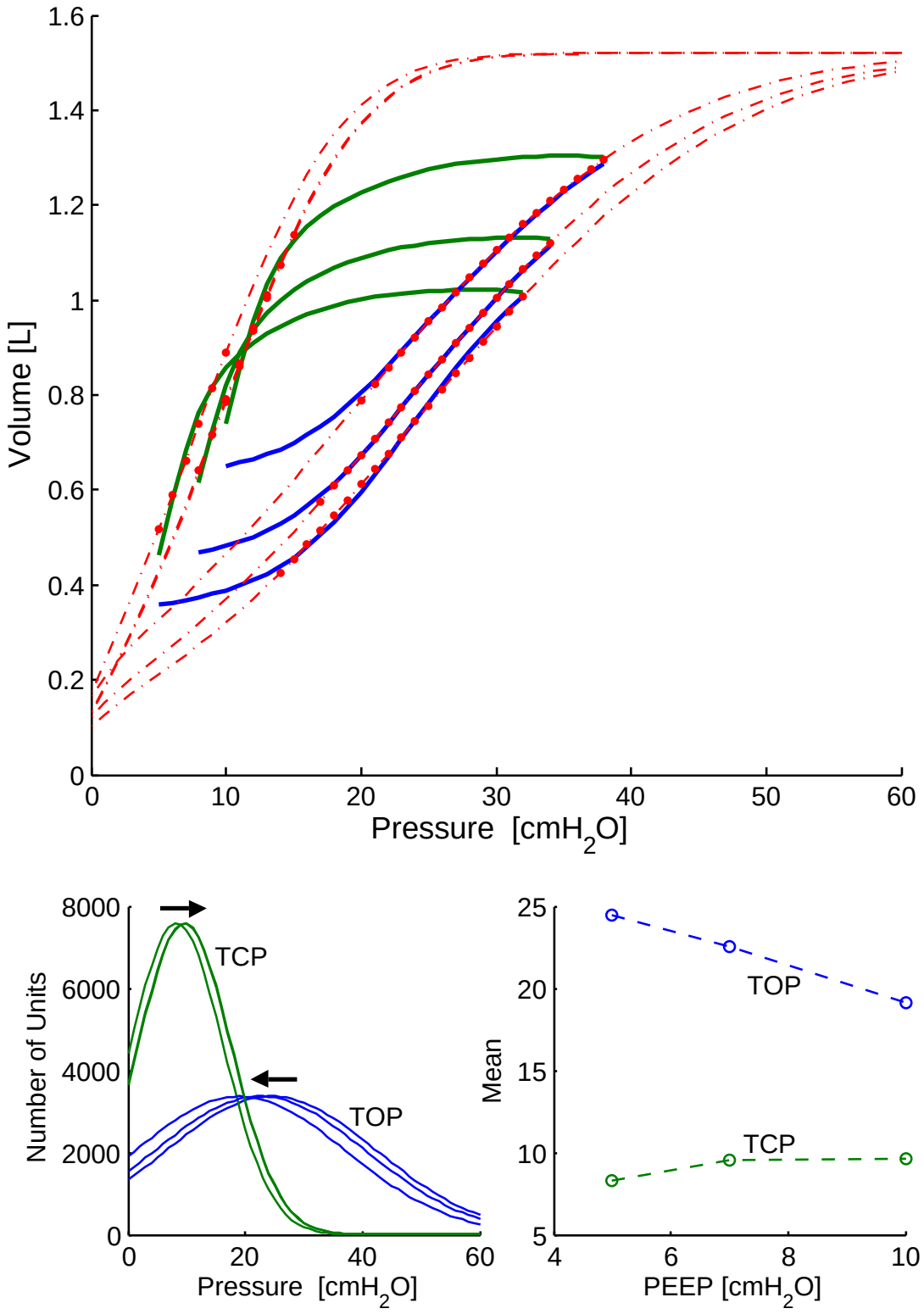

Figure 7.9 A model fit and the parameter for Data Set 3. The main plot shows clinical data (solid lines), fitted model (red dash lines), and fitted regions (red dots). Plot on the bottom left shows resulting TP distributions. Arrows indicate the movement of TP distribution mean with increasing PEEP. The plot on the bottom right shows the TP mean shifts.

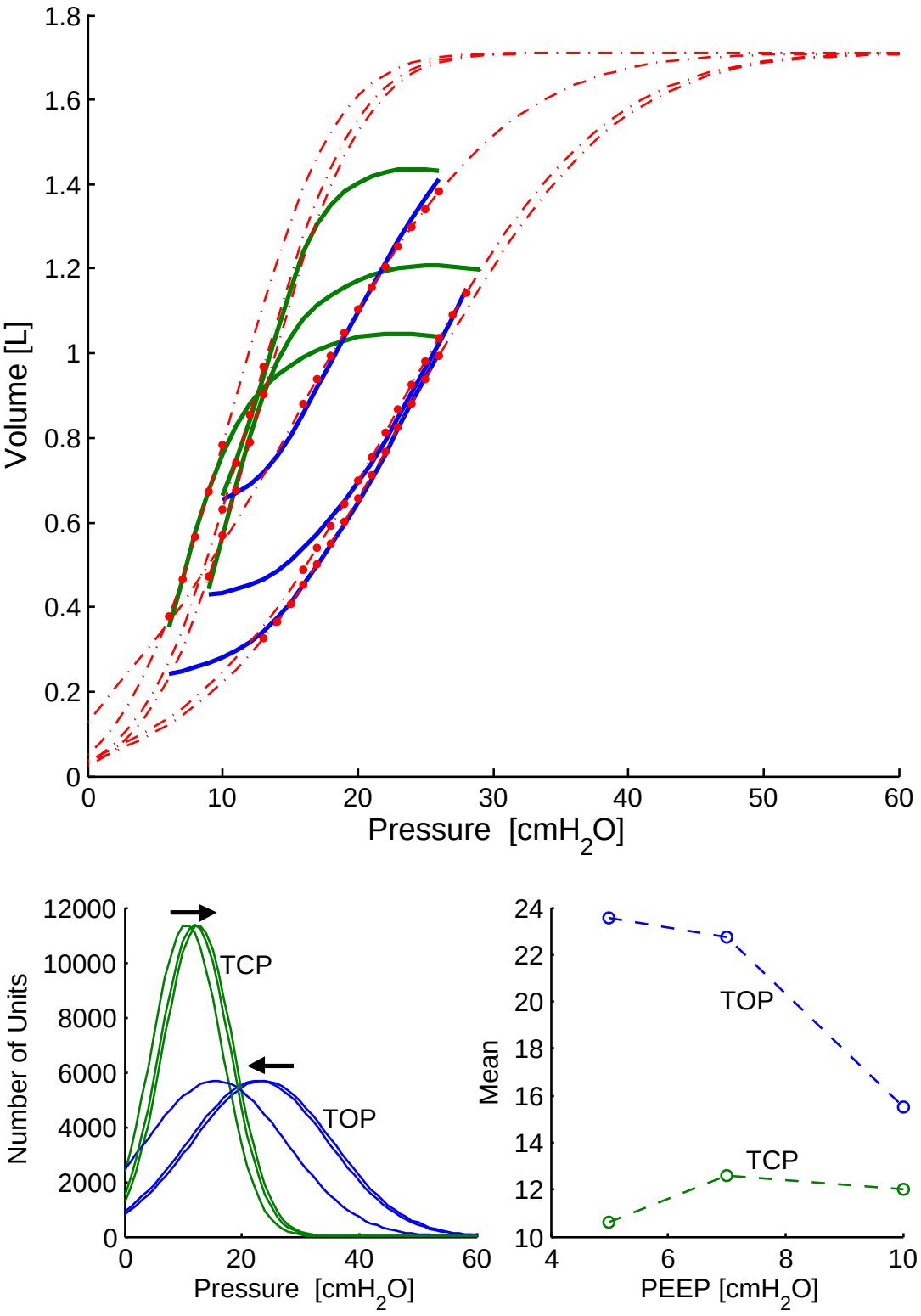

Figure 7.10 A model fit and the parameter for Data Set 4. The main plot shows clinical data (solid lines), fitted model (red dash lines), and fitted regions (red dots). Plot on the bottom left shows resulting TP distributions. Arrows indicate the movement of TP distribution mean with increasing PEEP. The plot on the bottom right shows the TP mean shifts.

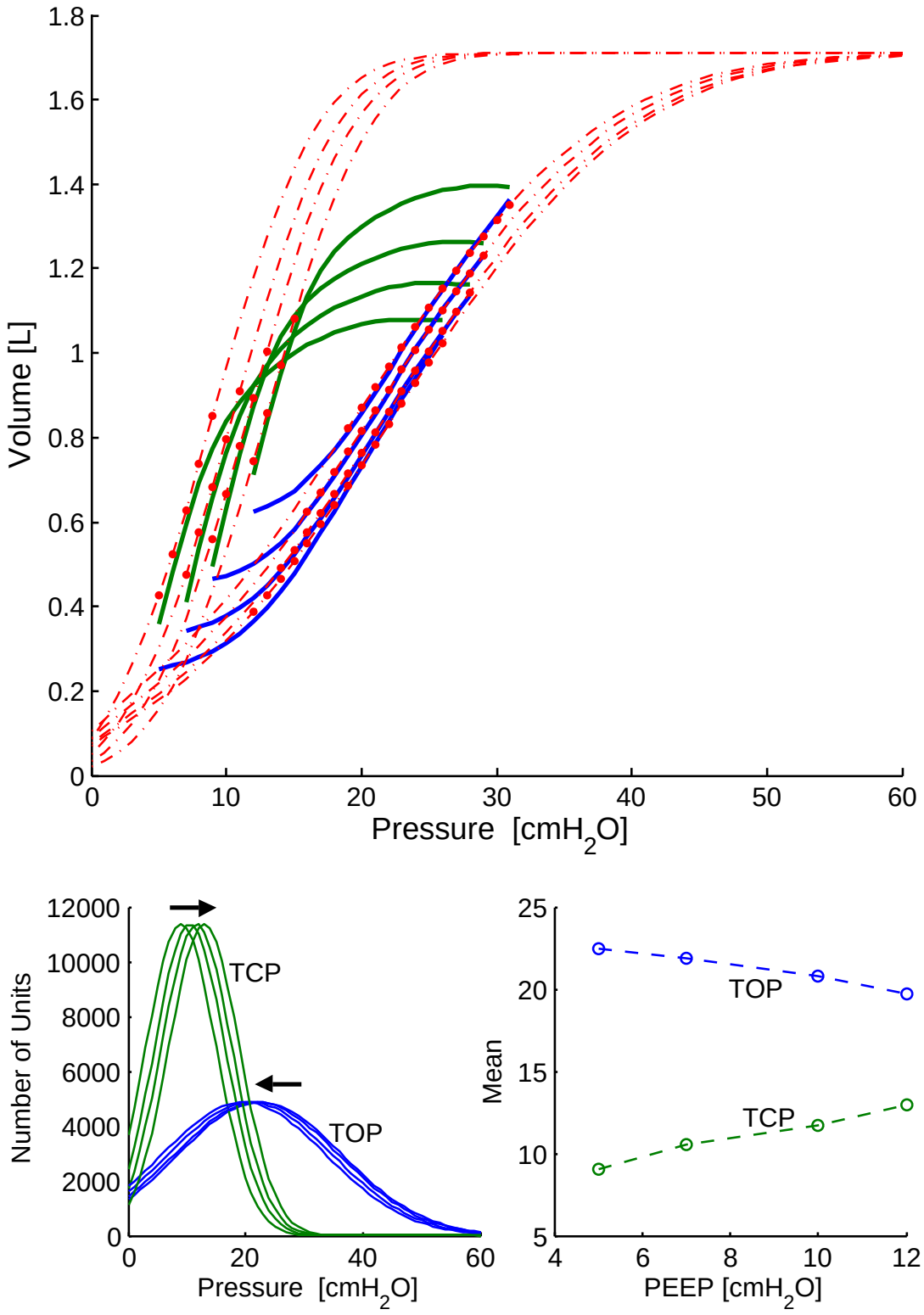

Figure 7.11 A model fit and the parameter for Data Set 5. The main plot shows clinical data (solid lines), fitted model (red dash lines), and fitted regions (red dots). Plot on the bottom left shows resulting TP distributions. Arrows indicate the movement of TP distribution mean with increasing PEEP. The plot on the bottom right shows the TP mean shifts.

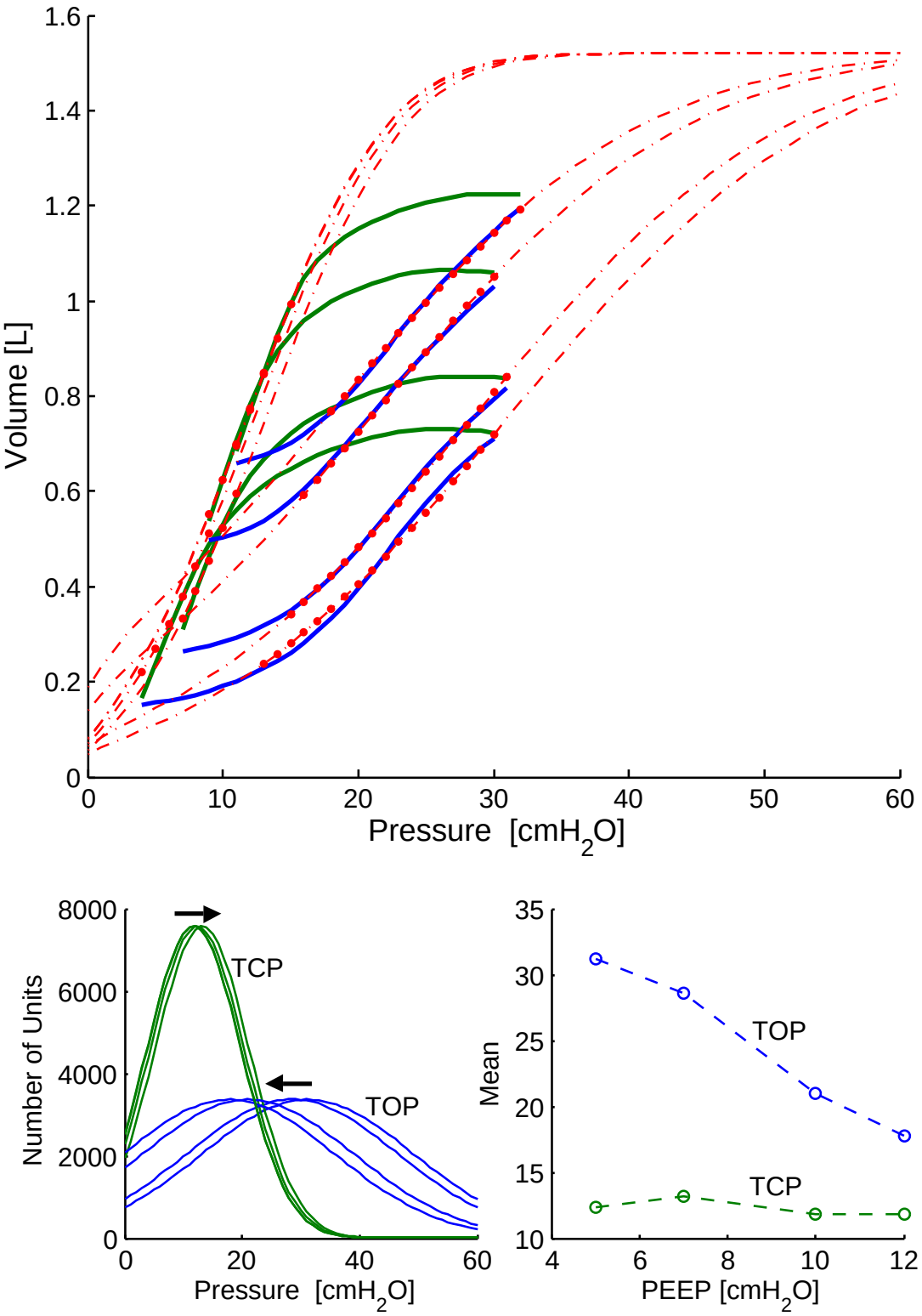

Figure 7.12 A model fit and the parameter for Data Set 6. The main plot shows clinical data (solid lines), fitted model (red dash lines), and fitted regions (red dots). Plot on the bottom left shows resulting TP distributions. Arrows indicate the movement of TP distribution mean with increasing PEEP. The plot on the bottom right shows the TP mean shifts.

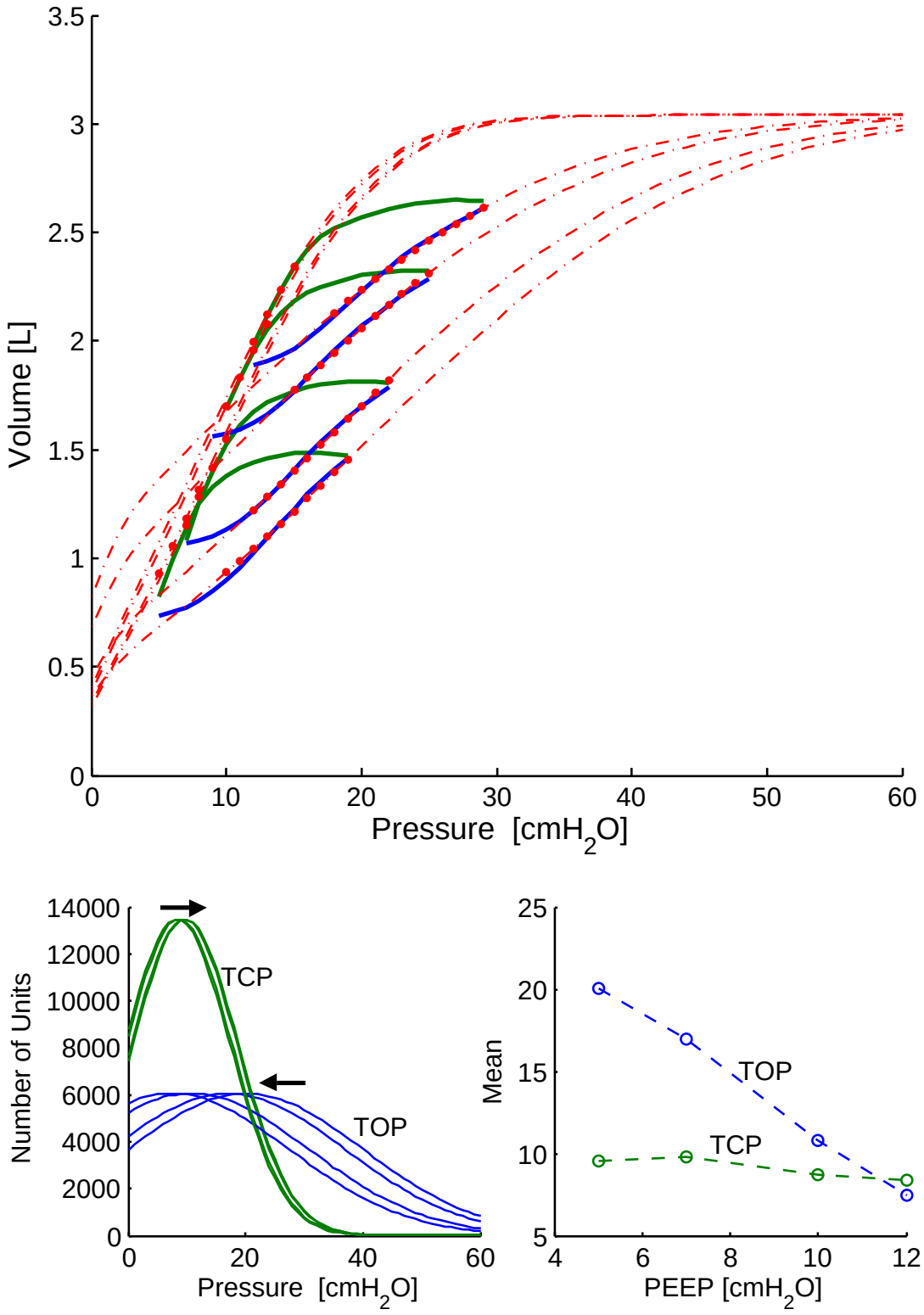

Figure 7.13 A model fit and the parameter for Data Set 7. The main plot shows clinical data (solid lines), fitted model (red dash lines), and fitted regions (red dots). Plot on the bottom left shows resulting TP distributions. Arrows indicate the movement of TP distribution mean with increasing PEEP. The plot on the bottom right shows the TP mean shifts.

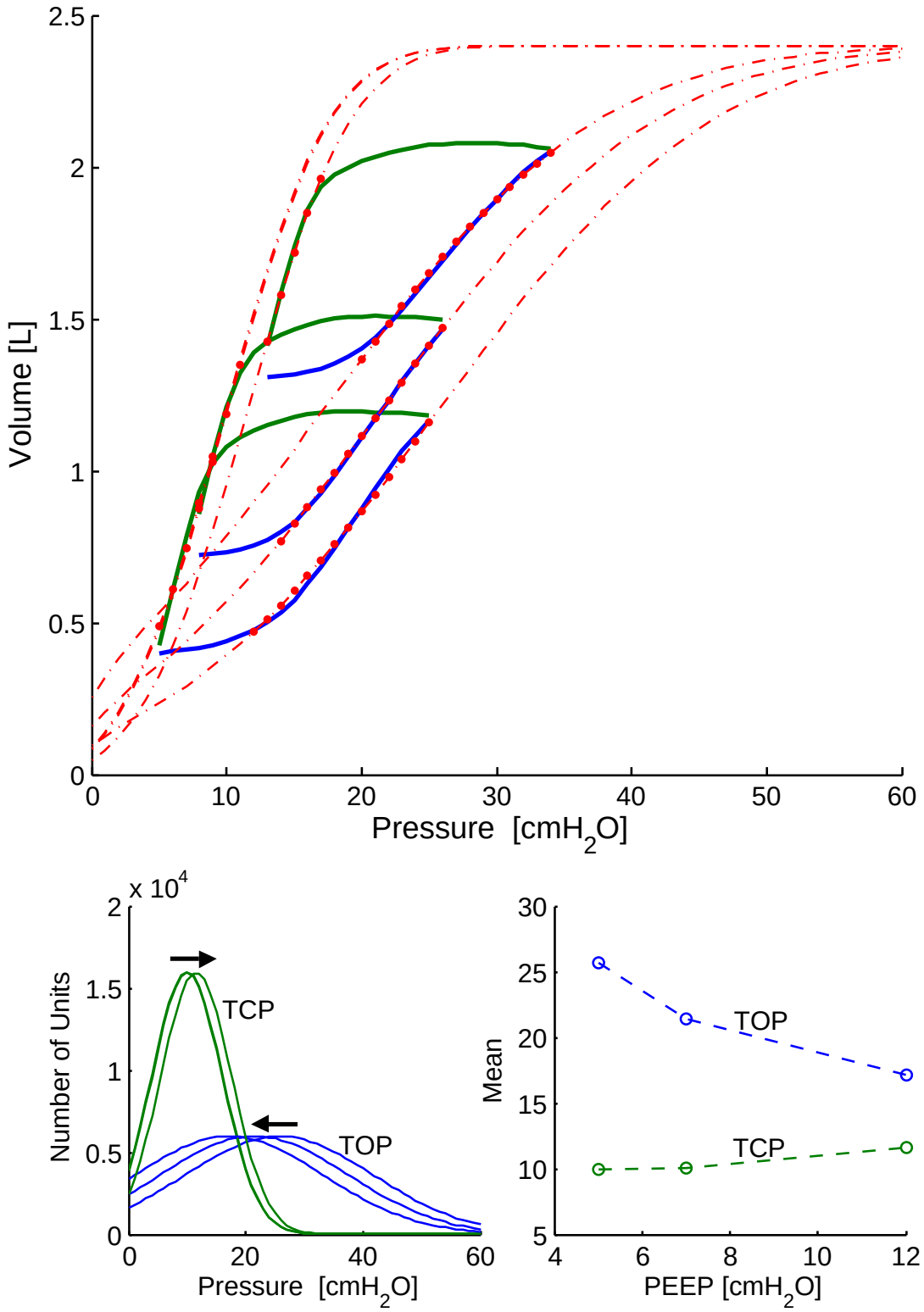

Figure 7.14 A model fit and the parameter for Data Set 8. The main plot shows clinical data (solid lines), fitted model (red dash lines), and fitted regions (red dots). Plot on the bottom left shows resulting TP distributions. Arrows indicate the movement of TP distribution mean with increasing PEEP. The plot on the bottom right shows the TP mean shifts.

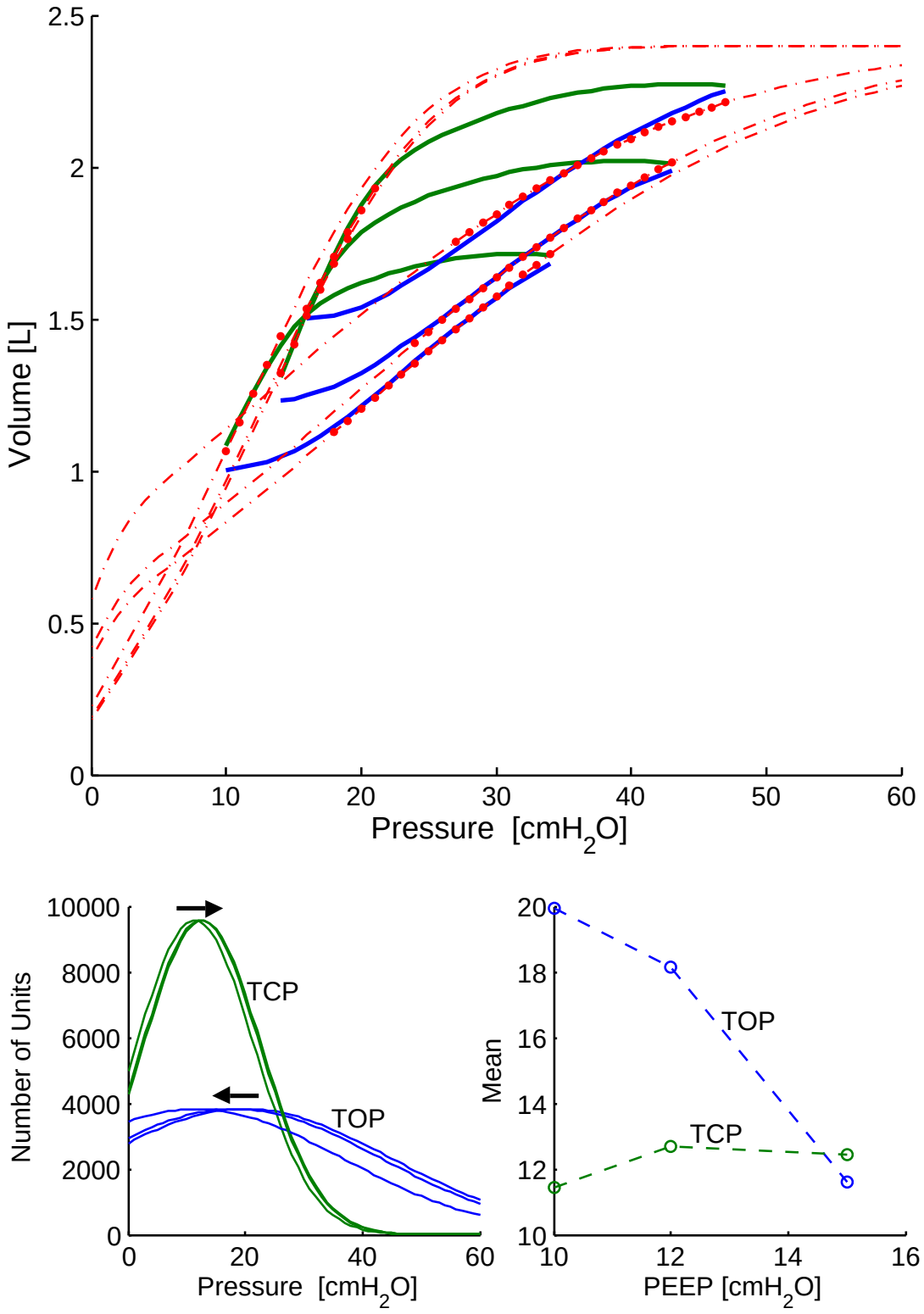

Figure 7.15 A model fit and the parameter for Data Set 9. The main plot shows clinical data (solid lines), fitted model (red dash lines), and fitted regions (red dots). Plot on the bottom left shows resulting TP distributions. Arrows indicate the movement of TP distribution mean with increasing PEEP. The plot on the bottom right shows the TP mean shifts.

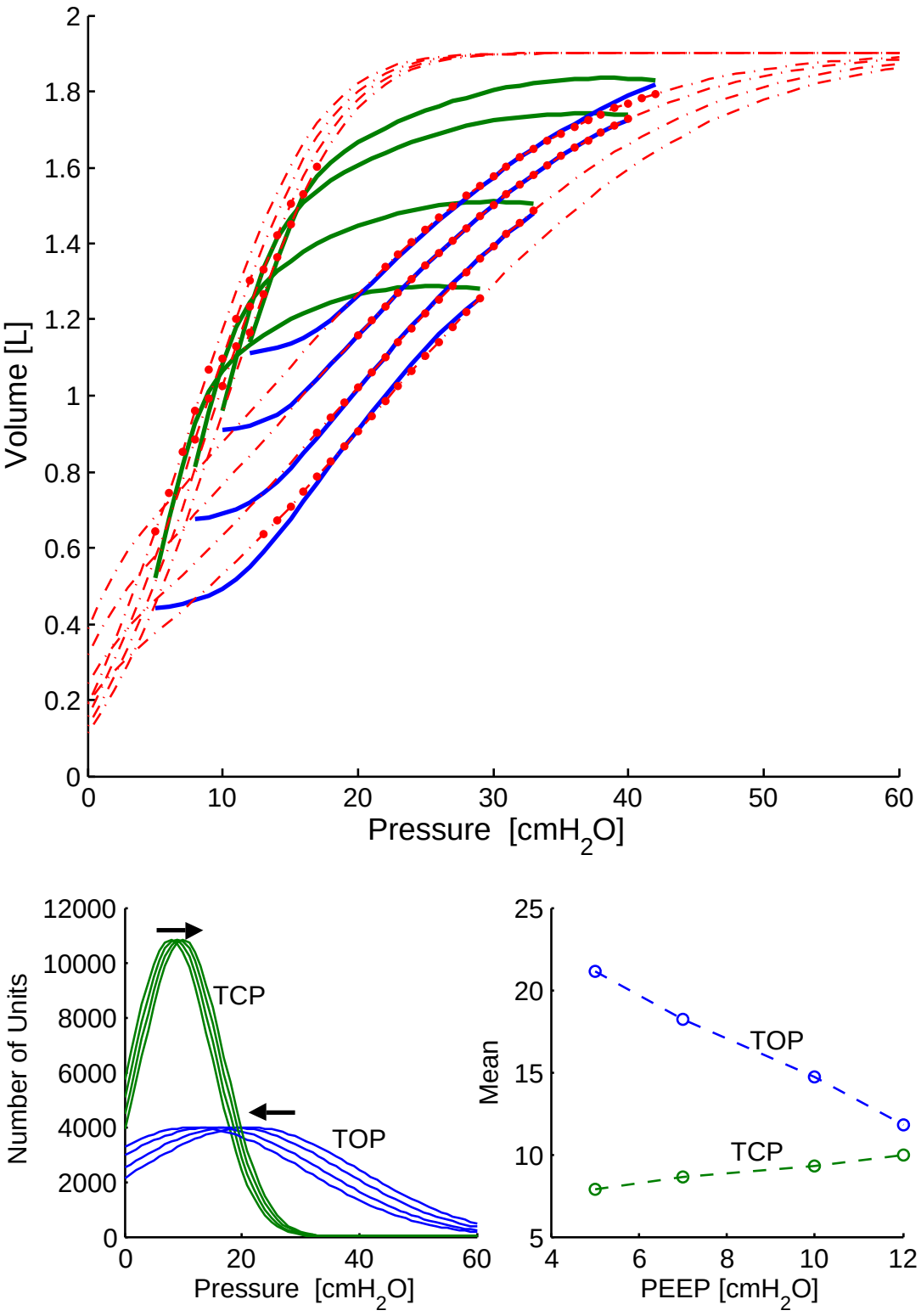

Figure 7.16 A model fit and the parameter for Data Set 10. The main plot shows clinical data (solid lines), fitted model (red dash lines), and fitted regions (red dots). Plot on the bottom left shows resulting TP distributions. Arrows indicate the movement of TP distribution mean with increasing PEEP. The plot on the bottom right shows the TP mean shifts.

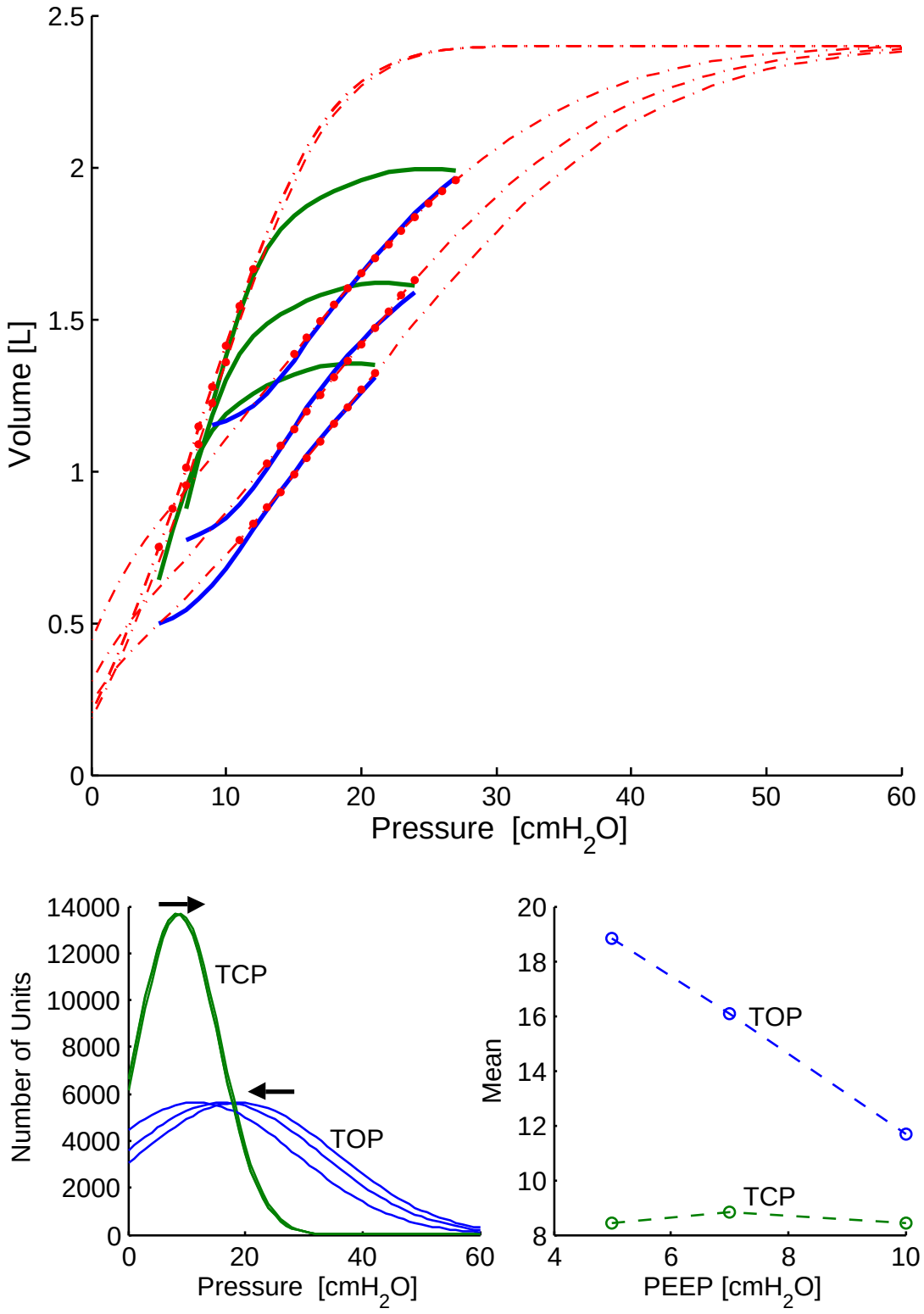

Figure 7.17 A model fit and the parameter for Data Set 11. The main plot shows clinical data (solid lines), fitted model (red dash lines), and fitted regions (red dots). Plot on the bottom left shows resulting TP distributions. Arrows indicate the movement of TP distribution mean with increasing PEEP. The plot on the bottom right shows the TP mean shifts.

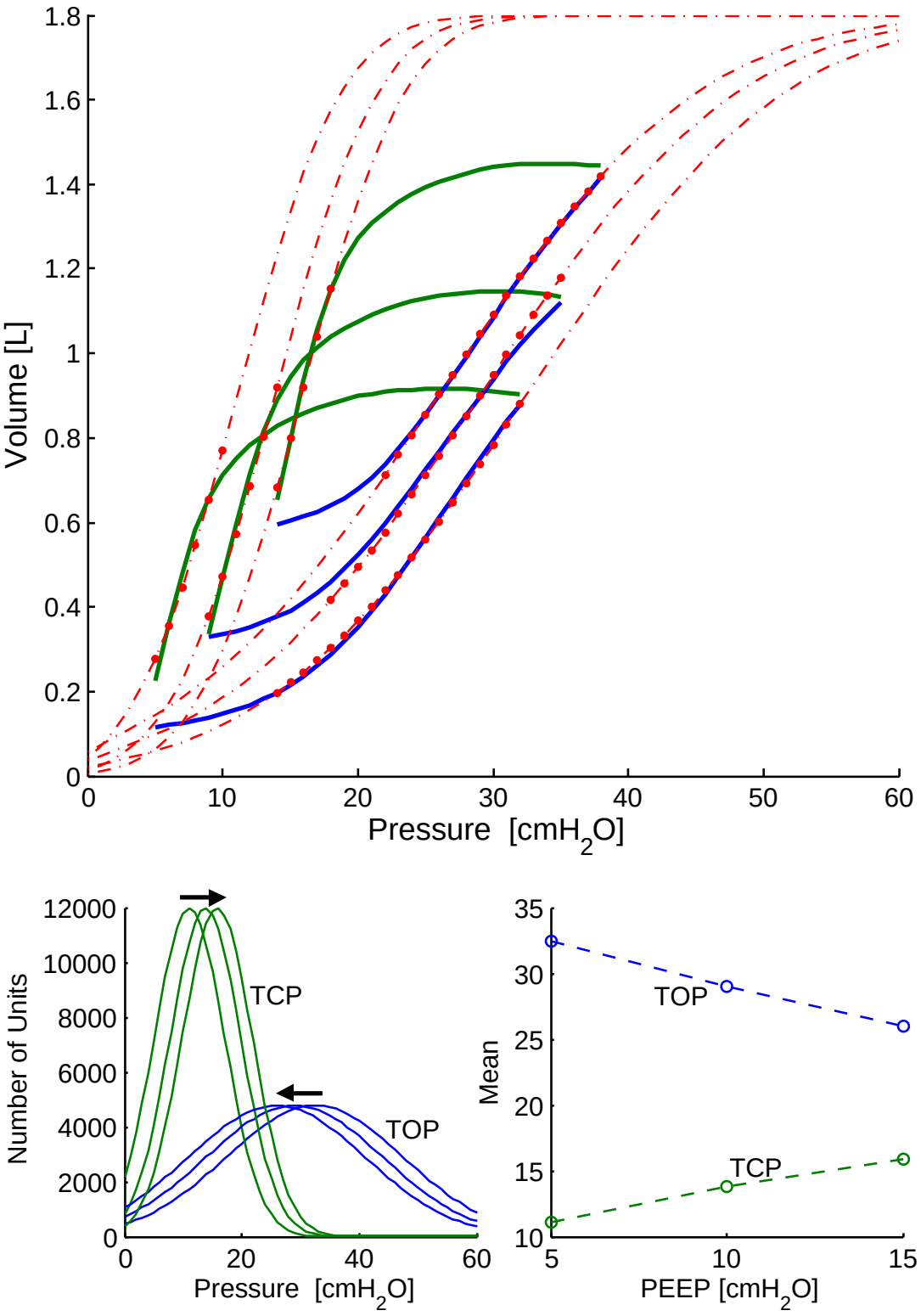

Figure 7.18 A model fit and the parameter for Data Set 12. The main plot shows clinical data (solid lines), fitted model (red dash lines), and fitted regions (red dots). Plot on the bottom left shows resulting TP distributions. Arrows indicate the movement of TP distribution mean with increasing PEEP. The plot on the bottom right shows the TP mean shifts.

7.4 Discussion and Limitations

These sets of clinical data are invaluable for validating the model. The data include the EEV measurement, which is crucial for better analysing each PV curve as part of a whole lung. Different PEEP levels clearly illustrated the clinically reported effects of PEEP on the lung mechanics and recruitment. The combination of this additional data allows the model to simulate the entire lung mechanics over therapeutic range and provide a solid level of validation that the model is physiologically and mechanically representative.

The model was able to fit the clinical data with minimal errors. The average absolute pressure point error in volume for inflation was less than 11 ml, which represents an average difference of less than 2% from the original data points. The average absolute error for deflation was about 28 ml or about 5% difference. However, it needs to be noted that because the percentage error is calculated using absolute volume, the value is exaggerated at lower volume and understated at higher volume. For example, 10 ml difference at an absolute volume of 100 ml is 10%, while the same 10 ml difference at 1000 ml is only 1%. This effect can be seen in Table 7.2, where the percentage error is larger at lower PEEP, in general. However, even after adjustment, these errors are well within clinical tolerance for changing therapy.

The grid search fitting produced a wide range of values for the total number of lung units. The lowest was 152,000 for Data Set 6, and the highest was twice as large at 304,000 for Data Set 7. This wide range of values is also observed in a clinical study [Gattinoni et al., 2006].

The number of units were a function of the maximum volume produced during the tidal ventilation and the compliance of the curve. For example, Data Sets 1 and 2, illustrated in Figures 7.7 and 7.8, produced similar maximum volumes during tidal ventilation of 1.84 L at PEEP=12 cmH_2O and 1.83 L at PEEP=10 cmH_2O, respectively. However, the compliance of Data Set 1 was significantly higher. As a result, the standard deviations for the TOP distribution, which essentially indicates the compliance, were 18 and 12 cmH_2O for Data Set 1 and 2, respectively. Consequently, the number of lung units was 180,000 for Data Set 1 and 220,000 for Data Set 2, indicating a potentially larger total inspiratory capacity. Similarly, Data Sets 9 and 11 resulted in the same number of lung units,

however the maximum volume during tidal ventilation was 2.3 and 2.0 litres with TOP standard deviation of 25 and 17 cmH_2O, respectively.

This relationship between inspiratory capacity and lung compliance indicates that physiologically the compliance of the lung is directly related to the EEV of tidal ventilation within the inspiratory capacity. When the lung is ventilated at a lower EEV, due to lower PEEP, more lung units are recruited during tidal ventilation compared to the lung starting at near the inspiratory capacity. As a direct result of the difference in recruitment, lower PEEP ventilation results in higher effective compliance. More specifically, at lower PEEP, the majority of volume increase is due to unit recruitment. However, at higher PEEP, when the lung is ventilated nearer inspiratory capacity, the majority of lung units are already recruited at the beginning of inspiration. Thus, the lung inflates to a greater extent by stretching the recruited units, resulting in lower compliance.

Alternatively, lower compliance at lower pressure may indicate reduced inspiratory capacity. One of the key symptoms of lung injury, such as ARDS, is a significant decrease in inspiratory capacity [Gattinoni et al., 2001; Puybasset et al., 1998]. Thus, this parameter may be used to directly analyse the condition of the lung and help quantify the level of injury. It would therefore be immensely valuable to compare the model results for the total number of lung units directly to the actual lung size for validation. Note that such a specific clinical study has never been performed at this date, but is an opened possibility resulting from this model.

Distribution means for TOP were significantly higher than that of TCP, indicating that the lung units are recruited at a significantly higher pressure than they are derecruited. The standard deviation of the TOP distribution was also significantly larger than that of TCP distribution. This width resulted in a wider distribution of TOP indicating significant recruitment throughout the range as reported in the literature [e.g. Carney et al., 1999; Schiller et al., 2003; Albaiceta et al., 2004]. The resulting TOP distribution is broad and concentrated at a higher pressure, while the TCP distribution is much narrower and concentrated at lower pressure. These characteristics are directly in agreement with clinical studies and expectation [Crotti et al., 2001; Pelosi et al., 2001].

The volume shifts between different PEEP levels were closely captured by shifting the distribution mean. In general, the TOP distribution mean decreased as PEEP increased, and the TCP distribution mean increased as PEEP increased. Physiologically, this shift indicates the varying nature of TOP and TCP under this therapy. More specifically, once a previously collapsed unit is recruited, it is easier to re-recruit the second time, which is the well accepted basis of a brief high pressure recruitment maneuvers to enhance recruitment [e.g. Foti et al., 2000; Henzler et al., 2005].

Mechanically, when PEEP is increased, the additional pressure recruits lung units that were not recruited during previous tidal ventilation at lower PEEP. Once recruited, the unit can then be re-recruited in subsequent cycles at the same PEEP at a lower pressure, essentially decreasing its unit TOP from the value it had at lower PEEP. Thus, the overall effect of higher PEEP is the recruitment of additional units at a given pressure and reduction of the associated TOP. The overall result is volume increase over the breathing cycle and at given pressure, which matches the clinical goal. Altering this alveolar mechanism using PEEP is also well observed in clinical studies [e.g. Chelucci et al., 2000; Halter et al., 2003; Malbouisson et al., 2001; McCann et al., 2001; Richard et al., 2001].

Furthermore, the slope of the mean shift was very close to constant for any given patient over all PEEP levels for both TOP and TCP. There were a few cases, however, where the slope changed significantly between different PEEP levels, such as Data Set 4, as illustrated in Figures 7.10. However, it is evident that the shape of the PV curve for PEEP=10 cmH_2O is drastically different from other PEEP levels in this case. This drastic difference signifies that the entire underlying mechanics has changed for this PEEP level, which the mean shift is not designed to fully capture. The clinical reasoning for this change is not known, however the model was able to clearly identify this change.

It is also important to note that the values of the mean, its shift, and the slope were significantly different between patients. This result indicates the uniqueness of the mean shift slope parameter. Hence, the model's ability to capture this complex patient specific mechanical behaviour is a significant level of added validation, particularly with regard to its clinical efficacy in predicting the outcome of the therapy changes.

Some data fits show an inflation curve crossing a deflation curve at low pressure. This behaviour is physiologically inaccurate, because it indicates that there are more units derecruited than recruited at that pressure and it results in a mismatch in the starting volume. However, because this model uses EEPs to relate EEVs, fitted curves below the data's associated PEEP level are not valid. Thus, each set of model fit parameters are only valid for the particular PEEP level fitted. This association between PEEP and the EEV is also observed in clinical studies [Cheng et al., 1995], adding another measure of validation.

A majority of the fitting error can be significantly improved by fitting the curves with different PEEP individually. There are also relatively larger differences in error between the lowest and the highest PEEP data for a given patient. This difference is caused by the limited number of parameters being used to fit the data, essentially restricting the flexibility of this minimal model. Even if one additional parameter, standard deviation for example, was varied between different PEEP levels, the overall fit would improve drastically. However, the additional varying parameter also makes it difficult to associate data between different PEEP levels for the same patient without additional measurements. Currently, the different PEEP settings are captured by a single parameter, the mean shift. The additional varying parameter would require a different metric to capture this trend, thus further complicating the fitting process. Given fitted model absolute errors of only 1-10% that are well within clinical significance, it is not necessary at this time to add additional variables or additional measurements.

Finally, this model is designed to simulate a fully mechanically ventilated patient. The work of breathing is thus done entirely by the ventilator. Clinically, such patients are referred to as "passively" breathing, which has been avoided here to avoid confusion with passive expiration mechanics. Spontaneously breathing patients, even partially, may have different mechanisms. This current model is thus limited to the fully mechanically ventilated patients. Further studies would have to be done to validate it for actively breathing cases.

7.5 Summary

The model was further validated in this chapter using clinical data. Each data set (of 12) was from one patient and included different PEEP levels and EEV measurements. The model was fitted using the Min-to-Max fitting method, simulating the entire range of lung mechanics. Preliminary fitting found that the unit compliance parameters have a relatively small effect on total lung mechanics, thus those parameters were kept constant for all data sets. Iterative grid search was performed after initial fitting for the rest of the parameters and the set of parameters that produced the least error was recorded.

The model was able to fit the clinical data well. The overall average absolute error was within 5% of the original data. The resulting parameters were also well within a clinically acceptable range, and the resulting threshold pressure distributions matched clinical observations and expectations well. The model was able to fit any given data set by capturing the trend of varying PEEP with just a single parameter, the threshold pressure distribution mean shift.

The following mechanical and physiological conclusions can be drawn from this clinical validation study:

- The shape of the TOP and TCP distributions uniquely reflect the clinically observed patient specific lung mechanics.
- The patient specific identified number of lung units may directly identify the patients' inspiratory capacity, and/or the level of lung injury.
- The slope of the mean shifts are effectively constant for a patient over all PEEP, which is a new and unique result in the area of pulmonary mechanics.
- The slope of the mean shifts are unique to a patient.
- The slope of the mean shifts represents the volume responsiveness of a patient to changes in PEEP therapy over a broad range of PEEP, which may have clinical significance.

Overall, the model was able to capture the key features of all the observed fundamental lung mechanics using a minimal number of parameters and dynamics.

The model fit produced a wide range of parameters to fit each patient specifically. Some of the parameters were distinctively identified for each data set or patient. These parameters may also directly indicate the condition of the lung. The minimal parameter approach of the model may result in certain restrictions, however the fitting of the data and the simulation are simple and clinically instantaneous. Thus, the model shows very good potential for clinical use in evaluating and modulating therapy.

Chapter 8

Model Prediction Validation and Clinical Use

It is widely known that given enough free parameters, a variety of physiological models can provide very accurate fits to most types of clinical data [Carson and Cobelli, 2001; Ben-Tal, 2006]. Therefore, a first level of validation assesses whether the model can provide accurate fits using uniquely identifiable parameters with physiologically realistic values. Clinically, however, models are most useful when they are effective at giving therapy selection to provide better or more robust care. Hence, the true test of any model is its ability, given a clinical data, to accurately predict the outcome of a therapy or intervention without knowing the actual response data. Specifically, accurate prediction of the unknown versus fitting of known data provides a second, more difficult level of validation.

Ventilator therapy is a treatment that still depends heavily on the experience and intuition of the intensive care clinician. As a result, the treatment varies widely between patients [Ferguson et al., 2005]. While there may exist set protocols for any given individual ICU, there is no global standard protocol [Deans et al., 2005]. There have been several attempts through clinical trials to standardise the protocol for ventilator treatment, particularly with regard to setting the optimal PEEP [Amato et al., 1998; Takeuchi et al., 2002] and tidal volume [ARDS Network, 2000; Kallet et al., 2005]. The end goals are always some combination of reduced length of mechanical ventilation, reduced ventilator effects, such as infection [Rello et al., 2002; van der Kooi et al., 2006], and reduced mortality. However, these studies have been challenged, both in theory and practice [Brochard et al., 1998; Brower et al., 2004; Deans et al., 2005; Eichacker et al., 2002]. There is thus no standard, well accepted protocol or approach for providing or managing mechanical ventilation.

One of the difficulties in achieving these goals may be that individual lung conditions and responses are highly variable. Each patient's lung mechanics may be fundamentally different from others, especially in injured or diseased lungs. Thus, one fixed protocol to treat an entire heterogeneous population with varying levels of lung injury may not be appropriate. Despite this difficulty, a fixed non-adaptive protocol was exactly the goal in many major studies [e.g. Amato et al., 1998; ARDS Network, 2000]. Therefore, ventilator therapy based on individualised lung mechanics using patient specific models may greatly improve the treatment, and benefit the patients [Lu and Rouby, 2000].

There are several potential clinical applications for this model. The model can individually identify the unique mechanics and condition of the patient's lung. Thus, it can be used to optimise patient specific ventilator treatment, if it can accurately predict the outcome of changes in therapy. Once the model identifies the unique patient specific parameters, it should, therefore, be able to predict the lung mechanics response at different ventilator settings. Using such a prediction, treatment can be optimised without unnecessary, time consuming procedures or trial and error analysis.

The model could also be used to analyse the state of disease and continuously monitor the patient, due to its ability to track recruitment status at a given pressure. Thus, beyond control of ventilator therapy, it offers the potential to track patient condition and disease state changes in the lung of the critical care patient. This latter application is generalisable to any mechanically ventilated ICU patient, not just those with ALI/ARDS.

8.1 Prediction

One of the difficulties with current methods of determining ventilator therapy, and PEEP in particular, is determining the optimal ventilator settings for a patient. Furthermore, the condition of the patient and the state of disease changes over time. Thus, the optimal setting is specific to a patient's condition at that time. In current practice, the ventilator is initially set to predefined levels and the parameters are varied depending on the resulting PV curves and blood oxygen concentration, as well as other clinical variables depending on the clinician. The

procedure is essentially a trial-and-error approach to evolve to an acceptable therapy.

Because the model can identify lung mechanics over an entire pressure range, it can be used to predict the lung mechanics at different ventilator settings and display the results as a well-known PV curve. It thus allows the clinicians to see the result before it is actually applied to the patient. Clinicians can then make a decision on whether to apply the changes.

Furthermore, the model can make predictions about multiple different settings in a relative instant. In contrast, the actual lung may take a several minutes to account for each change rendering this approach to optimising therapy both overly intensive and difficult. A relatively instantaneous result eliminates the need for trial-and-error procedures, and an optimum setting can be obtained immediately relative to normal clinical responses and time frames. However, this improvement in therapy selection can only occur if the predictions made by the model are accurate over the therapeutic ranges.

8.1.1 Prediction Method

Once all the model parameters are identified, the prediction process is relatively simple. The fundamental lung mechanics are captured by a single set of parameters for a patient, and changes in PEEP are captured by a single parameter, the mean shift. The trend of the mean shift can also be captured by fitting the data to known linear or polynomial equations. Thus using this equation, an appropriate mean shift can be calculated for any PEEP setting as long as the predicted trend is accurate.

The majority of fitted clinical data in Chapter 7 showed a mean shift relationship that was almost completely linear. Once this trend is captured using a minimum of 2 PV curves at different PEEP settings, the predicted mean shift for a new PEEP level is simply calculated from that equation. The predicted PV curve is then produced using the newly calculated TP mean values and the other already identified parameters.

The data sets from the study by Bersten [1998] that were used for model validation in Chapter 7 are used here to provide preliminary validation of the models predictive ability. For data with 3 PEEP values, 2 PEEP settings are used to fit the model and mean shift trend. The fitted model is then used to test the ability to predict the results of the third PV loop. For data with 4 PEEP values, 3 of the PV curves were used to predict the fourth. Any combination of PEEP values and PV curves may be used to test against the remaining unused PEEP value and PV curve. For this validation, all data sets from Chapter 7 are used. However, Data Sets 1 and 5 in particular are discussed in detail.

8.1.2 Prediction Results, Discussion and Limitations

The model was able to predict the missing mean shift and PV curve for the PEEP level with relatively small errors. The overall average absolute pressure point error for Data Set 1 was 13.9 ml (1.40%) and 60.7 ml (4.93%), for inflation and deflation respectively. For Data Set 5, the average absolute error was 15.6 ml (1.87%) and 41.9 ml (5.42%), for inflation and deflation respectively. Table 8.1 summarises the prediction errors for these 2 data sets for each predicted PEEP value.

Table 8.1 Summary of PV prediction errors for Data Set 1 and 5.

Data Set 1

	Inflation		Deflation	
PEEP	Error [ml]	Error [%]	Error [ml]	Error [%]
5	13.28	1.76	52.80	8.03
7	11.01	1.01	63.82	6.77
12	17.40	1.41	65.53	4.92

Data Set 5

	Inflation		Deflation	
PEEP	Error [ml]	Error [%]	Error [ml]	Error [%]
5	16.59	2.40	15.44	2.99
7	10.43	1.49	88.74	14.92
10	16.75	1.92	17.04	1.88
12	18.81	1.68	46.40	5.03

Table 8.2 summarises the overall prediction errors for all 12 sets. This table shows the maximum and average percentage absolute error for inflation and deflation at each predicted PEEP level, as well as interquartile range of errors. Data for PEEP of 0 cmH_2O was not included because there was only one set of

data that included a PEEP of 0. Note that the basic trend is a decreasing average and maximum absolute error as PEEP, and thus overall volumes, increases. This trend is caused by the difference in absolute values with which the percentage errors are calculated, as discussed in Chapter 7.

Table 8.2 Summary of PV prediction percentage errors for all data sets. The errors are listed according to predicted PEEP levels.

	Inflation			Deflation		
PEEP	Avg.	IQR	Max.	Avg.	IQR	Max.
5	8.11	2.08 - 9.24	33.22	11.22	7.79 - 12.22	39.33
7	4.56	1.01 - 7.99	15.28	11.74	6.38 - 14.92	28.91
10	6.55	1.98 - 6.27	28.38	12.63	6.35 - 13.18	43.94
12	5.89	1.81 - 8.35	16.90	4.28	1.28 - 6.19	9.58
15	3.81	2.87 - 4.75	5.70	9.19	8.16 - 10.23	11.27

Figure 8.1 illustrates the fitted mean shift and the actual mean for PEEP of 5 cmH_2O in Data Set 1 as predicted, having fitted the data for PEEP=7 and 12 cmH_2O. The predicted mean is marked with an asterisk ($*$). Figure 8.2 illustrates the resulting PV curve prediction, where the dashed lines are the original clinical data for the predicted PV loop. Because the model fitting avoided the highly dynamic transition area, the prediction was also made only for the steady portion of the curve, as illustrated with red dots in the figure. It is clear that the errors in Figure 8.2 are clinically insignificant.

Figures 8.3 and 8.4 illustrates the same prediction result for PEEP levels for 7 and 12 cmH_2O for Data Set 1, respectively. All results show minimal errors that are clinically insignificant. Finally, note that the linear mean shift trend lines in Figures 8.1 - 8.4 are all effectively identical with minimal differences.

Figures 8.5 - 8.8 illustrate the same results for all PEEP level predictions in the larger Data Set 5. In contrast to Data Set 1, the slope of these patient specific mean shift values is lower, indicating a patient less responsive to changes in PEEP. More specifically, this patient experiences far less of an increase in recruited lung volume for a given increase in PEEP, indicating less clinical effect in modifying therapy. Similar to the results for Data Set 1, all the predicted PV curves show clinically insignificant levels of error.

The mechanics of the lung at the missing PEEP values are readily predicted by linearly fitting the mean shift to identify the impact of this change. It also

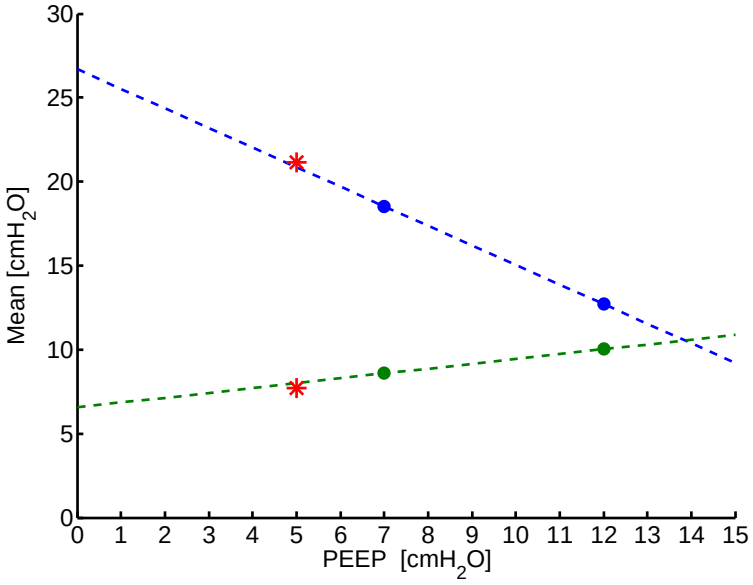

Figure 8.1 A fitted mean shift for prediction result for Data Set 1. PEEP=7 cmH_2O and PEEP=12 cmH_2O was used to predict PV data at PEEP=5 cmH_2O. The linear lines for mean shift (dashed lines) are identified from the 2 given data sets (solid dots). The red $*$ shows the original of the mean being predicted. Blue and green lines are for TOP and TCP distribution mean, respectively.

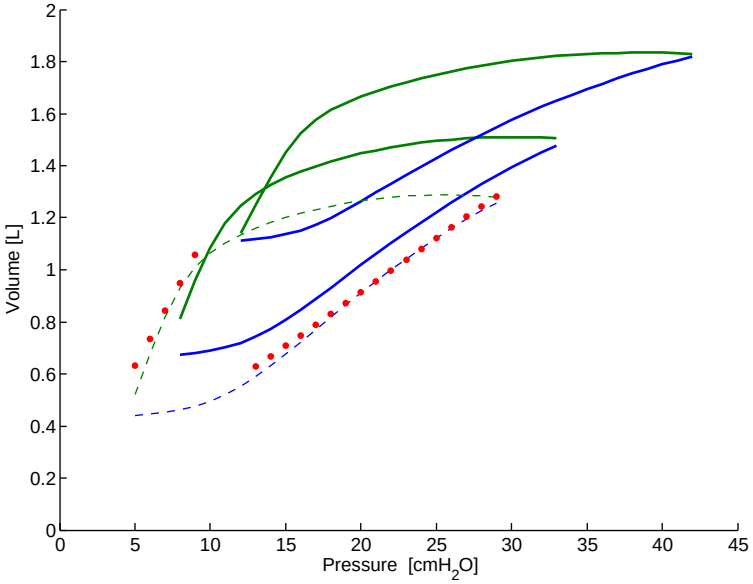

Figure 8.2 A prediction result for PEEP=5 cmH_2O of Data Set 1. The PV data was predicted by fitting 2 known PEEP levels (solid lines). The red dots indicate the predicted data and dashed lines show the original data.

allows the simplest method for predicting the mean at a new PEEP level. However, some of the means are not perfectly fitted and predicted by the linear fit, as best illustrated in Figure 8.4, where the dots are not exactly on the predictive line for this relatively extreme PEEP setting. This inaccuracy causes the relatively larger error of the predicted PV curve, which is still well within clinical

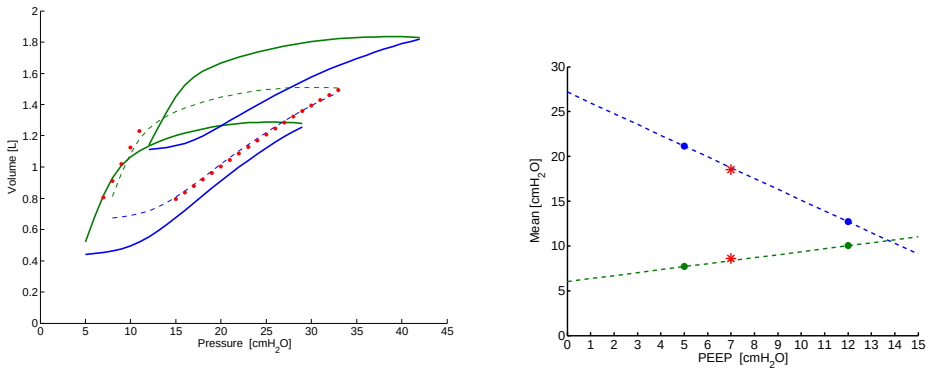

Figure 8.3 A prediction result for PEEP=7 cmH_2O of Data Set 1.

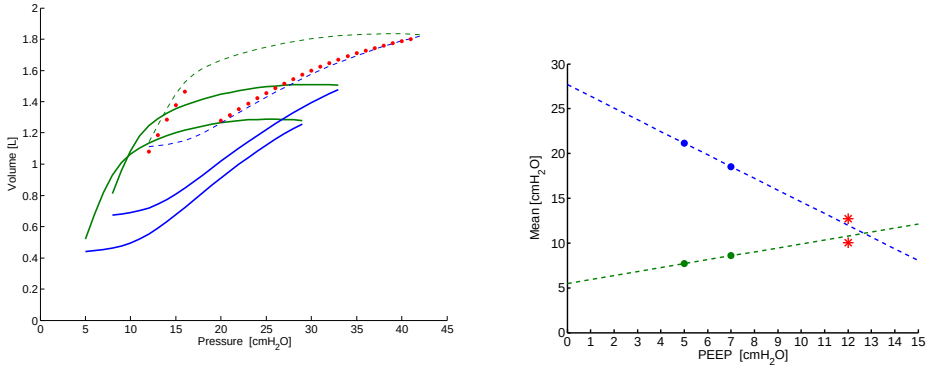

Figure 8.4 A prediction result for PEEP=12 cmH_2O of Data Set 1.

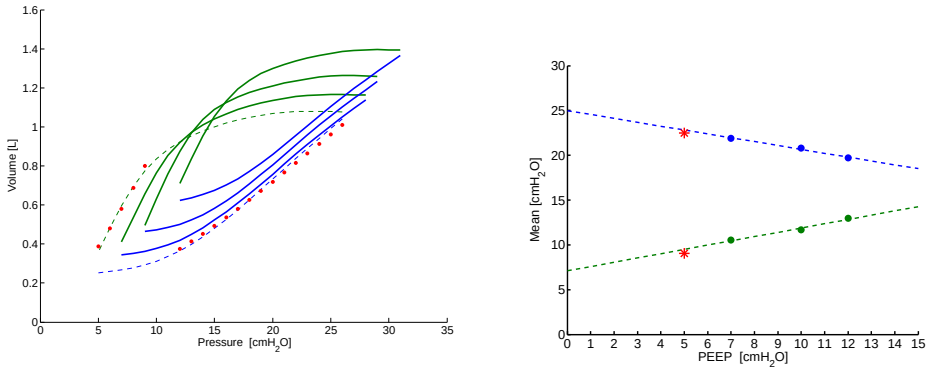

Figure 8.5 A prediction result for PEEP=5cmH_2O of Data Set 5.

expectations. It may be possible to predict the trend better by using some other equation for the mean shift fit in this specific case. This approach would require further investigation using additional clinical data and validation of the model that is not undertaken for this thesis. However, it is important to note that this error in the predicted mean shift is not clinically significant.

This prediction method utilises just a single parameter to predict between different PEEP settings. Thus, it is simple and easy to use, and can predict a patient specific response to the change in primary therapy. However, it limits

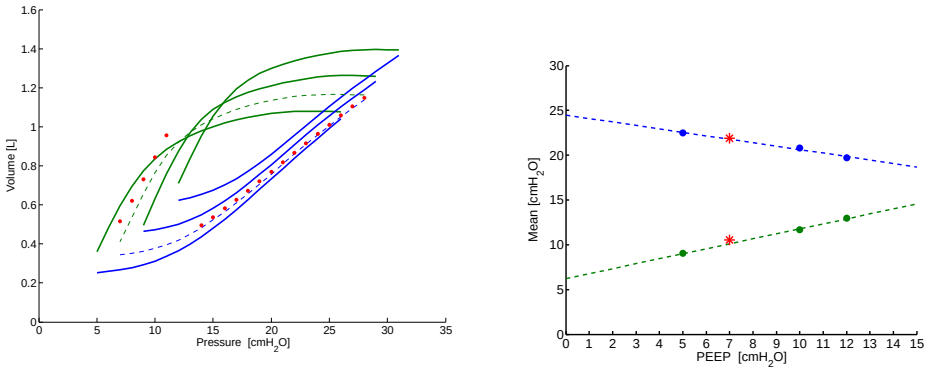

Figure 8.6 A prediction result for PEEP=7 cmH_2O of Data Set 5.

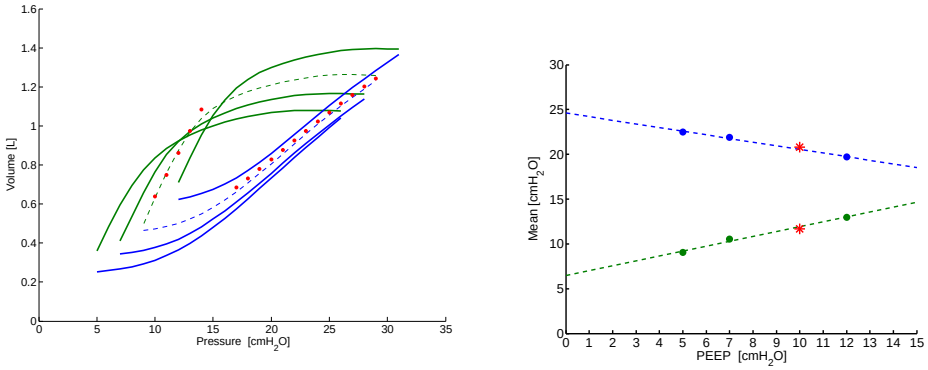

Figure 8.7 A prediction result for PEEP=10 cmH_2O of Data Set 5.

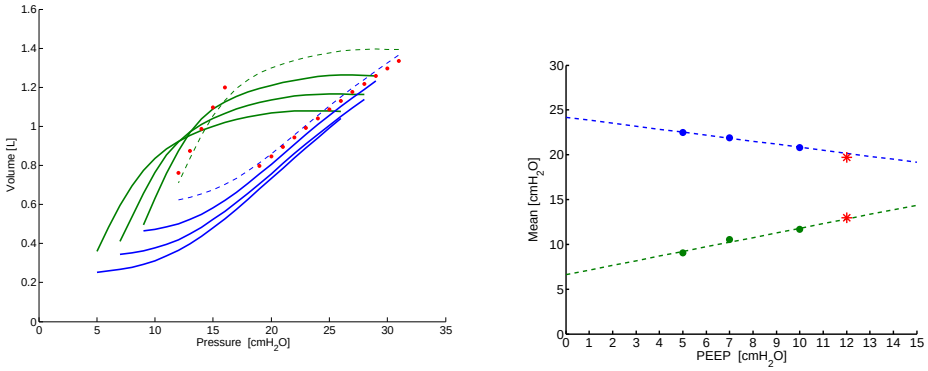

Figure 8.8 A prediction result for PEEP=12 cmH_2O of Data Set 5.

other ventilator settings. Since the model parameters were identified using PV loops, only the mechanisms that produced the PV loops are captured. Thus, this prediction method cannot be used to predict drastically different ventilator settings, such as ventilator mode, flow pattern, maximum inspiratory flow, etc.

However, it should be possible to predict the effect of different tidal volumes, since the EEV is only correlated to PEEP, as long as the flow rates do not change drastically. This impact of flow rates is distinct due to the use of proximal data

[Karason et al., 2000, 2001], and the airway resistance changes when flow rates change drastically, as discussed in Chapter 2 and 6. This limitation also implies that when the ventilator setting is changed drastically, the model needs to be refit and re-identified using 2 or more PV loops at that new setting.

That all said, such drastic changes are not typically part of standard ventilator therapy, which focuses more on gradual evolution of settings [Rouby et al., 2002]. In addition, the more detailed models of Chapter 4 could potentially manage such changes, but at a cost of much greater data requirements. Hence, it might be best noted that the model is limited to evolutionary prediction and changes typical of critical care.

This model has the ability to fit and follow the trend of any data including those from a ventilator. Thus, it can reproduce the shape and values of the particular data. For example, if the model was used to identify the parameters for ventilator data, then the model can predict the ventilator data at different settings. Similarly, if carina measurements like those of Karason et al. [2000] are used, then the model can be used to predict the PV curve at the carina for different settings. Thus, the model can be very generally applied to any data set or type that may be available.

It may also be possible to use this model to assess the true lung mechanics, if the ET tube and proximal airway resistances were better known or estimated empirically at the bedside. This approach would require a smarter, more automated ventilator and/or excessive clinical time. However, such smarter ventilators are being developed [e.g. Brunner and Iotti, 2002; Rees et al., 2002, 2006] and may appear in future.

This model and the prediction methods presented may avoid unnecessary additional interventions for a patient in ICU. However, the process requires data with at least 2 different PEEP settings and preferably those with EEV measurements, as well. These data are not always routinely measured in the ICU [Bersten and Soni, 2003; Stenqvist et al., 2002], and the effect of these measurements on the patient is not yet fully determined. It is, however, possible to measure them with relatively easy manoeuvres within short periods of time. It may even be possible to integrate them into the ventilator to be measured automatically [e.g. Rees et al., 2002].

8.2 Mean Shift Trend

The key parameter for predicting PV curves at different therapeutic PEEP levels in this study is the threshold pressure mean shift. This parameter essentially indicates the volume response of the lung mechanics to changes in PEEP. Thus, this parameter may be directly applicable and highly valuable in clinical situations.

8.2.1 Clinical and Physiological Relevance

The preliminary validations in this study found that, for a given patient and condition, this parameter is essentially linear with a constant slope across reasonable PEEP ranges. Figure 8.9 illustrates linearly fitted mean shifts for data set 1 (right) and data set 5 (left). Each line was fitted to just 2 identified mean values at different PEEP levels. Thus, there are 3 pairs of lines in total, one for each combination with the pair having one line for inflation and one for deflation. The lines are essentially indistinguishable regardless of the PEEP level mean value being predicted. This result clearly illustrates the effectively constant slope of the mean shift trend for these two patients within the given therapeutic range of PEEP levels examined.

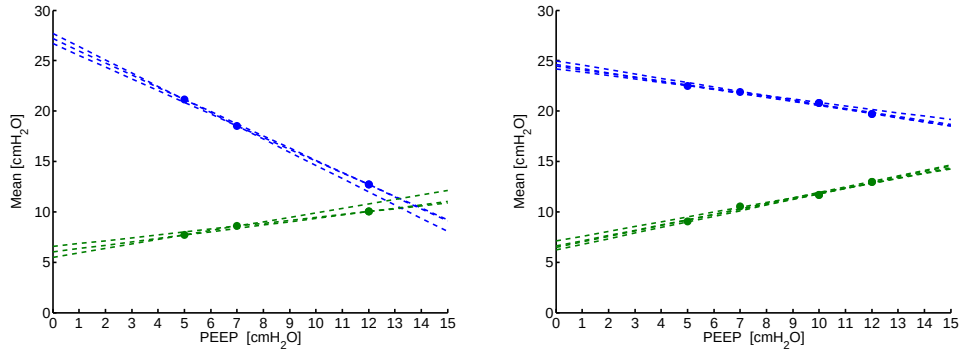

Figure 8.9 Mean shift slopes for Data Set 1 (right) and 5 (left). These linear lines are created by fitting 2 means at different PEEP levels. Blue and green lines show TOP and TCP distribution mean, respectively.

Finally, it should be noted that Bersten's study [1998] was examining lung over-inflation. Hence, these PEEP ranges may cover a relatively wider range, although well within accepted limits, than the typical PEEP range used clinically. This constant slope parameter over that range is thus a unique result in this field and offers significant potential in monitoring and assessing the patient response to the therapy.

In contrast, the slopes and the values of the mean are different between patients, as also illustrated in Figure 8.9. Given that both of these patients are ARDS/ALI affected to differing extents and have differing lung function, it is very likely that each patient responds differently to changes in PEEP. Figure 8.10 illustrates the identified mean shift for all 12 data sets. The value of the mean and the slope of the shift trend vary greatly between patients indicating a highly variable patient specific value.

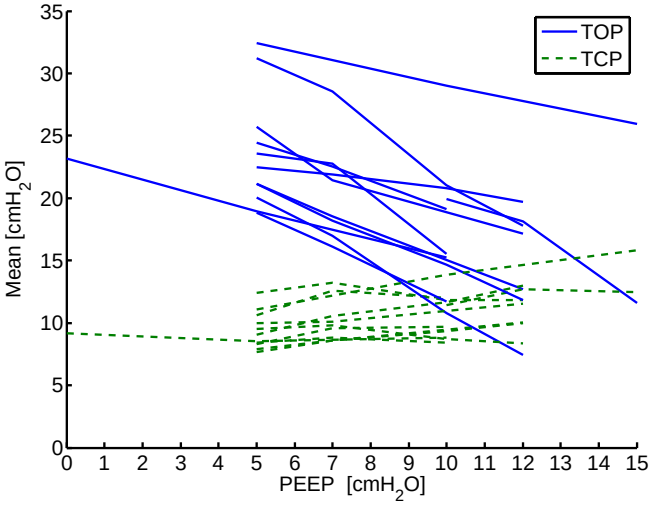

Figure 8.10 Mean shift for all 12 data sets. The values and the slope vary greatly between patients.

The distribution mean values over all PEEP levels are summarised in Table 8.3. The table also shows the fitted slope for each patient data set. This wide variation and the ability to track the patient specific response to PEEP change indicates that these parameters can uniquely reflect and assess the lung mechanics of the patient and their lung condition.

This variation between patients also explains, at least in part, the lack of a standard protocol for ventilator treatment. A majority of the studies to date have used a few discrete ventilator settings to search for optimal treatment [e.g. Amato et al., 1998; ARDS Network, 2000]. However, patient condition and lung mechanics vary greatly, as illustrated by the broad and continuous variation of mean shifts and slopes between patients in Figure 8.10. Therefore, the optimal settings for individual patients will also vary broadly and continuously. In other words, a single standard protocol for all patients may not be possible in the light of this data. Instead, these results show that patient's lung mechanics and condition must be considered individually to determine the specific optimal setting for the patient.

Table 8.3 Summary of TP distribution mean and the slope of its shifting trend.

	TOP mean				TCP mean			
Data Set	Min.	Max.	Avg.	Slope	Min.	Max.	Avg.	Slope
1	12.7	21.1	17.5	-1.20	7.7	10.0	8.8	0.32
2	15.2	23.2	19.1	-0.80	8.5	9.2	8.8	-0.03
3	19.1	24.5	22.0	-1.07	8.3	9.7	9.2	0.26
4	15.5	23.5	20.6	-1.67	10.6	12.6	11.7	0.24
5	19.7	22.5	21.2	-0.39	9.0	13.0	11.0	0.53
6	17.8	31.2	24.6	-2.01	11.8	13.2	12.3	-0.14
7	7.4	20.1	13.8	-1.84	8.4	9.8	9.1	-0.20
8	17.2	25.7	21.4	-1.15	10.0	11.6	10.5	0.24
9	11.6	19.9	16.6	-1.71	11.4	12.7	12.2	0.18
10	11.8	21.1	16.5	-1.31	7.9	10.0	9.0	0.28
11	11.7	18.8	15.5	-1.43	8.4	8.8	8.6	0.00
12	26.0	32.4	29.1	-0.65	11.1	15.8	13.6	0.47
Avg.	15.4	23.7	19.8	-1.27	9.4	11.3	10.4	0.18
Min.	7.4	18.8	13.8	-2.01	7.7	8.8	8.6	-0.20
Max.	26.0	32.4	29.1	-0.39	11.8	15.8	13.6	0.53

Gattinoni et al. [2006] recently conducted a study on lung recruitment using CT scans. The study showed that there is significant patient variability in the amount of potentially recruitable lung, which is strongly associated with the responsiveness to the PEEP change. This result correlates well to the variability identified by this model, as illustrated in Figure 8.10. Furthermore, they found a link between amount of potentially recruitable lung and mortality. Thus, this mean shift parameter may have further clinical perspective and impact.

8.2.2 Airway Resistance and True Lung Mechanics

Tube resistance, as discussed in Section 2.1, plays a significant role in the shape of the exterior, proximal PV curve. The more direct representation of the true(r) lung mechanics at the carina can be significantly different from what is indicated by the dynamic PV data, especially for proximal data measured before the ET tube. This effect is further magnified for data taken inside the ventilator due to the additional connectors and air spaces. Such effects are best illustrated in Figures 6.9 and 6.10. Thus, using such data may not fully reflect the true condition of the lung, and the usefulness of fitting the model and analysing the data may be questioned.

However, in most ICUs, the true lung, or carina, measurement is not a routine protocol and often the only data available comes from inside of a ventilator. Hence, the validation and predictive results presented still provide an (potentially limited) advantage over current practice. However, the question remains as to how well proximal data can be extrapolated to represent the true lung mechanics.

The patient specific mean shift parameter identified by this model is a direct result of analysing raw proximal PV data, which includes dynamic and resistive effects. Therefore, the parameter identified may not directly represent the true lung mechanism. However, because the model is based on the fundamental mechanics, the slope of the mean shift and its clinical relevance can be readily related to the true lung mechanics. One such method to show this relation is to use the estimated carina measurement. Carina measurement can be estimated with reasonable accuracy without additional intervention to the patient, as long as the flows are measured [Lichtwarck-Aschoff et al., 2003]. An example of that process is presented here.

It is relatively straight forward to estimate the true lung, or carina, pressure from proximally measured pressure. The ET tube is essentially a pipe with a known diameter and length, and the fluid flow in a pipe and its resistance has been well studied and established [e.g. Zamir, 2000]. Therefore, its resistive effect can be calculated from its dimensions and the flow rate, which is a part of a routine PV measurement in the ICU. Physiologically more accurate parameters may then be identified by analysing the estimated true lung PV loops.

Figure 8.11 illustrates an example of PV data and its estimated inspiration carina measurement using the data from Chapter 7 (Data Set 1). The patient was ventilated with a constant inspiratory flow rate, thus the resulting resistive pressure loss is also constant during the steady portion of inspiration. Therefore, the carina pressure is easily estimated in this case using a constant pressure reduction. This estimation is appropriate for this data and this model because the parameters are identified using this steady portion of the data. Different cases would require some (limited) extended flow-resistance analysis to achieve a similar result.

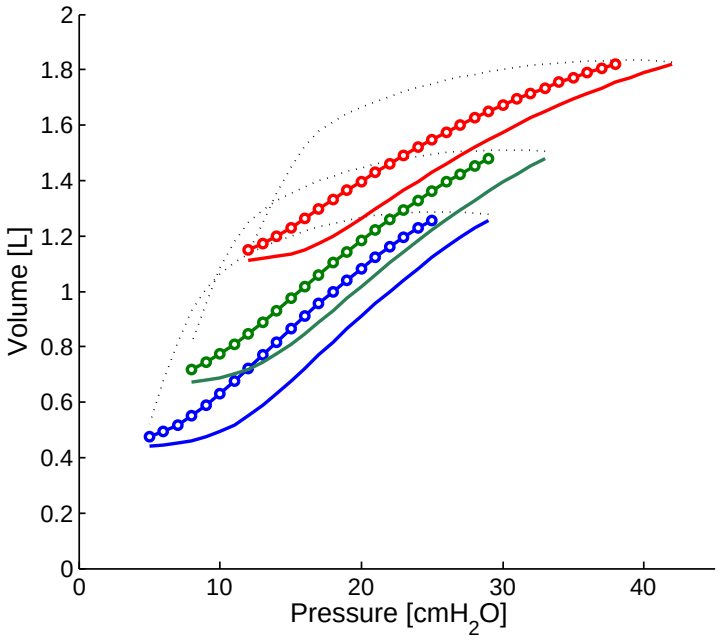

Figure 8.11 An example PV data (Data Set 1) with estimated carina inflation PV. The PV curve is estimated as a constant pressure reduction because of the constant flow rate used. The solid lines shows the original proximal PV curves and the lines with *open circles* shows the estimated carina PV curves for all PEEP levels (Blue, green, and red for PEEP=5, 7, and 12 cmH_2O, respectively).

The estimated PV data is then fitted to the model and the parameters are re-identified. Figure 8.12 illustrates the fitted carina PV data. The plot illustrates the original, proximal, PV data and the estimated carina PV data, and their fits. Figure 8.13 illustrates the resulting TP distribution mean shifts for the proximal and carina data. As can be seen from the plot, the means are simply shifted to a lower value, and the slope of the mean shift is exactly the same as for the proximal measurement. This difference simply represents the additional pressure required to overcome the tube resistance.

The model's fundamental mechanics allows the identification of this principal lung parameter, regardless of the location or types of measurement. The slope of the mean shift, representing the responsiveness of the lung, is valid for both proximal and estimated carina data. This result indicates that this parameter captures the essential features of the dynamic data that signifies the basic underlying lung mechanics. Therefore, this parameter determined from the dynamic and resistive data may be directly applicable to the true lung mechanics and, more importantly, can be readily implemented clinically. An independent clinical study has also found that the true lung mechanics can be derived using the proximally measured dynamic PV data [Stahl et al., 2006], validating this result.

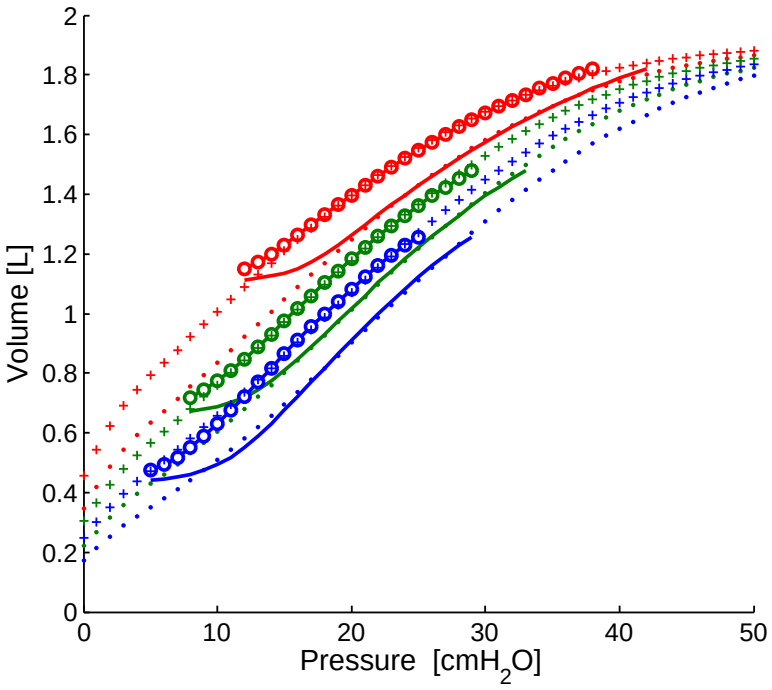

Figure 8.12 An example of model fit to proximal and estimated carina PV data (Data Set 1). The solid lines shows the original proximal PV curves and the lines with *open circles* shows the estimated carina PV curves for all PEEP levels (Blue, green, and red for PEEP=5, 7, and 12 cmH_2O, respectively). Dots and + symbols shows the model fit to proximal and estimated carina data, respectively.

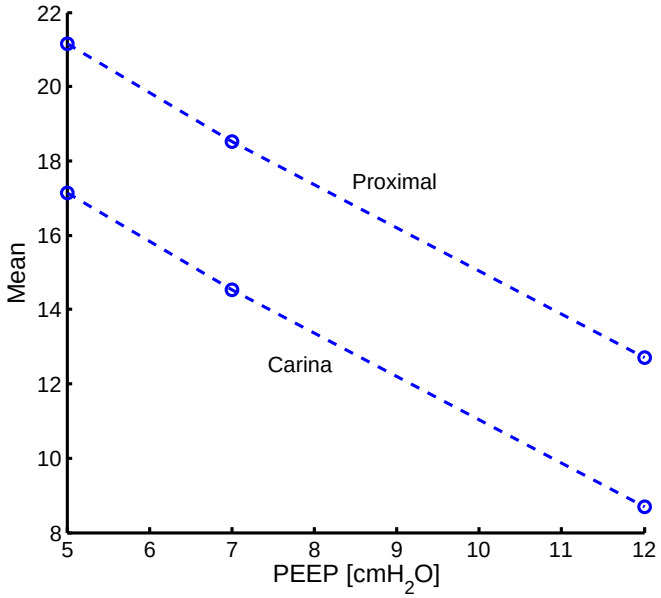

Figure 8.13 Mean shifts for proximal and estimated carina data. The means for the estimated carina PV curve simply moves to lower values, indicating the additional pressure required to overcome resistance. The slope of mean shift is the same as proximal.

The example presented here uses simple, but clinically typical, constant flow rate data. Other data with more complex variable flow patterns, including the deflation limb, can also be processed in a similar manner. However, the resistive pressure needs to be estimated using the associated flow data at each pressure point to account for variable flows. This calculation is well defined and only requires the dimension of the tube and flow data, which are part of routine PV data measurement. Fitting the model to this data allows identification of the true lung parameters. More importantly, the essential mechanics may be identified regardless of the location of the pressure measurement.

8.2.3 Summary

The mean shift parameter is directly related to the response of lung mechanics to the PEEP change. Therefore, this parameter may be used to assess the effectiveness of certain ventilator treatments, such as recruitment maneuvers, where the main goal is to use pressure changes (i.e. PEEP) to increase the amount of recruitment. More specifically, this model can predict the recruitment status and response of a given patient directly using the mean shift parameters. Therefore, it can indicate how effective such a maneuver may be for a particular patient and condition. This is an extremely important piece of information that will better inform clinician about the effectiveness (or lack thereof) of their ventilatory therapy.

Given that the data analysed here are from patients with different extents or indication of ARDS/ALI, as well as different lung mechanics, it is possible to draw the following clinically relevant conclusions:

- The mean shift slopes are a measure of a patient's unique volume responsiveness, and thus recruitment responsiveness, to change in PEEP.
- The volume responsiveness may be linked to mortality [Gattinoni et al., 2006], indicating that the slope of the mean shift may have additional clinical perspective and impact.
- The slopes are likely to change with condition and thus offer the ability to assess and track condition on a regular or as needed basis.

- The slopes should likely be checked before applying a change in therapy or at an interval (daily or more frequent) that would enable them to be relevant when the therapy is changed using this approach.

- It may be necessary for relatively large changes in PEEP therapy to assess the slope in different PEEP regimes (as with data set 5) to ensure accuracy. A refitting at the final selected PEEP value and re-evaluation of the slope is straightforward computationally and would verify any such significant action taken.

- It is often difficult for the clinicians to know if the change in pulmonary mechanics is due to a true change in patient's condition or due to sub-optimal ventilation. The ability to track changes while delivering more optimal ventilation will inform the clinicians about the true changes in pulmonary mechanics.

Overall, these results indicate that the mean shift slope, which is the direct product of the methods and models developed in this thesis, provides both a validated physiological method for assessing lung function, as well as a validated clinical predictive ability to guide this unique critical care therapy.

8.3 Other Potential Clinical Use

This model has other potential uses in clinical situations. Some parameters, such as the total number of units and standard deviation of the TOP distribution, may be used to directly indicate the condition of the patient and the level of injury or disease. Hence, it has a role that is strictly related to patient specific disease monitoring.

Furthermore, ventilator induced lung injury (VILI), such as barotraumas and over-inflation, can be caused by suboptimal ventilator treatment or error [Dreyfuss and Saumon, 1998]. However, identifying the injury in real time may be difficult. One of the ways to detect the over-inflated lung is to use the slope or compliance of the inflation PV curves [Bersten, 1998]. This metric is directly related to the standard deviation of the TOP distribution. Thus, it can be easily

implemented in the model for detecting over-inflation or managing injury status. This implementation enables the model to optimise the ventilator, as well as detect VILI, further enhancing its potential practicality in clinical situation.

Because the model is completely software based, it can be integrated directly into any modern ventilator. This integration allows a continuous monitoring of the patient condition and easy therapeutic decision support. Similar integration could be obtained by placing the sensors in breathing circuits or the use of carina sensors.

The model based system could thus automatically track the disease state over time, detect VILI, optimise the ventilator settings as the patients' condition changes, and alarm clinicians if the condition changes drastically. Tracking of clinical condition obviates the need for further investigations, such as repeated micro-biological sampling, and adds consistency to each patient's care. Finally, the system model is computationally simple enough that it may be implemented into smaller devices to be used in ambulances, for example, or into a PDA for extra portability.

Part IV

Conclusions and Future Work

Chapter 9

Conclusions

Overview

Mechanical ventilation is the one of the most common treatments a patient receives in the ICU with significant implication for both mortality and cost outcomes. However, a convenient and practical method for determining and quantifying the underlying condition of the individual patient lung is lacking. As a result, the optimal setting of the ventilator is not clearly defined, and the clinical studies designed to clarify this difficulty have been controversial at best. They provided no clinically effective answers to the critical care community.

A quasi-static minimal model is developed that captures all the essential features of lung mechanics using readily available non-invasive clinical PV data. It is able to identify unique patient specific parameters, as well as a clinically meaningful patient responsiveness to the treatment. The model therefore has significant potential to provide a method to evaluate the lung mechanics in clinical real-time to aid diagnosis and predict the outcome of therapy changes at the bedside in critical care.

Full Conclusions

Mechanical ventilation is one of the most widely used, and one of the most costly treatments for ICU patients. It is used to aid the patient with breathing difficulty due to lung injury, such as ARDS, by reducing the work of breathing and thus reducing patient effort. Many patients in ICU are fully sedated and thus fully dependent on ventilator. However, sub-optimal ventilator settings can interfere with efficient gas transfer, hindering patient recovery. Moreover, a wrongly set ventilator can cause additional damage to the lung. Therefore, optimising venti-

lator treatment requires a delicate trade-off between larger volume to maximise gas transfer and smaller volume to minimise further lung injuries.

Currently, there are no established or accepted protocols for ventilator treatment. There have been a number of clinical studies attempting to standardise the treatment, however none has been accepted as a global standard. As a result, protocols vary greatly between different institutions and clinicians, and the final decision often depends on the experience and intuition of the intensive care clinician.

This lack of global protocol is caused, at least in part, by the variable condition and lung mechanics between patients and over time as patient condition evolves. These evolutions and differences require a specific optimal treatment for each individual patient and thus a patient specific approach to achieve significant result. However, this need for customisation is hindered by the lack of a convenient method to measure and quantify the underlying disease condition and lung mechanics of the individual patient at the bedside.

This research, therefore, developed a novel model of lung mechanics that captures the fundamental mechanics of the mechanically ventilated lung. The model is based on physiologically relevant and mechanically accurate components, using newly hypothesised and clinically observed lung mechanics. It is the first clinically focused lung model to base its mechanics on the primary mechanism of recruitment and derecruitment. Patient specific parameters are thus able to be identified using readily available clinical PV data providing the necessary patient specific identification of lung status and condition.

Three models are developed using the same principal components, but utilising different numbers and types of lung units. The first full physiological model consists of 4 unit types, accounting for all unit types present in the ARDS lung. This full model provides the most physiological detail and the highest resolution, however it is limited in clinical situation due to excessive number of parameters that needed to be uniquely identified. The second model utilises 2 unit types, representing ARDS and healthy lung units. This reduction essentially halves the number of parameters to a more manageable level, however the number of parameters is still clinically impractical and the information it provides may not all be directly relevant at the bedside.

The third and final model consists of a single unit type, specifically focusing on clinical practice. Using clinically observed values and mechanics, the parameter identification process is further simplified, and the model is able to identify patient specific lung mechanics using just 2 parameters for each respiration limb. This final model can uniquely identify lung mechanics of a patient from readily available data in ICU without requiring additional test or equipment. In particular, its assessment of lung function via distributions of lung unit recruitment provides several novel and unique clinical features that are relevant to clinical practice and therapy selection.

The model was initially validated using a physiologically relevant mechanical lung simulator. It produces PV data closely matching that of clinically reported data including proximal and carina measurements, while providing a wide range of physiological compliances and lung mechanics. The lung model was validated by fitting it to the simulator data. The model captured all key features of the data with minimal errors of less than 3%, showing the ability and versatility of the model to capture all the essential features and fit a wide range of lung mechanics.

The model was further validated using the clinical data consisting of different PEEP levels and EEVs for several different patients. The model identified each patient uniquely with average absolute errors of less than 5%. These results indicate a high level of clinical relevance, while capturing all distinguishably different patient specific mechanics. The clinical practicality was further validated by assessing the model's predictive ability to changes in therapy using the same clinical data. The model was able to predict the PV response to different PEEP levels within 10% on average, as well as identifying unique patient specific parameters.

A particularly useful and novel result is that the system model can identify a parameter that directly indicates the patient's responsiveness to changes in therapy. Such a parameter has significant relevance for practically assessing the patient's condition and optimising treatment in clinical situations. In addition, this parameter, while patient specific, was uniquely identifiable across the clinical cohort. A parameter of this nature has not been reported in the literature to this date.

Overall, the minimal model of lung mechanics developed in this research is based on the fundamental physiology and mechanics of the mechanically ventilated lung. The model is able to fit a variety of different clinical and simulated data with minimal error while capturing the essential characteristics. A preliminary validation of its predictive ability showed good results and identified patient specific parameters of high clinical significance. While a full clinical validation of the model and further evaluation of the system are required, the model shows great potential to be used as both a clinical diagnostic decision support tool and a continuous patient monitoring tool in critical care.

Chapter 10

Future Work

10.1 Full Clinical Validation

The validation of the model using the simulator and clinical data presented in this thesis have laid a strong foundation for this model and show very good potential for clinical applications to optimise ventilator treatment. However, an extensive clinical study is required to fully validate the ability of the model and the effectiveness of the system.

For a full validation, the study requires additional clinical data from a variety of different patients with different disease conditions. These sets of data will allow a full validation of the model fit and identification of the unique parameters. The ideal data set would include all necessary data, such as EEV and different PEEP levels, to fully validate the model's potential. It would be valuable to include data that may indicate the severity of the disease, such as CT scans, so that the identified parameters can be directly compared. This additional data and the comparison would lead to development of a database which can be used to identify the severity of disease using the model parameters.

Hence, there are at least three trials that could be done embedded into the fourth overall randomised trial. Alternatively, they could be done separately or in parts. Specifically:

1. Evaluate metrics of recruitment using CT scan and PV data:

   This test will evaluate the effectiveness of mean and SD of TOP and TCP as a overall recruitment indicator by directly comparing the result with that

of CT scans. Multiple PEEP level trials will allow evaluation of mean shift as a metric for patient specific responsiveness to change in PEEP.

2. Evaluate change in therapy prediction with different PEEP:

   This test will evaluate the model's predictive ability as well as the prediction method of the system model. The linearity of mean shift and its limits can also be evaluated.

3. Evaluate the ability to monitor and track patient and disease condition:

   The data would be collected on a regular basis daily along with a CT scan to compare with model results. This test will evaluate the model's monitoring and tracking ability as patient condition and disease status change over time.

4. Randomised controlled trial (RCT) for ventilator optimisation:

   This large RCT will evaluate the overall effect of applying this model as a part of mechanical ventilator treatment in critical care and compare outcomes with conventional treatment. Several aspects of the treatment, such as length of MV, cost, and outcome will be compared and studied.

The first and the second trials can be conducted at the same time to fully and clinically validate the model and its methods. The third trial can also be done at the same time, however it will need to be conducted over a several days. Finally, the RCT can be conducted to evaluate the overall effect of the applied model methods. Additional clinical studies could be done to compare against other therapy protocols.

10.2 Model Components

The model presented in this thesis is not necessarily a final form. The model was validated against a significant, but limited, number of clinical data sets. This validation showed excellent results, however, a few model components and their governing equations require further investigation to create potential improvements.

10.2.1 Mean Shift Equations

One of the parameters for uniquely identifying the key mechanics of the lung is the threshold pressure distribution mean shift between different PEEP settings. It was the key parameter used in prediction of change in therapy. The current model presented in this thesis uses a linear equation to fit the shift with good results within the therapeutic PEEP ranges given. However, some data showed a trend that was not completely linear and may be fitted better with some other equation.

For example, it can be speculated based on lung physiology that at an excessively high PEEP, the lung tissue is fully stretched and the increase in volume at a given pressure with increasing PEEP reduces. Therefore, the amount of mean shift is also reduced at this PEEP level, and the slope of the shift decays to zero. This trend cannot be described by a simple linear equation. Instead, this physiological trend may be better described by an equation that includes this decay (e.g. second-order) at relatively high PEEP levels.

It is also possible that within clinically reasonable PEEP levels, the mean shift is close enough to linear and thus can be described by the linear equation. However, depending on the severity of lung injury, patient may be ventilated at near maximum lung capacity. At this level, the linear equation may not be suitable to effectively describe the trend. Alternatively, such changes in this range may be due to lung obstruction or other unmodelled behaviours. Additional clinical data and further evaluation of the model is required to clarify these issues.

10.2.2 Threshold Pressure Distribution Equations

The threshold pressures and their distributions are the most fundamental mechanics in this model. The current model presented in this thesis describes the distribution using a normal distribution function for greatest simplicity. As a result, the distribution is symmetrical about the mean. However, it is known that ALI/ARDS affects a lung heterogeneously, and the healthy and injured lung units are present in the same lung. It is also known that healthy and injured lung units exhibit significantly different mechanisms of volume change. Therefore, the

true lung mechanics and condition may be better described by incorporating the differences between these units. The second, 2 unit type, model was developed based directly on this concept, but requires a much greater amount data or other measurements to identify the model.

However, rather than doubling the number of parameters by having a separate unit types, as with the 2 unit type model, it may be possible to include the effect of different unit mechanics in a single curve. One such method is to use the skew-normal distribution, which require only 1 additional parameter. The major difference between healthy and injured lung unit mechanics is their TOP. The healthy units are recruited at a lower pressure in relatively small pressure range, resulting in a narrow high peak distribution. In contrast, the injured units are recruited at a higher pressure and over a wider range, resulting in a broader flatter distribution. The skew-normal distribution may be able to describes this overall effect of fast recruiting healthy units and slow recruiting injured units with a single curve.

Furthermore, the skewness of the distribution may directly indicate the level of lung injury of the patient producing another patient specific parameter. The use of this distribution function will add at least one more parameter that needs to be uniquely identified, which may or may not require additional data or testing. However, compared to using 2 unit types, one additional parameter is clinically plausible. Finally, even more direct identification of the level of lung injury that this distribution may provide would be very advantageous in clinical situations.

10.3 System Models

Preliminary validation of the system model, as it would be used clinically, showed a great potential for the system to be useful in several clinical situations. The uniquely identified parameters were not only able to predict and reconstruct the patient specific PV curve, but also may be able to indicate the condition of the patient directly. Furthermore, the model may be readily integrated with additional mechanics of ventilation to supplement the PV data, so that it can reflect the true lung mechanics for direct analysis or assessment. Additional research and validation is required to fully evaluate these parameters' potential improvements. A few possible improvements are briefly described here.

10.3.1 Inspiratory Capacity Estimation

As discussed briefly in Chapter 7, the model resulted in variable number of lung units between patients. In this model, the total number of units is associated with the amount of recruitable lung units and thus directly related to the absolute maximum volume of the lung. Physiologically, this available volume from the relaxed lung at atmospheric pressure to the maximum inflation is called Inspiratory Capacity (IC). A reduction in this volume is one of the marked symptoms of ARDS and thus, its identification is clinically very relevant for diagnosis and treatment.

Validation of this potential correlation and clinical diagnostic requires direct comparison between the model results and clinical measurement. However, this data is not easily obtainable in clinical situations. Measurement of IC requires inflating the lung to maximum capacity, which is clinically and ethically impossible due the additional lung injury that it will most likely cause. It may be possible to use other less risky methods, such as CT scans, to estimate IC, however validation of this metric requires a practical method of measuring or estimating the IC of a mechanically ventilated critical care patient.

10.3.2 Airway Resistance Evaluation/Estimation

Airway resistances have a significant effect on measured PV curves, especially the ones measured inside the ventilator, which is the most common practice currently in ICU. The artificial airways between the ventilator and the patient, such as the connecting and ET tubes, can create significant resistance that serve to mask the true lung mechanics in the PV curves obtained.

The validation study in this thesis showed the model's ability to fit and identify PV data both with (proximal) and without (carina) these resistance effects. However, for direct clinical relevance, PV curves of true lung mechanics should be used for patient condition analysis. Therefore, it may be valuable to develop and integrate airway resistance estimation systems in the model and apply them to the data before analysis. Resistance characteristics of tubes are easy to test and measure, thus the development of a resistance database for each

common brand of ET and breathing circuit tube and their combinations under variety of different flow patterns is realistically feasible. The integration of this system would ease the analysis and increase the accuracy of bedside diagnosis.

10.3.3 Spontaneously Breathing Patients

Not all patients on mechanical ventilators are fully dependent on the ventilator. Some patients have lowered lung function, however they still have some level of spontaneous breathing. Therefore, the ventilator is used as a supportive tool, rather than completely taking over the work of breathing. The lung mechanics of these patients may be more complex and difficult to capture due to additional mechanics, patient variability, and lack of direct measurement of the total patient breathing effort.

The current model developed in this research is designed and validated only for paralysed passively breathing patients. Therefore, it cannot be applied directly to the spontaneously breathing patient at this point, regardless of the extent of their breathing effort. However, because there are a significant number of patients on mechanical ventilation who have some level of breathing effort, it will be valuable to develop and integrate a metric that allows analysis of such spontaneously breathing patients. In addition, many patients are completely passively ventilated for short periods of time without muscle relaxants. Hence, this model is likely to be applicable in this case, as well.

The primary difficulty will be to find a metric that detects the presence of spontaneous breathing and identify the level of effort exerted by the patient. It may be possible, for example, to quantify the effort from sudden or unnatural changes in pressure, or may require direct measurement of patient's muscular movement. In any case, additional research is required to identify and validate this metric. However, incorporating these additional mechanics into the system model will significantly broaden the potential clinical applications for the system. Finally, elements of this model would be incorporated into a model for non-ventilated spontaneously breathing patients outside of intensive care. This application would enable disease and physiological changes to be tracked and more appropriately managed.

10.3.4 Automated System

Finally, the model requires a full or semi-automated system to incorporate all the features of the system model, including data acquisition, processing, and analysis. Because this system is designed to be clinically useful, the entire system must be packaged in such way that requires least effort from the intensive care staff to operate, and the data and the information must be presented in easy to understand, intuitively clear manner. Hence, a greater automation in either sensored, smart breathing circuits and/or smarter ventilators is the long-term clinical goal for this research.

References

Albaiceta, G. M., Piacentini, E., Villagra, A., Lopez-Aguilar, J., Taboada, F., and Blanch, L. (2003). Application of continuous positive airway pressure to trace static pressure-volume curves of the respiratory system. *Crit Care Med*, 31(10):2514–9.

Albaiceta, G. M., Taboada, F., Parra, D., Luyando, L. H., Calvo, J., Menendez, R., and Otero, J. (2004). Tomographic study of the inflection points of the pressure-volume curve in acute lung injury. *Am J Respir Crit Care Med*, 170(10):1066–72. Epub 2004 Aug 18.

Amato, M. B., Barbas, C. S., Medeiros, D. M., Magaldi, R. B., Schettino, G. P., Lorenzi-Filho, G., Kairalla, R. A., Deheinzelin, D., Munoz, C., Oliveira, R., Takagaki, T. Y., and Carvalho, C. R. (1998). Effect of a protective-ventilation strategy on mortality in the acute respiratory distress syndrome. *N Engl J Med*, 338(6):347–54.

Artigas, A., Bernard, G. R., Carlet, J., Dreyfuss, D., Gattinoni, L., Hudson, L., Lamy, M., Marini, J. J., Matthay, M. A., Pinsky, M. R., Spragg, R., and Suter, P. M. (1998). The american-european consensus conference on ards, part 2: Ventilatory, pharmacologic, supportive therapy, study design strategies, and issues related to recovery and remodeling. acute respiratory distress syndrome. *Am J Respir Crit Care Med*, 157(4 Pt 1):1332–47.

Ashbaugh, D. G., Bigelow, D. B., Petty, T. L., and Levine, B. E. (1967). Acute respiratory distress in adults. *Lancet*, 2(7511):319–23.

Atabai, K. and Matthay, M. A. (2002). The pulmonary physician in critical care. 5: Acute lung injury and the acute respiratory distress syndrome: definitions and epidemiology. *Thorax*, 57(5):452–8.

Ben-Tal, A. (2006). Simplified models for gas exchange in the human lungs. *J Theor Biol*, 238(2):474–95.

Bersten, A. D. (1998). Measurement of overinflation by multiple linear regression analysis in patients with acute lung injury. *Eur Respir J*, 12(3):526–32.

Bersten, A. D., Edibam, C., Hunt, T., and Moran, J. (2002). Incidence and mortality of acute lung injury and the acute respiratory distress syndrome in three australian states. *Am J Respir Crit Care Med*, 165(4):443–8.

Bersten, A. D. and Soni, N., editors (2003). *Oh's Intensive Care Manual*. Butterworth-Heinemann, London, UK, 5th edition.

Borges, J. B., Okamoto, V. N., Matos, G. F., Caramez, M. P., Arantes, P. R., Barros, F., Souza, C. E., Victorino, J. A., Kacmarek, R. M., Barbas, C. S., Carvalho, C. R., and Amato, M. B. (2006). Reversibility of lung collapse and hypoxemia in early acute respiratory distress syndrome. *Am J Respir Crit Care Med*, 174(3):268–78.

Brochard, L., Roudot-Thoraval, F., Roupie, E., Delclaux, C., Chastre, J., Fernandez-Mondejar, E., Clementi, E., Mancebo, J., Factor, P., Matamis, D., Ranieri, M., Blanch, L., Rodi, G., Mentec, H., Dreyfuss, D., Ferrer, M., Brun-Buisson, C., Tobin, M., and Lemaire, F. (1998). Tidal volume reduction for prevention of ventilator-induced lung injury in acute respiratory distress syndrome. the multicenter trail group on tidal volume reduction in ards. *Am J Respir Crit Care Med*, 158(6):1831–8.

Brower, R. G., Lanken, P. N., MacIntyre, N., Matthay, M. A., Morris, A., Ancukiewicz, M., Schoenfeld, D., and Thompson, B. T. (2004). Higher versus lower positive end-expiratory pressures in patients with the acute respiratory distress syndrome. *N Engl J Med*, 351(4):327–36.

Brunner, J. X. and Iotti, G. A. (2002). Adaptive support ventilation (asv). *Minerva Anestesiol*, 68(5):365–8.

Carney, D. E., Bredenberg, C. E., Schiller, H. J., Picone, A. L., McCann, U. G., Gatto, L. A., Bailey, G., Fillinger, M., and Nieman, G. F. (1999). The mechanism of lung volume change during mechanical ventilation. *Am J Respir Crit Care Med*, 160(5):1697–1702.

Carson, E. R. and Cobelli, C. (2001). *Modelling methodology for physiology and medicine*. Academic Press Series in Biomedical Engineering. Academic Press, San Diego.

Chase, J. G., Yuta, T., Mulligan, K. J., Shaw, G. M., and Horn, B. (2006). A novel mechanical lung model of pulmonary diseases to assist with teaching and training. *BMC Pulm Med*, 6:21.

Chelucci, G. L., Dall'Ava-Santucci, J., Dhainaut, J. F., Chelucci, A., Allegra, A., Lockhart, A., Zin, W. A., and Milic-Emili, J. (2000). Association of peep with two different inflation volumes in ards patients: effects on passive lung deflation and alveolar recruitment. *Intensive Care Med*, 26(7):870–7.

Cheng, W., DeLong, D. S., Franz, G. N., Petsonk, E. L., and Frazer, D. G. (1995). Contribution of opening and closing of lung units to lung hysteresis. *Respir Physiol*, 102(2-3):205–15.

Crotti, S., Mascheroni, D., Caironi, P., Pelosi, P., Ronzoni, G., Mondino, M., Marini, J. J., and Gattinoni, L. (2001). Recruitment and derecruitment during acute respiratory failure: a clinical study. *Am J Respir Crit Care Med*, 164(1):131–40.

Dasta, J. F., McLaughlin, T. P., Mody, S. H., and Piech, C. T. (2005). Daily cost of an intensive care unit day: the contribution of mechanical ventilation. *Crit Care Med*, 33(6):1266–71.

Deans, K. J., Minneci, P. C., Cui, X., Banks, S. M., Natanson, C., and Eichacker, P. Q. (2005). Mechanical ventilation in ards: One size does not fit all. *Crit Care Med*, 33(5):1141–3.

Dreyfuss, D. and Saumon, G. (1998). Ventilator-induced lung injury: lessons from experimental studies. *Am J Respir Crit Care Med*, 157(1):294–323.

Edibam, C., Rutten, A. J., Collins, D. V., and Bersten, A. D. (2003). Effect of inspiratory flow pattern and inspiratory to expiratory ratio on nonlinear elastic behavior in patients with acute lung injury. *Am J Respir Crit Care Med*, 167(5):702–7.

Eichacker, P. Q., Gerstenberger, E. P., Banks, S. M., Cui, X., and Natanson, C. (2002). Meta-analysis of acute lung injury and acute respiratory distress syndrome trials testing low tidal volumes. *Am J Respir Crit Care Med*, 166(11):1510–4.

Esteban, A., Anzueto, A., Frutos, F., Alia, I., Brochard, L., Stewart, T. E., Benito, S., Epstein, S. K., Apezteguia, C., Nightingale, P., Arroliga, A. C., and

Tobin, M. J. (2002). Characteristics and outcomes in adult patients receiving mechanical ventilation: a 28-day international study. *Jama*, 287(3):345–55.

Ferguson, N. D., Frutos-Vivar, F., Esteban, A., Anzueto, A., Alia, I., Brower, R. G., Stewart, T. E., Apezteguia, C., Gonzalez, M., Soto, L., Abroug, F., and Brochard, L. (2005). Airway pressures, tidal volumes, and mortality in patients with acute respiratory distress syndrome. *Crit Care Med*, 33(1):21–30.

Foti, G., Cereda, M., Sparacino, M. E., De Marchi, L., Villa, F., and Pesenti, A. (2000). Effects of periodic lung recruitment maneuvers on gas exchange and respiratory mechanics in mechanically ventilated acute respiratory distress syndrome (ards) patients. *Intensive Care Med*, 26(5):501–7.

Gattinoni, L., Caironi, P., Cressoni, M., Chiumello, D., Ranieri, V. M., Quintel, M., Russo, S., Patroniti, N., Cornejo, R., and Bugedo, G. (2006). Lung recruitment in patients with the acute respiratory distress syndrome. *N Engl J Med*, 354(17):1775–86.

Gattinoni, L., Caironi, P., Pelosi, P., and Goodman, L. R. (2001). What has computed tomography taught us about the acute respiratory distress syndrome? *Am J Respir Crit Care Med*, 164(9):1701–11.

Gattinoni, L. and Pesenti, A. (2005). The concept of "baby lung". *Intensive Care Med*, 31(6):776–84.

Girgis, K., Hamed, H., Khater, Y., and Kacmarek, R. M. (2006). A decremental peep trial identifies the peep level that maintains oxygenation after lung recruitment. *Respir Care*, 51(10):1132–9.

Guyton, A. C. and Hall, J. E. (2000). *Textbook of medical physiology*. W. B. Saunders, Philadelphia, 10th edition.

Halter, J. M., Steinberg, J. M., Schiller, H. J., DaSilva, M., Gatto, L. A., Landas, S., and Nieman, G. F. (2003). Positive end-expiratory pressure after a recruitment maneuver prevents both alveolar collapse and recruitment/derecruitment. *Am J Respir Crit Care Med*, 167(12):1620–6. Epub 2003 Feb 25.

Hamilton Medical (2006). Galileo gold ventilator brochure and technical specifications.

Henzler, D., Pelosi, P., Dembinski, R., Ullmann, A., Mahnken, A. H., Rossaint, R., and Kuhlen, R. (2005). Respiratory compliance but not gas exchange

correlates with changes in lung aeration after a recruitment maneuver: an experimental study in pigs with saline lavage lung injury. *Crit Care*, 9(5):R471–82.

Hickling, K. G. (1998). The pressure-volume curve is greatly modified by recruitment. a mathematical model of ards lungs. *Am J Respir Crit Care Med*, 158(1):194–202.

Hickling, K. G. (2001). Best compliance during a decremental, but not incremental, positive end-expiratory pressure trial is related to open-lung positive end-expiratory pressure: a mathematical model of acute respiratory distress syndrome lungs. *Am J Respir Crit Care Med*, 163(1):69–78.

Hickling, K. G. (2002). Reinterpreting the pressure-volume curve in patients with acute respiratory distress syndrome. *Curr Opin Crit Care*, 8(1):32–8.

Iotti, G. A. and Braschi, A. (1999). *Measurements of Respiratory Mechanics During Mechanical Ventilation*. Hamilton Medcal AG, Rhazuns, Swirzerland.

Jonson, B. (2005). Elastic pressure-volume curves in acute lung injury and acute respiratory distress syndrome. *Intensive Care Med*, 31(2):205–12. Epub 2004 Dec 17.

Jonson, B., Richard, J. C., Straus, C., Mancebo, J., Lemaire, F., and Brochard, L. (1999). Pressure-volume curves and compliance in acute lung injury: evidence of recruitment above the lower inflection point. *Am J Respir Crit Care Med*, 159(4 Pt 1):1172–8.

Jonson, B. and Svantesson, C. (1999). Elastic pressure-volume curves: what information do they convey? *Thorax*, 54(1):82–7.

Kacmarek, R. M. (2005). Lung protection: the cost in some is increased work of breathing. is it too high? *Respir Care*, 50(12):1614–6.

Kallet, R. H., Campbell, A. R., Dicker, R. A., Katz, J. A., and Mackersie, R. C. (2006). Effects of tidal volume on work of breathing during lung-protective ventilation in patients with acute lung injury and acute respiratory distress syndrome. *Crit Care Med*, 34(1):8–14.

Kallet, R. H., Jasmer, R. M., Pittet, J. F., Tang, J. F., Campbell, A. R., Dicker, R., Hemphill, C., and Luce, J. M. (2005). Clinical implementation of the ards

network protocol is associated with reduced hospital mortality compared with historical controls. *Crit Care Med*, 33(5):925–9.

Karason, S., Karlsen, K. L., Lundin, S., and Stenqvist, O. (1999). A simplified method for separate measurements of lung and chest wall mechanics in ventilator-treated patients. *Acta Anaesthesiol Scand*, 43(3):308–15.

Karason, S., Sondergaard, S., Lundin, S., Wiklund, J., and Stenqvist, O. (2000). Evaluation of pressure/volume loops based on intratracheal pressure measurements during dynamic conditions. *Acta Anaesthesiol Scand*, 44(5):571–7.

Karason, S., Sondergaard, S., Lundin, S., Wiklund, J., and Stenqvist, O. (2001). Direct tracheal airway pressure measurements are essential for safe and accurate dynamic monitoring of respiratory mechanics. a laboratory study. *Acta Anaesthesiol Scand*, 45(2):173–9.

Lee, W. L., Stewart, T. E., MacDonald, R., Lapinsky, S., Banayan, D., Hallett, D., and Mehta, S. (2002). Safety of pressure-volume curve measurement in acute lung injury and ards using a syringe technique. *Chest*, 121(5):1595–601.

Lichtwarck-Aschoff, M., Helmer, A., Kawati, R., Lattuada, M., Sjostrand, U. H., Zugel, N., Guttmann, J., and Hedenstierna, G. (2003). Good short-term agreement between measured and calculated tracheal pressure. *Br J Anaesth*, 91(2):239–48.

Lim, C. M., Soon Lee, S., Seoung Lee, J., Koh, Y., Sun Shim, T., Do Lee, S., Sung Kim, W., Kim, D. S., and Dong Kim, W. (2003). Morphometric effects of the recruitment maneuver on saline-lavaged canine lungs. a computed tomographic analysis. *Anesthesiology*, 99(1):71–80.

Lu, Q. and Rouby, J. J. (2000). Measurement of pressure-volume curves in patients on mechanical ventilation: methods and significance. *Crit Care*, 4(2):91–100. Epub 2000 Mar 21.

Luhr, O. R., Antonsen, K., Karlsson, M., Aardal, S., Thorsteinsson, A., Frostell, C. G., and Bonde, J. (1999). Incidence and mortality after acute respiratory failure and acute respiratory distress syndrome in sweden, denmark, and iceland. the arf study group. *Am J Respir Crit Care Med*, 159(6):1849–61.

Maeda, Y., Fujino, Y., Uchiyama, A., Taenaka, N., Mashimo, T., and Nishimura, M. (2003). Does the tube-compensation function of two modern mechanical ventilators provide effective work of breathing relief? *Crit Care*, 7(5):R92–7.

Malbouisson, L. M., Muller, J. C., Constantin, J. M., Lu, Q., Puybasset, L., and Rouby, J. J. (2001). Computed tomography assessment of positive end-expiratory pressure-induced alveolar recruitment in patients with acute respiratory distress syndrome. *Am J Respir Crit Care Med*, 163(6):1444–50.

Manzano, F., Yuste, E., Colmenero, M., Aranda, A., Garcia-Horcajadas, A., Rivera, R., and Fernandez-Mondejar, E. (2005). Incidence of acute respiratory distress syndrome and its relation to age. *J Crit Care*, 20(3):274–80.

Maquet Medical Systems (2006). Servo-i ventilator brochure.

Martynowicz, M. A., Minor, T. A., Walters, B. J., and Hubmayr, R. D. (1999). Regional expansion of oleic acid-injured lungs. *Am J Respir Crit Care Med*, 160(1):250–8.

Martynowicz, M. A., Walters, B. J., and Hubmayr, R. D. (2001). Mechanisms of recruitment in oleic acid-injured lungs. *J Appl Physiol*, 90(5):1744–53.

McCann, U. G., n., Schiller, H. J., Carney, D. E., Gatto, L. A., Steinberg, J. M., and Nieman, G. F. (2001). Visual validation of the mechanical stabilizing effects of positive end-expiratory pressure at the alveolar level. *J Surg Res*, 99(2):335–42.

McLean, S. E., Jensen, L. A., Schroeder, D. G., Gibney, N. R., and Skjodt, N. M. (2006). Improving adherence to a mechanical ventilation weaning protocol for critically ill adults: outcomes after an implementation program. *Am J Crit Care*, 15(3):299–309.

Mergoni, M., Martelli, A., Volpi, A., Primavera, S., Zuccoli, P., and Rossi, A. (1997). Impact of positive end-expiratory pressure on chest wall and lung pressure-volume curve in acute respiratory failure. *Am J Respir Crit Care Med*, 156(3 Pt 1):846–54.

Mols, G., Priebe, H. J., and Guttmann, J. (2006). Alveolar recruitment in acute lung injury. *Br J Anaesth*, 96(2):156–66.

Ochs, M., Nyengaard, J. R., Jung, A., Knudsen, L., Voigt, M., Wahlers, T., Richter, J., and Gundersen, H. J. (2004). The number of alveoli in the human lung. *Am J Respir Crit Care Med*, 169(1):120–4.

Otis, A. B., Fenn, W. O., and Rahn, H. (1950). Mechanics of breathing in man. *J Appl Physiol*, 2(11):592–607.

Pelosi, P., Croci, M., Ravagnan, I., Vicardi, P., and Gattinoni, L. (1996a). Total respiratory system, lung, and chest wall mechanics in sedated-paralyzed postoperative morbidly obese patients. *Chest*, 109(1):144–51.

Pelosi, P., Crotti, S., Brazzi, L., and Gattinoni, L. (1996b). Computed tomography in adult respiratory distress syndrome: what has it taught us? *Eur Respir J*, 9(5):1055–62.

Pelosi, P., Goldner, M., McKibben, A., Adams, A., Eccher, G., Caironi, P., Losappio, S., Gattinoni, L., and Marini, J. J. (2001). Recruitment and derecruitment during acute respiratory failure: an experimental study. *Am J Respir Crit Care Med*, 164(1):122–30.

Pereira, C., Bohe, J., Rosselli, S., Combourieu, E., Pommier, C., Perdrix, J. P., Richard, J. C., Badet, M., Gaillard, S., Philit, F., and Guerin, C. (2003). Sigmoidal equation for lung and chest wall volume-pressure curves in acute respiratory failure. *J Appl Physiol*, 95(5):2064–71.

Puybasset, L., Cluzel, P., Chao, N., Slutsky, A. S., Coriat, P., and Rouby, J. J. (1998). A computed tomography scan assessment of regional lung volume in acute lung injury. the ct scan ards study group. *Am J Respir Crit Care Med*, 158(5 Pt 1):1644–55.

Puybasset, L., Cluzel, P., Gusman, P., Grenier, P., Preteux, F., and Rouby, J. J. (2000). Regional distribution of gas and tissue in acute respiratory distress syndrome. i. consequences for lung morphology. ct scan ards study group. *Intensive Care Med*, 26(7):857–69.

Rees, S. E., Allerod, C., Murley, D., Zhao, Y., Smith, B. W., Kjaergaard, S., Thorgaard, P., and Andreassen, S. (2006). Using physiological models and decision theory for selecting appropriate ventilator settings. *J Clin Monit Comput*, 20(6):421–429.

Rees, S. E., Kjaergaard, S., Perthorgaard, P., Malczynski, J., Toft, E., and Andreassen, S. (2002). The automatic lung parameter estimator (alpe) system: non-invasive estimation of pulmonary gas exchange parameters in 10-15 minutes. *J Clin Monit Comput*, 17(1):43–52.

Rello, J., Ollendorf, D. A., Oster, G., Vera-Llonch, M., Bellm, L., Redman, R., and Kollef, M. H. (2002). Epidemiology and outcomes of ventilator-associated pneumonia in a large us database. *Chest*, 122(6):2115–21.

Reynolds, H. N., McCunn, M., Borg, U., Habashi, N., Cottingham, C., and Bar-Lavi, Y. (1998). Acute respiratory distress syndrome: estimated incidence and mortality rate in a 5 million-person population base. *Crit Care (Lond)*, 2(1):29–34.

Richard, J. C., Maggiore, S. M., Jonson, B., Mancebo, J., Lemaire, F., and Brochard, L. (2001). Influence of tidal volume on alveolar recruitment. respective role of peep and a recruitment maneuver. *Am J Respir Crit Care Med*, 163(7):1609–13.

Rouby, J. J., Lu, Q., and Goldstein, I. (2002). Selecting the right level of positive end-expiratory pressure in patients with acute respiratory distress syndrome. *Am J Respir Crit Care Med*, 165(8):1182–6.

Rouby, J. J., Puybasset, L., Cluzel, P., Richecoeur, J., Lu, Q., and Grenier, P. (2000). Regional distribution of gas and tissue in acute respiratory distress syndrome. ii. physiological correlations and definition of an ards severity score. ct scan ards study group. *Intensive Care Med*, 26(8):1046–56.

Rubenfeld, G. D., Caldwell, E., Peabody, E., Weaver, J., Martin, D. P., Neff, M., Stern, E. J., and Hudson, L. D. (2005). Incidence and outcomes of acute lung injury. *N Engl J Med*, 353(16):1685–93.

Rylander, C., Hogman, M., Perchiazzi, G., Magnusson, A., and Hedenstierna, G. (2004). Functional residual capacity and respiratory mechanics as indicators of aeration and collapse in experimental lung injury. *Anesth Analg*, 98(3):782–9, table of contents.

Schiller, H. J., Steinberg, J., Halter, J., McCann, U., DaSilva, M., Gatto, L. A., Carney, D., and Nieman, G. (2003). Alveolar inflation during generation of a quasi-static pressure/volume curve in the acutely injured lung. *Crit Care Med*, 31(4):1126–33.

Sebel, P., Stoddart, D. M., Waldhorn, R. E., Waldmann, C. S., and Whifield, P. (1985). *Respiration: the breath of life*. The Human Body. Torstar Books Inc., New York.

Seeley, R. R., Stephens, T. D., and Tate, P. (2003). *Anatomy & Physiology*. McGraw-Hill, New York, NY, 6th edition.

Sondergaard, S., Karason, S., Hanson, A., Nilsson, K., Hojer, S., Lundin, S., and Stenqvist, O. (2002). Direct measurement of intratracheal pressure in pediatric respiratory monitoring. *Pediatr Res*, 51(3):339–45.

Stahl, C. A., Moller, K., Schumann, S., Kuhlen, R., Sydow, M., Putensen, C., and Guttmann, J. (2006). Dynamic versus static respiratory mechanics in acute lung injury and acute respiratory distress syndrome. *Crit Care Med*, 34(8):2090–8.

Stenqvist, O. (2003). Practical assessment of respiratory mechanics. *Br J Anaesth*, 91(1):92–105.

Stenqvist, O., Olegard, C., Sondergaard, S., Odenstedt, H., Karason, S., and Lundin, S. (2002). Monitoring functional residual capacity (frc) by quantifying oxygen/carbon dioxide fluxes during a short apnea. *Acta Anaesthesiol Scand*, 46(6):732–9.

Straus, C., Louis, B., Isabey, D., Lemaire, F., Harf, A., and Brochard, L. (1998). Contribution of the endotracheal tube and the upper airway to breathing workload. *Am J Respir Crit Care Med*, 157(1):23–30.

Suchyta, M. R., Clemmer, T. P., Elliott, C. G., Orme, J. F., J., Morris, A. H., Jacobson, J., and Menlove, R. (1997). Increased mortality of older patients with acute respiratory distress syndrome. *Chest*, 111(5):1334–9.

Takeuchi, M., Goddon, S., Dolhnikoff, M., Shimaoka, M., Hess, D., Amato, M. B., and Kacmarek, R. M. (2002). Set positive end-expiratory pressure during protective ventilation affects lung injury. *Anesthesiology*, 97(3):682–92.

The Acute Respiratory Distress Syndrome Network (2000). Ventilation with lower tidal volumes as compared with traditional tidal volumes for acute lung injury and the acute respiratory distress syndrome. *N Engl J Med*, 342(18):1301–8.

van der Kooi, T. I., de Boer, A. S., Mannien, J., Wille, J. C., Beaumont, M. T., Mooi, B. W., and van den Hof, S. (2006). Incidence and risk factors of device-associated infections and associated mortality at the intensive care in the dutch surveillance system. *Intensive Care Med*.

Vander, A., Sherman, J., and Luciano, D. (2001). *The Mechanism of Body Function*. Human Physiology. McGraw-Hill, New York, NY, 8th edition.

Venegas, J. G., Harris, R. S., and Simon, B. A. (1998). A comprehensive equation for the pulmonary pressure-volume curve. *J Appl Physiol*, 84(1):389–95.

Walsh, T. S., Dodds, S., and McArdle, F. (2004). Evaluation of simple criteria to predict successful weaning from mechanical ventilation in intensive care patients. *Br J Anaesth*, 92(6):793–9. Epub 2004 Apr 30.

Ware, L. B. and Matthay, M. A. (2000). The acute respiratory distress syndrome. *N Engl J Med*, 342(18):1334–49.

Yuta, T., Chase, G., Shaw, G., and Hann, C. (2004). Dynamic models of ards lung mechanics for optimal patient ventilation. In *26th Annual International Conference of the IEEE Engineering in Medicine and Biology Society*, San Francisco, CA.

Zamir, M. (2000). *The Physics of Pulsatile Flow*. Biological Physics. Springer-Verlag, New York.

Zilberberg, M. D. and Epstein, S. K. (1998). Acute lung injury in the medical icu: comorbid conditions, age, etiology, and hospital outcome. *Am J Respir Crit Care Med*, 157(4 Pt 1):1159–64.